Mapping Groundwater with Geophysics:

Locating and Characterizing Aquifers in the Beaufort Watershed with Electrical Resistivity Surveying

by

Savanna Yamamoto

A Thesis Submitted in Partial Fulfillment of the
Requirements of the

HONOURS PROGRAM

in the School of Earth and Ocean Sciences

Supervisors: Lucinda Leonard and Mike Wei

We acknowledge and respect the Lək̓ʷəŋən (Songhees and Xʷsepsəm/Esquimalt) Peoples on whose territory the university stands, and the Lək̓ʷəŋən and W̱SÁNEĆ Peoples whose historical relationships with the land continue to this day.

Abstract

In the Beaufort Watershed study area on eastern Vancouver Island, groundwater is the primary freshwater supply. More data are needed to improve characterization of the groundwater resource, in order to protect and manage it. Electrical resistivity surveying is a cost-effective remote sensing technique that allows the types of subsurface materials to be inferred, and therefore allow for qualitative and quantitative characterizations of aquifers to be made. Working with the Beaufort Watershed Stewards, I collected, modelled, and interpreted 11 vertical 1D profiles (~83 m deep) and two vertical 2D profiles (81 m long x 17 m deep) in the study area. I was able to distinguish between different types of geological materials such as sand and gravel, till, clay, and various bedrock types and also identify where potential aquifers exist among these materials. Extensive sand and gravel units, which are commonly major sources of groundwater, were only identified throughout the southern part of the study area. Most of these units were determined to be water-bearing, yielding moderate-high quantities of water, and being only partially confined. They had an average thickness of ~17.5 metres, and were all located at ground level. A potential source of groundwater spanning the entire study area was the sedimentary bedrock identified in nearly all profiles, which was determined to be a relatively confined, low-yielding aquifer. This aquifer had an average depth of approximately 32 metres and an undefined thickness. A non-permeable, aquitard unit composed of clay, till, or both was also determined to span the entire region, averaging approximately 30.5 metres thick. The average depth to the aquitard was determined to vary between the northern and southern parts of the study area, where the aquitard in the former averaged roughly 2.5 metres depth, and the aquitard in the latter averaged roughly 18 metres depth. The 2D profiles, on either side of the Ships Point peninsula near Fanny Bay, both indicated the presence of saltwater within a sand and gravel aquifer unit, implying the occurrence of subsurface seawater proximal to shorelines.

Table of Contents

List of Figures

List of Tables

Acknowledgements

I respectfully acknowledge that the land this project was completed on is the Unceded Traditional Territory of the K'ómoks First Nation, the traditional keepers of this land. Additionally, I would like to thank members of the Beaufort Watershed Stewards – Mark Lake, Mike Mesford, Lise Laguë, Lynne Ray, Pam Lengyel, and Paul Anders – for their enthusiastic help setting up and running electrical resistivity surveys on those long, hot, summer days. I also express my gratitude to Juan Suarez, of Fisheries and Oceans Canada, for providing access to the Rosewall Creek Hatchery property and for sharing his knowledge. A special thanks to Mike Mesford, of the BWS, for hosting Dr. Lucinda Leonard and I during the week of data collection, and Mark Lake, of the BWS, for his instrumental part in creating this project, as well as being the correspondent between UVic and the BWS. This research was supported by the Jamie Cassels Undergraduate Research Awards, University of Victoria.

My sincerest appreciation is offered to Lucinda Leonard and Mike Wei who provided dedicated guidance, support, and wisdom to me over the last ten months. Each of them showed excellent care to my work and me throughout this project, helping me grow as a student and as a person. While both Lucinda and Mike have taught me in other courses, it is abundantly clear after being supervised by them for this study that they have a true passion for nurturing and inspiring their students. I feel privileged to have had the opportunity to get to know and learn from them, and I hope that I can make the same kind of impact they have made for me one day.

Lastly, I want to recognize my family, including my parents, siblings, grandparents, aunts, and uncles. During the past year while I worked on this project they have shared in all the excitement that came along, from the stages of field work to the completion of my thesis, and for this I am fortunate and grateful. Since grade school they have encouraged me to strive for my personal best and I believe this was one of the most significant factors in my success throughout my thesis and education as a whole.

1. Introduction

1.1. Groundwater Resources

Freshwater is an ecologically and societally valuable resource, important to the well being of all life on earth, and yet less than 3% of all water on Earth is fresh (e.g., Shiklomanov, 2000). While it provides hydration and habitat for organisms, humans use freshwater for drinking, sanitation, producing food, generating power, and manufacturing products. Although freshwater is stored in various environments including glaciers and ice caps, lakes, rivers, and ground ice/permafrost, and the atmosphere, a large portion of the freshwater humans rely on is stored beneath Earth's surface as groundwater. Roughly 30% of freshwater is held in aquifers below ground (e.g., Shiklomanov, 2000), where water fills the pore spaces of geological materials and is referred to as groundwater. An aquifer is a geological unit that is permeable and water-saturated, and supplies useful quantities of water; aquitards are geological units that are less permeable and therefore are incapable of supplying useful quantities of water. Humans access the water in aquifers via natural springs where groundwater is expressed at Earth's surface, or more commonly, by pumping of wells dug or drilled into the aquifers.

According to Berardinucci and Ronneseth (2002), in British Columbia, groundwater supplies roughly 25% of all municipal water needs, excluding the major metropolitan areas of Greater Victoria and Vancouver. In many places, groundwater is the only freshwater source available and with continuously increasing demands, protection of the quality and quantity of groundwater resources is significant. Identifying and studying aquifers in British Columbia is an important step in the protection and management of the hidden resource. Where the quality of groundwater is of concern, especially in areas without alternative freshwater sources, contamination by anthropogenic activity (fertilizers, septic systems, transportation activities, etc.) or natural phenomena such as saltwater intrusion (e.g., Berardinucci & Ronneseth, 2002) can be mitigated and reduced, or fully eliminated, with the knowledge of aquifer locations and characteristics. The Water Sustainability Act (WSA), introduced to British Columbia in 2016, aims to protect the environmental flow needs, groundwater levels and flow, and the rights of water users (surface or groundwater), particularly following the First-in-Time; First-in-Right concept (Province of BC, 2016). Mapping and characterizing aquifers are key to following the statutory laws of protection

in the WSA, as they allow for proper allocation of water uses, and help avoid and resolve conflicts between water users and aquatic habitats.

1.2. The Beaufort Watershed Study Area

On the central east coast of Vancouver Island, between Fanny Bay and Royston, BC (Fig. 1.2.0), communities rely almost solely on groundwater for their freshwater supply. The Beaufort Watershed Stewards (BWS; https://beaufortwater.org/), a group of local volunteers who work to protect the freshwater in the region, are dedicated to improving the knowledge on surface and groundwater sources in the area in order to ensure their communities have a healthy, sustainable supply. In most of the populous areas on the east coast of Vancouver Island, the spatial coverage of groundwater data is quite dense, but this is not true for the area of interest (Fig. 1.2.1). Although the communities between Fanny Bay and Royston are much smaller than those where groundwater data are more concentrated, sufficient information is no less important.

Figure 1.2.0. Study area between Fanny Bay and Royston, showing the relative location of the Beaufort Mountain Range and the Strait of Georgia.

To be able to determine the projected health of groundwater in the region, the Beaufort Watershed Stewards desire greater understanding of the location, extent, and size of the aquifers within the Beaufort Watershed as well as the groundwater chemistry in the coastal area. Groundwater wells are distributed throughout the study area of approximately 200 square kilometres, yet the aquifers that have been previously mapped cover only ~85 square kilometres within this region (Fig. 1.2.1). As a result, aquifers have not been mapped in areas where many of the wells are located, making protection and management of the groundwater resource more difficult.

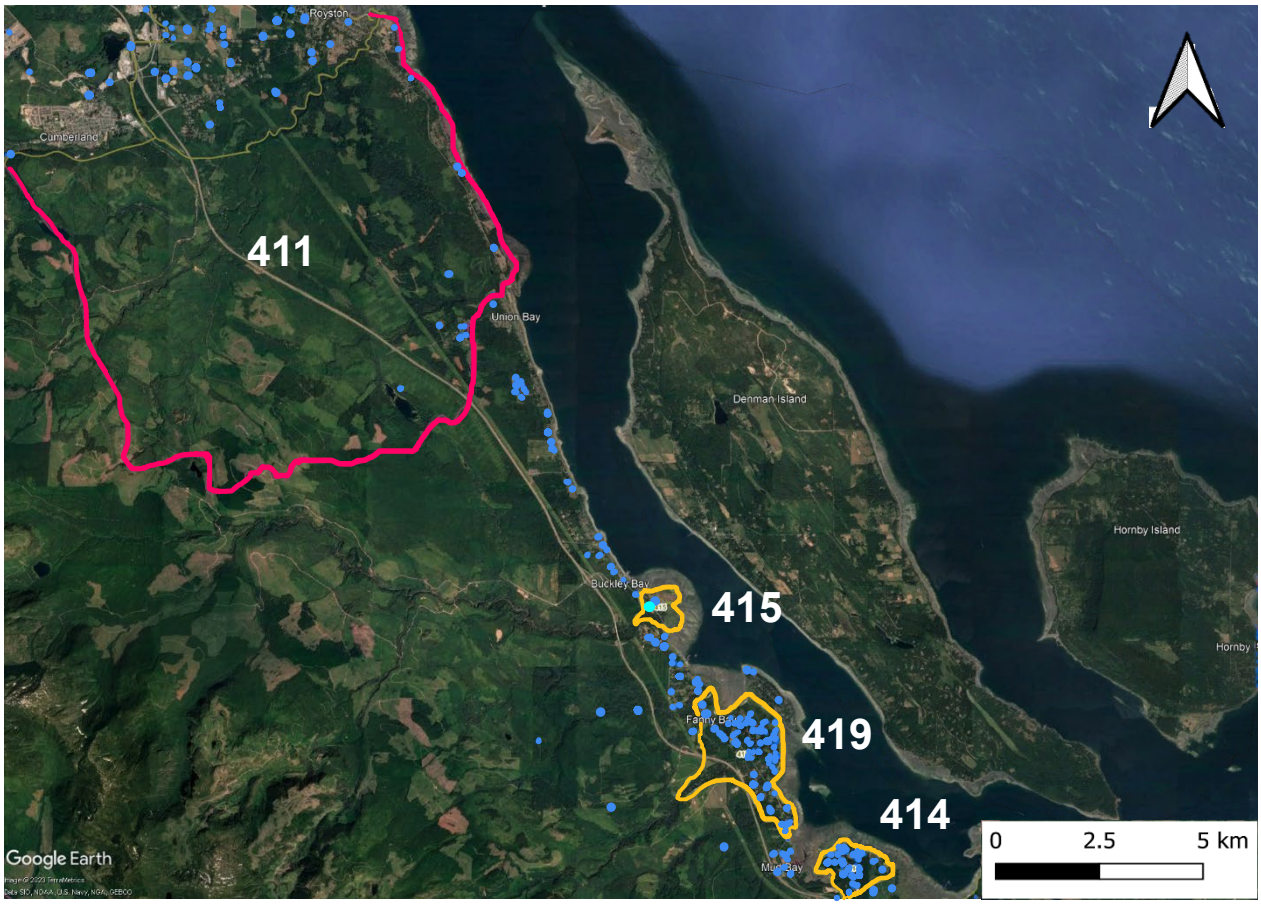

Figure 1.2.1. Groundwater data in the study area. The aquifers currently mapped in the study area are outlined in pink and yellow, indicating bedrock and sand and gravel materials, respectively. Aquifer numbers associated with these aquifers are written in, or beside the corresponding polygons. Groundwater wells are depicted as blue dots, with the cyan dot symbolizing a provincial observation well (GWELLS, https://apps.nrs.gov.bc.ca/gwells/).

Traditionally, the process of mapping aquifers consists of drilling wells, analysing the lithology, interpolating lithological layers between boreholes, and then extracting an aquifer boundary based on the location of the wells, the geomorphology of the geological unit, and the surrounding topography. The ease and confidence in mapping aquifers are improved with higher concentrations of well log lithologies (e.g., Berardinucci & Ronneseth, 2002). Due to the expense and difficulty of mapping aquifers in this manner, the Beaufort Watershed Stewards desire a more cost-effective method to fill in the data gaps between wells and add to the knowledge of the groundwater resource.

1.3. Objectives

The main objective of my Honours thesis research is to improve the mapping and understanding of aquifer units in the Beaufort Watershed area. Using a geophysical remote sensing technique called electrical resistivity surveying, I have collected resistivity data at sites chosen by the BWS. In this thesis, I analyze the resistivity data and use them to interpret lithological sequences throughout the study area. From this, I infer the spatial and vertical distribution of aquifers and aquitards, as well as their thickness, depth, and the degree to which aquifers are confined. Knowledge of aquifers and confining layers is useful from a protection and management perspective to better understand groundwater recharge, the vulnerability of aquifers to contamination from activities at the land surface, and the hydraulic connection between surface water and groundwater, for example. Lastly, using the resistivity data I examine part of the study area to determine if there is evidence of saltwater presence within aquifers, to address the concerns of community members living in close proximity to the ocean.

1.4. Thesis Outline

In total, this thesis consists of six sections, including the current one providing an introduction. The following sections include the background, methods, results and interpretations, discussion, and conclusion. The background in the second section provides context for this study including the geological and hydrogeological setting, the applied geophysical concepts, and previous research completed for similar studies. In the third section, the geophysical method of electrical resistivity surveying is described in detail, broken into two different experiment types, and the overall design of the study is described. The results and interpretations of the geophysical surveys comprise the fourth section. A discussion of the interpretations takes place in section five, summarizing the regional geology and hydrogeology,

and reviewing the implications for the Beaufort Watershed study area. The sixth and final section concludes the study and provides recommendations to improve this research in the future.

2. Background

2.1. Geological Setting

The Beaufort Range on Vancouver Island (Fig. 2.1.0) is part of the Insular Belt that forms much of coastal British Columbia. The narrow, NW-trending mountain range is located ~ 6 km inland and roughly parallels the central east coast of Vancouver Island. The eastern slopes of the mountain range act to funnels water to the east into stream systems and to recharge aquifers, supply the coastal communities between Royston and Bowser with freshwater in the form of groundwater and surface water. Situated along the Strait of Georgia, the Beaufort Watershed region has been accumulating sediment for tens of millions of years (e.g., Earle, 2002).

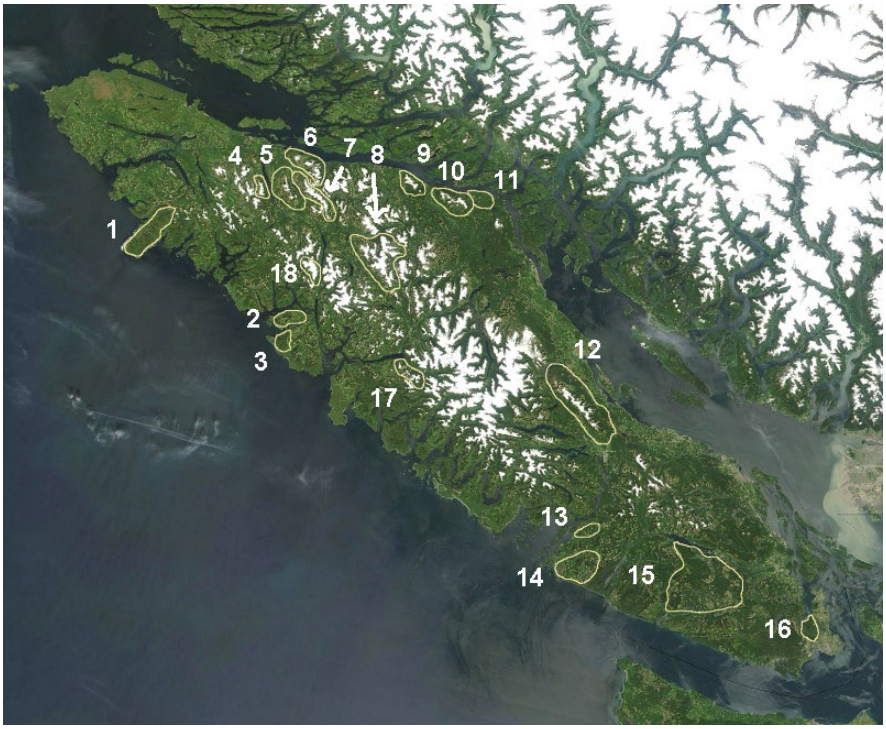

Figure 2.1.0. Mountain ranges on Vancouver Island. Number 12 on the east coast correlates to the Beaufort Range located west of the study area. (Satellite imagery from NASA, Public domain, via Wikipedia Commons).

2.1.1. Regional Bedrock Geology

The igneous Wrangellia terrane forms most of Vancouver Island; following accretion of this terrane to the west coast of ancestral North America, clastic sediments were deposited in a

trough-shaped basin of the Georgia Depression (e.g., Clague, 1976) located to the east of the terrane during the upper part of the Cretaceous, between 85 and 66 million years ago (e.g., Earle, 2002). It is widely accepted that most of these sediments were deposited in a marine setting, specifically as gravity flows or submarine fans (e.g., Mustard, 1994). Lithification of these deposits formed the Nanaimo Group of sedimentary rocks (Fig. 2.1.1.0) ranging in coarseness from mudstones (shales) to conglomerates and reaching nearly five kilometres thick in areas (e.g., Earle, 2002). On a regional scale, the Nanaimo Group alternates between the coarser-grained and finer-grained units and is generally eastward-dipping (e.g., Hamblin, 2015). Cathyl-Bickford (1992) divided the Nanaimo Group bedrock into 15 different units called members, after first dividing it into five formations, and it is these members I use for reference in this study.

In the study area between Fanny Bay and Royston, the most commonly mapped unit of the Nanaimo Group bedrock is the Willow Point Member, generally between 120 and 150 metres thick, consisting mainly of shale and siltstone, and minor sandstone (Cathyl-Bickford, 1992). Other important members in the study area include the Royston, Tsable, Browns, and Puntledge members, each composed of different proportions of shale, siltstone, sandstone, and conglomerate and ranging in thickness from 5 to 220 metres (Cathyl-Bickford, 1992). These units are shown in an example of a map by Cathyl-Bickford and Hoffman (1998) in Figure 2.1.1.1. Just south of the study area, between Nanoose Bay and Deep Bay, Nanaimo Group bedrock has been determined to be fractured (e.g., Benoit et al., 2015; Hamblin, 2015), while on the neighbouring Gulf Islands to the east, it is proposed that shale-dominated Nanaimo Group lithologies have greater fracture intensities than the coarser-grained lithologies (e.g., Lapcevic, Kenny & Wei, 2006). This suggests that the Nanaimo Group bedrock in the study area is also fractured to some degree. Although there was one outcrop of bedrock I observed between study sites, the weathered surface made it difficult to determine whether or not the bedrock was indeed fractured; it did, however, confirm the presence of bedding which provide natural planes for fractures to occur. This outcrop also confirmed the eastward-dipping nature of the Nanaimo Group.

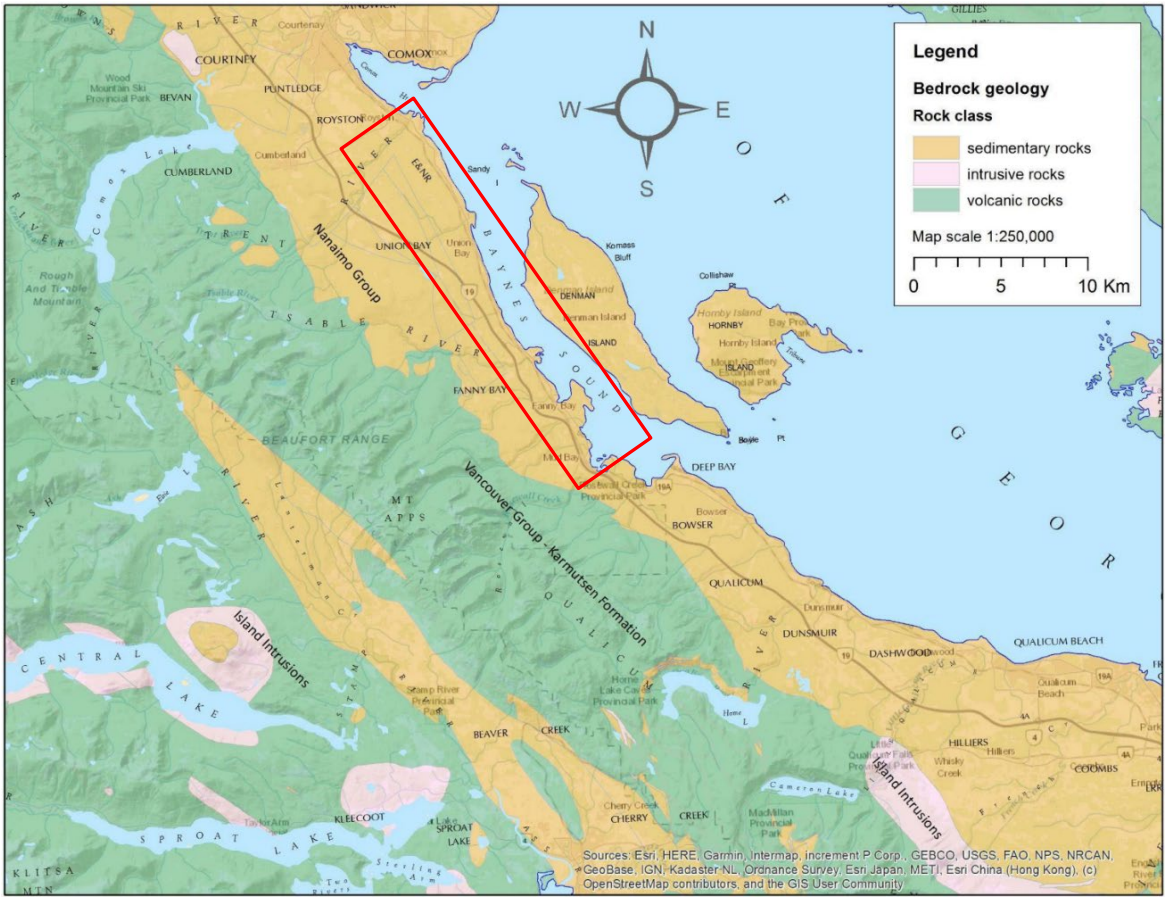

Figure 2.1.1.0. General bedrock geology mapped within the study area highlighted by the red box (modified from Pereversoff et al., 2022).

2.1.2. Regional Unconsolidated Sediments

Unconsolidated sediments that blanket Vancouver Island are the result of a complex depositional history including two periods of glaciation bounded by non-glacial intervals (Fig. 2.1.2.0). Seven lithostratigraphic units (Table 2.1.2.0) are identified and recognized in the Beaufort Watershed region, each distinguished by their lithologies, climatostratigraphies, depositional environments, and/or age. These materials can be over 100 metres thick on the coastal lowlands, but in many areas, they are commonly thinner due to the irregular bedrock topography underlying the region (e.g., Bednarski, 2015). While there have been no exposures found that demonstrate the stratigraphic relationship of all seven units together, numerous exposures to the south of the study area have been determined to fully relate all units to one another with respect to time, including the underlying bedrock (e.g., Bednarski, 2015). Fyles

(1960; 1963b) mapped the distribution of these sediments throughout the study area, as shown in an example map in Figure 2.1.2.1.

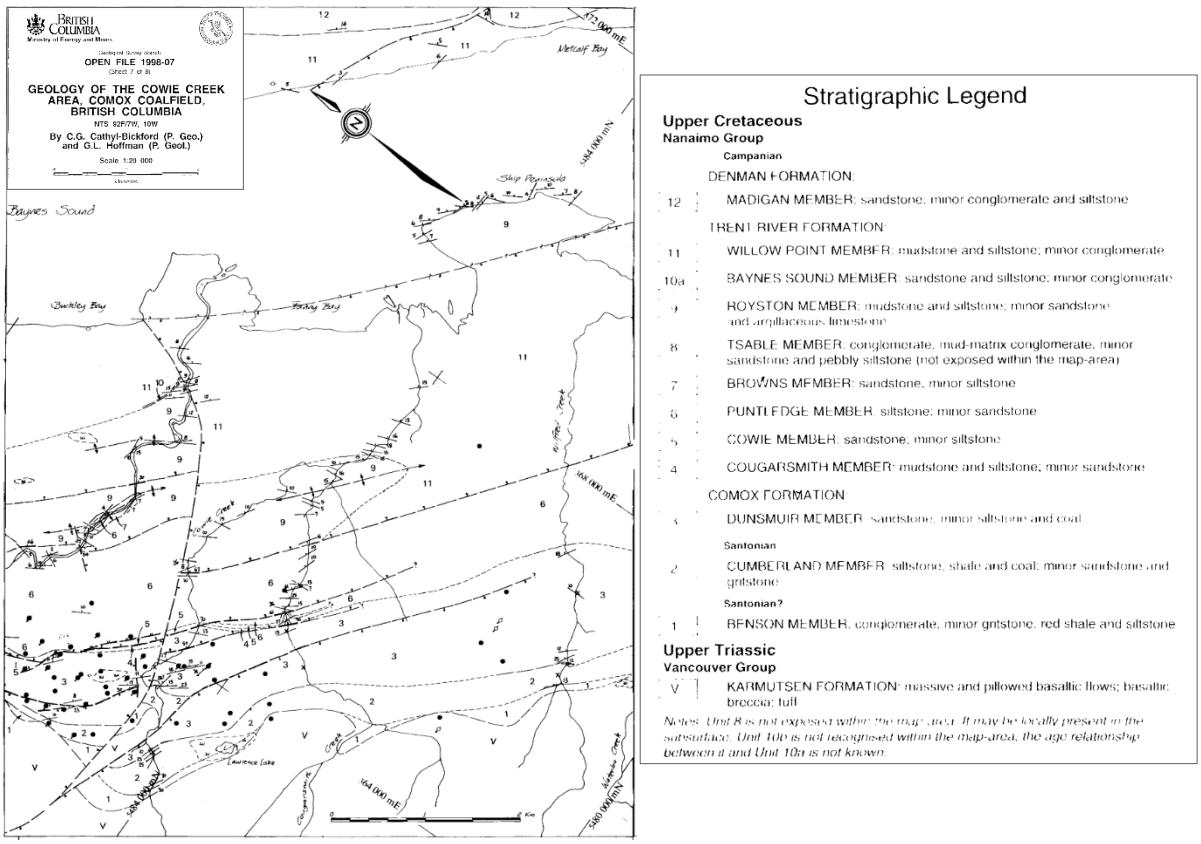

Figure 2.1.1.1. Example of a local bedrock geology map modified from Cathyl-Bickford and Hoffman (1998), showing part of the southern region of the study area (Fanny Bay).

The oldest units of unconsolidated material in the Beaufort Watershed region were deposited prior to, and during, the penultimate glaciation over 50 ka; these sediments are known as the Mapleguard Sediments and the Dashwood Drift and comprise outwash and glacial deposits, respectively (e.g., Bednarski, 2015; Benoit et al., 2015). The Mapleguard Sediments include minor gravel with bedded sand, silt, and clay in packages that most commonly are up to 10 metres thick but have been recorded as more than 20 metres thick in certain locations (e.g., Bednarski, 2015; Benoit et al., 2015). Stratigraphically higher, the Dashwood Drift consisting of clays, stoney silts, sands, gravels, and cobbles in a sequence of glaciofluvial, ice-contact, and (glacio-) marine sediments bounding a single till that is 3 to 9 metres thick (e.g., Bednarski, 2015). Overall, this unit is commonly observed to be no more than 10 metres thick (e.g., Benoit et al., 2015). Although mapped at the surface on eastern Vancouver Island and in the broader Beaufort Watershed region, these units are not observed in the study area in surficial sediments.

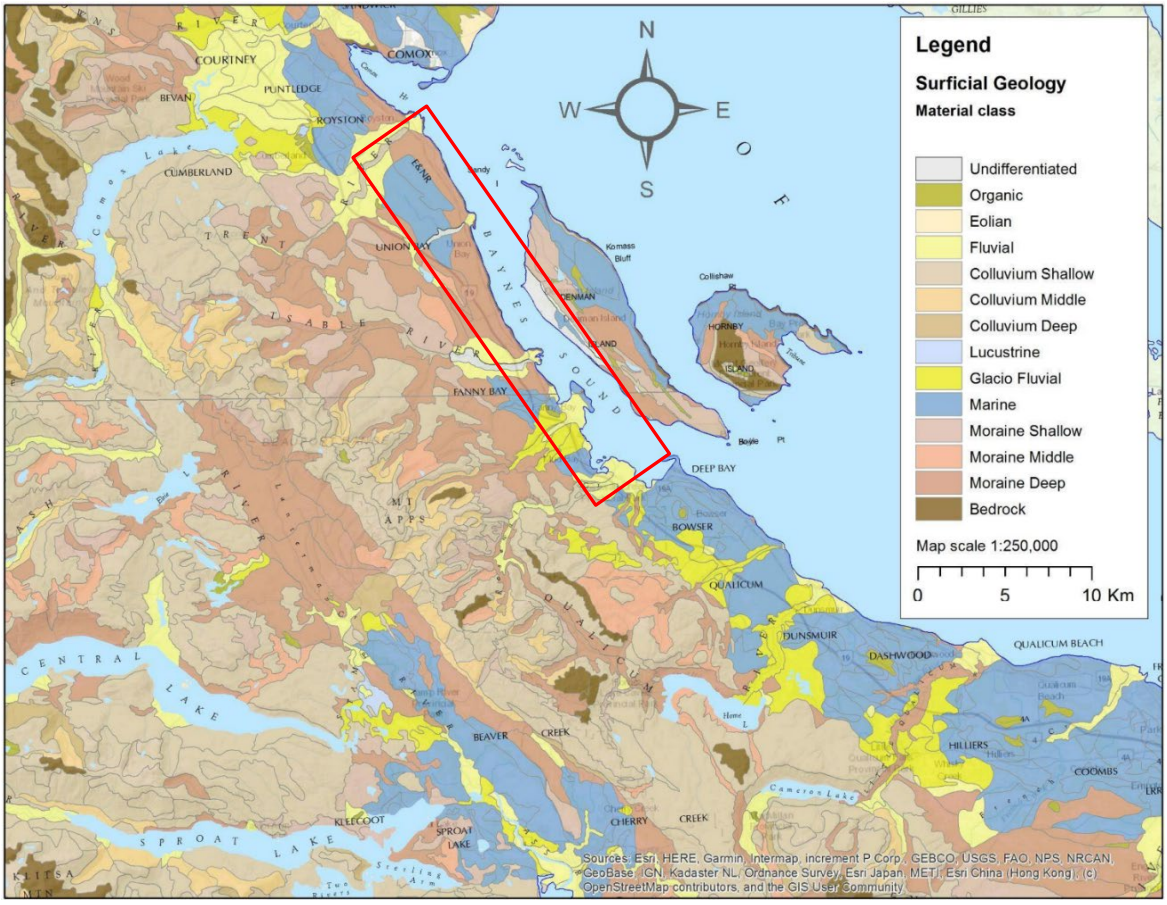

Figure 2.1.2.0. General surficial geology of the region; study area outlined in red (modified from Pereversoff et al., 2022).

After the penultimate glaciation, the Cowichan Head Formation was deposited between ~50 and 31 ka, during the Olympia nonglacial interval (e.g., Bednarski, 2015). It is divided into two sections, an upper and lower member, where the former is proposed to be estuarine and fluvial in nature, composed of sandy silt and gravel, and the latter is marine in nature with clayey silt and sand (Armstrong & Clague, 1977). Sediments of the Cowichan Head Formation can be up to 21 metres thick (e.g., Bednarski, 2015; Benoit et al., 2015) . Like the Mapleguard Sediments and Dashwood Drift, the Cowichan Head Formation has been mapped as surficial deposits in the general Beaufort Watershed region, but it has not been observed in the study area.

Table 2.1.2.0. Summary of the seven lithostratigraphic units present in the overall study region (modified from Bednarski, 2015). The colours are associated with the common lithologies in the lithostratigraphic units: light yellow = sand and gravel, grey = clay, light green = till, gold = sand, and brown = sedimentary bedrock. The Nanaimo Group could be any of the 15 members recognized by Cathyl-Bickford (1992). Yields of aquifers are predicted from the dominant lithologies according to Table 6 of Berardinucci and Ronneseth (2002). *Date from Earle (2019).

Radiocarbon Age	Stage/Substage	Climatostratigraphy	Lithostratigraphic Unit	Main Lithologies	Legend
ka BP ka cal BP	Holocene	Postglacial	Salish Sediments	sand and gravel; minor silt and clay	Yield of Aquifers in Study Area
10 11.6	Late-Wisconsinan	Postglacial	Capilano Sediments	gravel, sand, silt and clay	Higher Yield
13 15.6	Late-Wisconsinan	Fraser Glaciation	Vashon Drift	till	
18 21.8	Late-Wisconsinan	Fraser Glaciation	Quadra Sands	sand and gravel	Lower Yield
27.1 31.1	Mid-Wisconsinan	Olympia Nonglacial Interval	Cowichan Head Formation	NA	
40 43.6	Mid-Wisconsinan	Olympia Nonglacial Interval	Cowichan Head Formation	NA	Aquitard
>50 *beyond the range of radiocarbon dating*	Pre-Wisconsinan	Penultimate Glaciation	Dashwood Drift (including Mapleguard Sediments)	NA	
90-65 Ma*	Upper Cretaceous	NA	Nanaimo Group	shale, siltstone, sandstone; minor conglomerate	

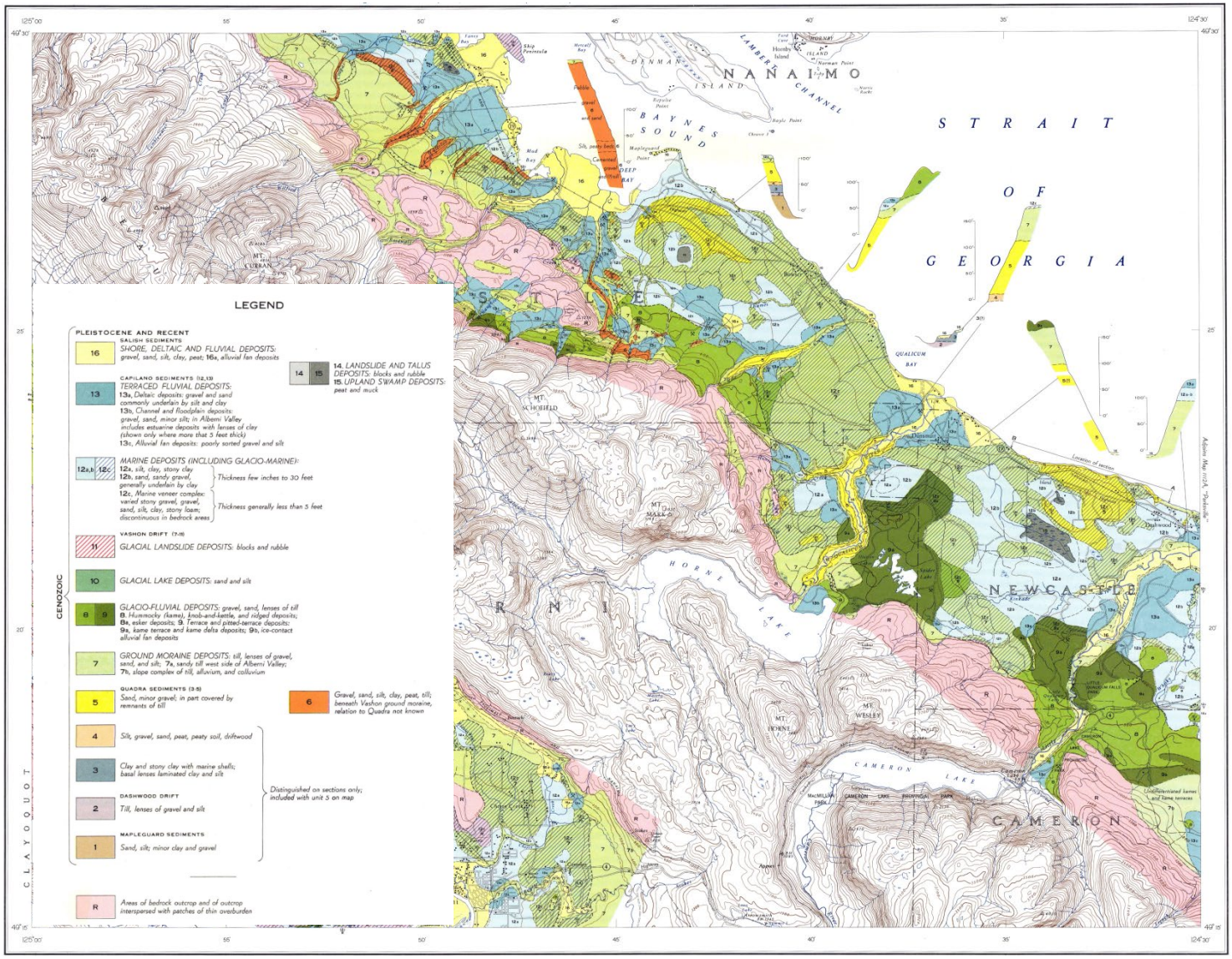

Figure 2.1.2.1. Example of a local surficial geology map modified from Fyles (1963b), showing the southern most part of the study area as well as further south along the east coast of Vancouver Island.

During the transition from a non-glacial interval to a glacial interval, the advancement of glaciers formed a unit of sediment referred to as the Quadra Sand. These deposits are interpreted to have formed in the outwash plains of the advancing glaciers during the onset of the Fraser Glaciation approximately 25,000 years ago (e.g., Bednarski, 2015; Benoit et al., 2015; Pike et al., 2010). Where the Quadra Sand unit exceeds 75 metres in thickness, it comprises minor silt and gravel among well-sorted sand (e.g., Bednarski, 2015; Benoit et al., 2015). An unnamed sediment package that may be synchronous with the Quadra Sand unit is found at the surface in numerous locations throughout the study area, and is composed of gravel, sand, silt, clay, and till, depicted on the map as orange (Fig. 2.1.2.1) by Fyles (1963b). Sediments of the Quadra Sand are mapped near the surface just south of the study area between the communities of Bowser and Deep Bay (Fig. 2.1.2.1) and are therefore relevant to this study, along with the supposedly contemporaneous unit according to Fyles (1960; 1963a).

Stratigraphically above the Quadra Sand is the Vashon Drift. This unit coincides with the Fraser Glaciation that occurred between ~25 and 10 ka (e.g., Pike et al., 2010), and contains tills, including in the form of moraines, and various ice-proximal deposits including eskers, kame terraces, and ice-contact fans and deltas (e.g., Bednarski, 2015; Benoit et al., 2015). In the lowlands, the till is generally sandier as opposed to in valleys where it is more clay-rich, while the ice-proximal deposits are dominantly sand and gravel. The thickness of this unit is commonly observed at a maximum of 30 metres; however, in locations where the underlying Quadra Sand has been eroded significantly, Vashon Drift has been seen to approach 60 metres in thickness (e.g., Bednarski, 2015; Benoit et al., 2015). When the ice sheet began to thin, sea level reached an elevation of ~150 metres or more above its present level (e.g., Bednarski, 2015; Benoit et al., 2015). In particular, distribution of the till in this stratigraphic unit is widespread throughout the study area (Fig. 2.1.2.1), making the Vashon Drift essential to this study.

Capilano Sediments represent the transition out of the Fraser Glaciation similar to how the Quadra Sand represents the transition into the glacial interval. Capilano Sediments were deposited during the early stages of deglaciation (~15 ka; e.g., Pike et al., 2010) as glaciofluvial outwash sands and gravels but also as glaciomarine and marine sediments (clays, silts, sands, and gravels) in isostatically depressed areas, until isostatic rebound caused relative sea level to fall by ~135 metres leading to fluvial and deltaic deposits becoming more dominant (e.g., Bednarski, 2015; Benoit et al., 2015). The typical maximum thickness of Capilano Sediments is ~25 metres;

however, they are often much thinner and appear as a marine veneer over Vashon Drift, or, in some cases, Quadra Sand (e.g., Bednarski, 2015; Benoit et al., 2015). These veneers are mapped at the surface in multiple locations throughout the study area, usually adjacent to the surficial deposits of deltaic and fluvial Capilano Sediments (Fig. 2.1.2.1).

Most recently, during the Holocene epoch (since ~11 ka), Salish Sediments were deposited. Stratigraphically the top unit, Salish Sediments are distinguished, albeit imperfectly, from the preceding Capilano Sediments by their elevation relative to present day base levels (sea, lake, and river), generally occurring within the first 5 metres above base level (e.g., Bednarski, 2015; Benoit et al., 2015). Since sea level has been relatively stable at present day base level for the last ~6 thousand years (e.g., Bednarski, 2015; Benoit et al., 2015), this differentiating factor is not without uncertainty. Salish Sediments are composed of gravel, sand, silt, and clay in shore and deltaic deposits (Fyles, 1960; Fyles, 1963a; Fyles, 1963b); however, fluvial deposits are the most common (e.g., Bednarski, 2015), making the Salish Sediments most typically a coarse-textured, permeable unit. Figure 2.1.2.1 shows the prominent occurrence of these sediments in the study area, making them a main focus of this research.

2.1.3. Regional Aquifers and Aquitards

Each of the previously described stratigraphic units, including the Nanaimo Group bedrock, contributes to the hydrogeology of the Beaufort Watershed study area, whether that be acting as an aquifer or an aquitard. Typically, geological materials containing high proportions of fine grain sizes, such as shale, siltstone, clay, and till, behave as aquitards; however, fine-grained bedrock such as shale and siltstone can alternatively behave as an aquifer if fractured sufficiently to be permeable for water flow (e.g., Lapcevic, Kenny & Wei, 2006). Fractures in bedrock are considered to create secondary porosity that influence the permeability of a rock. Aquifers can be either unconsolidated sand and/or gravel or bedrock that is porous and/or fractured, generally yielding higher and lower quantities of water, respectively (Berardinucci & Ronneseth, 2002; Moore et al., 2002). The sorting of the unconsolidated sands and gravels may influence the yield of the aquifer, where silty sand and gravel may produce moderate instead of the high yields of better sorted, clean sand and gravel (Berardinucci & Ronneseth, 2002). Aquifers can also be classified as unconfined or confined to varying degrees, where confined aquifers are overlain by aquitards and unconfined aquifers are not (Fig. 2.1.3.0).

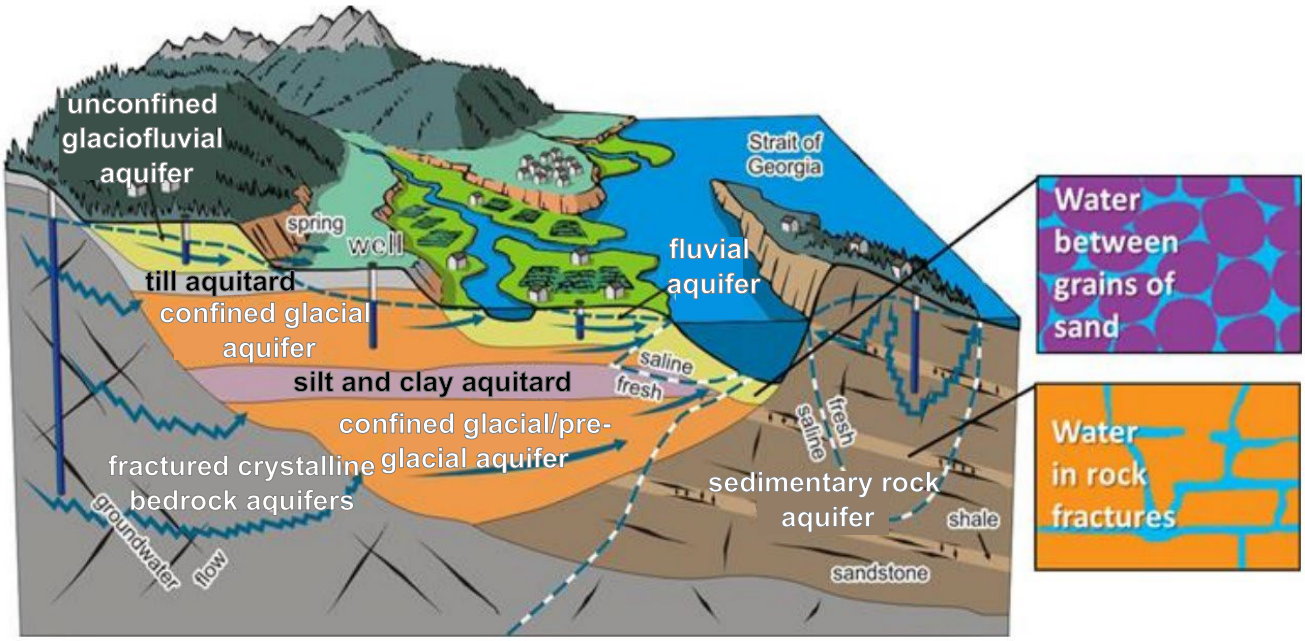

Figure 2.1.3.0. Illustration of the typical materials of aquifers and aquitards in British Columbia, as well as insets showing the types of porosity in unconsolidated versus consolidated materials (modified from Barroso, Ormond & Lepcevic, 2016).

Aquitards in the study area include deposits of both the Dashwood and Vashon Drifts (tills) as well as the Cowichan Head Formation and Capilano Sediments (marine clays). It is important to note that the heterogeneous nature of these deposits can result in lenses of sand and/or gravel that may form small, local sources of groundwater. Although much of the Nanaimo Group bedrock is shale and siltstone, these lithologies are not considered aquitards in this study since they have been observed to be well fractured in neighbouring areas (e.g., Benoit et al., 2015; Hamblin, 2015; Lapcevic, Kenny & Wei, 2006) and are expected to also be fractured in the study region. It is from these fractures, saturated in groundwater, that wells and springs may yield their water. For this reason, all Nanaimo Group bedrock units in the study area are regarded as aquifer materials, presumed to have relatively low yields, as suggested by Berardinucci and Ronneseth (2002). Other regional stratigraphic units have lithologies suitable for high yield aquifers including the Cowichan Head Formation, Quadra Sand, Capilano and Salish Sediments. Similar to the local sources of groundwater within aquitards, the marine clays of the Cowichan Head Formation and the Capilano Sediments may form lenses that behave as local aquitards, partially confining underlying aquifers. While the Quadra Sand is the most exploited aquifer on the east coast of Vancouver Island (e.g., Bednarski, 2015), Nanaimo Group aquifers are commonly

utilized in the absence of Quadra Sand (e.g., Benoit et al., 2015). The hydrogeological classification of each stratigraphic unit in the region is shown in Table 2.1.2.0.

2.1.4. Previously Mapped Aquifers in the Beaufort Watershed

In the Beaufort Watershed study area, there are currently four aquifers mapped: aquifer numbers 411, 415, 419, and 414 (Fig. 1.2.1; GWELLS: https://apps.nrs.gov.bc.ca/gwells/aquifers). Of these four, just one is an aquifer of bedrock material. Aquifer number 411 occurs in the northern part of the study area, between Union Bay and Royston (GWELLS, https://apps.nrs.gov.bc.ca/gwells/aquifers/411). It comprises of fractured sedimentary bedrock of the Nanaimo Group lithostratigraphic unit. Extending in area beyond the boundaries of this study (731.9 km^2), the provincial government reports this aquifer to be low in vulnerability to contamination, with a low median well yield (~2.5 GPM) and a median water depth of 5.94 metres below ground surface (ENV, 2022a). In the central part of the study area, aquifer number 415 is located around the mouth of Tsable River covering just 0.8 km^2 (GWELLS, https://apps.nrs.gov.bc.ca/gwells/aquifers/415). As a sand and gravel aquifer thought to correspond with Salish Sediments, it is unconfined and considered highly vulnerable to contamination. Lacking data to estimate a median well yield or median water depth, the aquifer is proposed to have high productivity, directly related to well yield, and have a seasonally variable water level that approaches a maximum of ~5 metres below ground surface between August and September (ENV, 2022b). At Ships Point peninsula in Fanny Bay, aquifer number 419 is indicated as a Quadra Sand, sand and gravel aquifer, 4.3 km^2 in area (GWELLS, https://apps.nrs.gov.bc.ca/gwells/aquifers/419). The characteristics of this aquifer are currently much better understood than the other three in the study area, as hydraulic properties of the aquifer are known, quantifying how the aquifer responds to pumping (ENV, 2022c). The median well yield is ~40 GPM, and the median water depth is 2.44 metres below the ground surface (ENV, 2022c). This aquifer is reported to be partially confined and moderately vulnerable to contamination. Aquifer number 414 is a sand and gravel aquifer, located at the furthest southern extent of the study area at the mouth of Rosewall Creek, and is said to be correlated to the Salish Sediments lithostratigraphic unit (GWELLS, https://apps.nrs.gov.bc.ca/gwells/aquifers/414). This aquifer is mapped to be 1.5 km^2 and has insufficient data for estimating the median well yield but is determined to have high productivity which relates to well yield (ENV, 2022d). The provincial government has deemed this aquifer to be highly vulnerable to contamination due to its

unconfined nature (ENV, 2022d). The boundaries of each sand and gravel aquifer were delineated using surficial geology boundaries, groundwater development areas, and air photos. Table 2.1.4 summarizes the characteristics of the previously mapped aquifers.

Tables 2.1.4. Summary of characteristics of previously mapped aquifers in the study area (GWELLS: https://apps.nrs.gov.bc.ca/gwells/aquifers).

Aquifer #	**411**	**414**	**415**	**419**
Material	Bedrock	Sand & Gravel	Sand & Gravel	Sand & Gravel
Lithostratigraphic Unit	Nanaimo Group	Salish Sediments	Salish Sediments	Quadra Sand
Area (km^2)	731.9	1.5	0.8	4.3
Confinement	Majorly Confined	Unconfined	Unconfined	Partially Confined
Vulnerability	Low	High	High	Moderate
Median Well Yield (GPM)	~2.5	-	-	~40
Median Water Depth (m)	5.94	-	-	2.44

2.2. Saltwater Intrusion

Saltwater intrusion, or seawater intrusion, is the phenomenon that occurs when the groundwater gradient favours the flow of seawater into a coastal aquifer due to drawdown of the water table or simply groundwater extraction (Fig. 2.2.0; e.g., Freeze & Cherry, 1979). This poses an issue for the population that relies on the coastal aquifer for their freshwater, as saltwater intrusion can result in non-potable water. In the study area, community members in Fanny Bay on the Ships Point peninsula are particularly interested in knowing whether or not they are inducing saltwater intrusion and degrading the quality of their freshwater. According to iMapBC, an interactive mapping website from the Government of British Columbia (https://maps.gov.bc.ca/ess/hm/imap4m/), classification of the risk of saltwater intrusion is high

on the southeast side of the Ships Point peninsula (Fig. 2.2.1), suggesting reason for investigation.

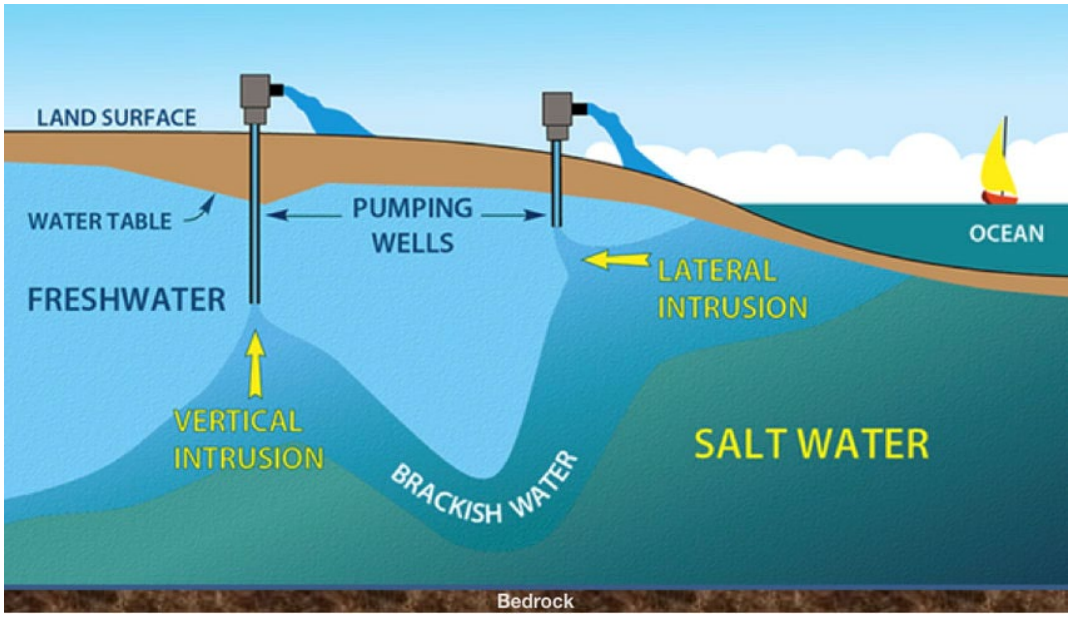

Figure 2.2.0. Schematic showing lateral and vertical saltwater intrusion induced by pumping wells (from Buzzanga, 2017).

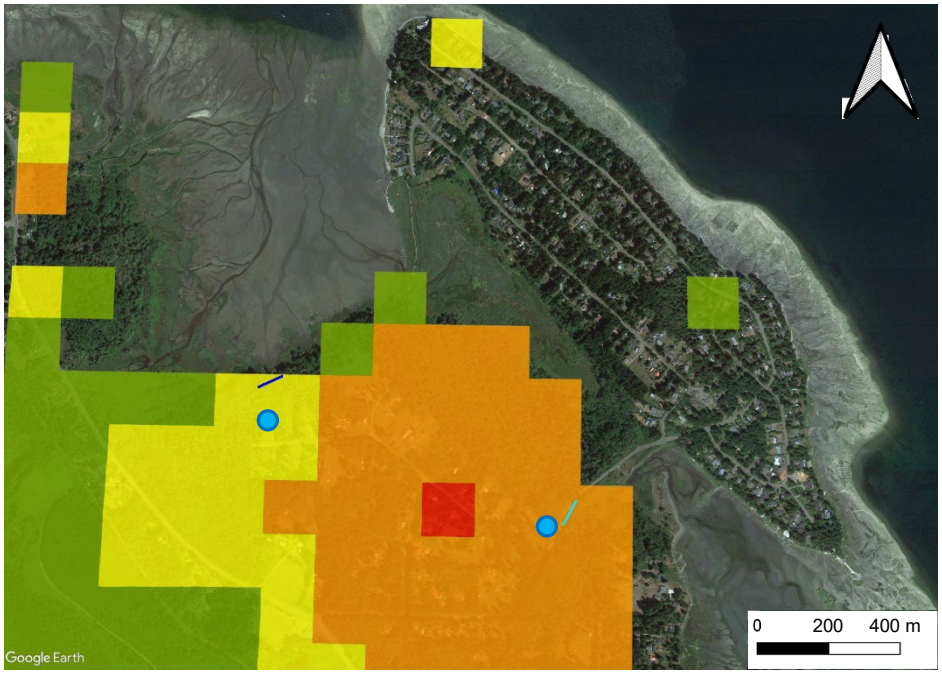

Figure 2.2.1. Aquifer vulnerability to saltwater intrusion at Ships Point Peninsula. Coloured contours indicate levels of risk: red = high, orange = moderately high, yellow = moderate, and green = moderately low (data from Province of B.C., 2022). On either side of the peninsula, blue lines show locations of resistivity profiles for this study, and blue dots show nearby wells (GWELLS, https://apps.nrs.gov.bc.ca/gwells/).

2.3. Resistivity

Conductivity is an intrinsic electrical property that quantitatively describes how well a material can transmit an electric current. The inverse of conductivity is a property called resistivity that defines how effectively a material opposes the flow of an electric current. In Ohm's Law (Equation 2.3.1), voltage, *V*, is equal to the product of the current, *I*, and the resistance, *R*. Voltage is an electric pressure that forces movement of charged electrons and allows for work to be done; this property is measured in volts [V]. Current, in this case, is defined as the rate of flow of an electric charge and is measured in amperes [A] while resistance is defined as the degree to which a material or medium can oppose the flow of a current and is measured in Ohm's [Ω]. Resistivity (ρ), or apparent resistivity (ρ_a), is related to Ohm's Law (Equation 2.3.1), where the change in resistance of a material (δR) across a given unit volume (defined by its cross-sectional area (A) and length (L)), provides a measurement of resistivity (Equation 2.3.2), most often calculated in ohm-metres or Ωm. Resistivity is an intrinsic property (similar to density or magnetic susceptibility), being independent of material volume (e.g., Freeze & Cherry, 1979), and relies heavily on the composition and structure of the material.

Equation 2.3.1.

$$V = IR$$

$$V = \text{voltage [V]}$$
$$I = \text{current [A]}$$
$$R = \text{resistance [}\Omega\text{]}$$

Equation 2.3.2.

$$\rho_a = \delta R \frac{\delta A}{\delta L} = \frac{\delta V}{I}\frac{\delta A}{\delta L}$$

$$\rho_a = \text{apparent resistivity [}\Omega\text{m]}$$
$$\delta R = \text{change in resistance [}\Omega\text{]} = \frac{\delta V}{I} = \frac{\text{potential difference [V]}}{\text{current [A]}}$$
$$\frac{\delta A}{\delta L} = \frac{\text{cross} - \text{sectional area [m}^2\text{]}}{\text{length [m]}} = \text{unit volume}$$

Geological materials exhibit great ranges in resistivities, with massive sulfides represented by values as low as 10^{-2} and a few other geological materials reaching values as high as 10^5 (Palacky, 1988). Resistivities of geological materials are therefore scaled logarithmically when

displayed graphically. Electrical properties of geological materials are dominantly controlled by electrolytic conduction which is governed by the salinity of saturating porewater as well as the porosity and permeability of the saturated material (e.g., Burger, Sheehan & Jones, 2006; Freeze & Cherry, 1988). The variability of these factors across the scope of geological materials, and within individual materials, provides an explanation for the large range in resistivities commonly observed in typical geological materials (Fig. 2.3.0). While electronic conduction also influences the resistivity of geological materials such as metals, it is less significant in the context of hydrogeology.

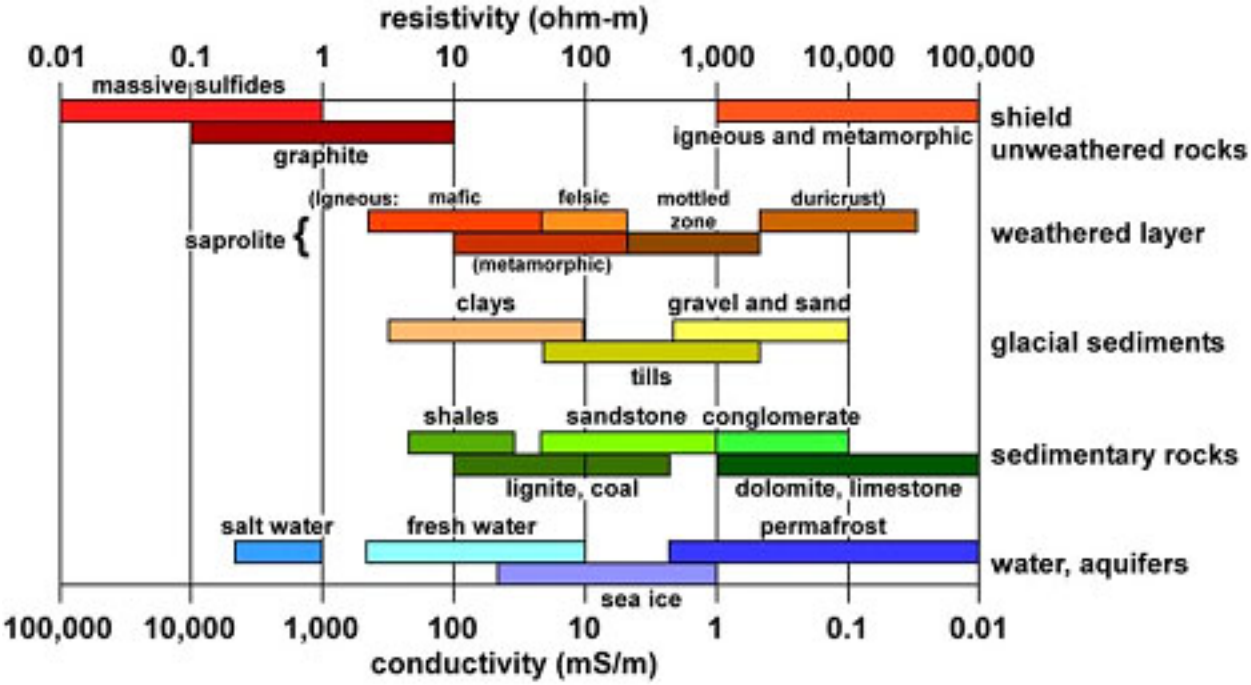

Figure 2.3.0. Ranges of resistivity characteristic of common geological and hydrological materials (Palacky, 1988).

Given that resistivity is material dependent, measurements of the property can be used to infer the geological materials being represented. However, this method is subject to significant uncertainty, as the ranges of resistivity characteristic of each geological material typically demonstrate overlap with the ranges of other materials (Fig. 2.3.0). With respect to the study area, where sedimentary rocks and glacial sediments comprise the local geology, there is partial overlap of the potential resistivity ranges expected within both the unconsolidated and bedrock lithologies, as well as between the two. In this situation, any sedimentary rock type could be interpreted as a type of glacial sediment, while most glacial sediments could be interpreted as sedimentary rock; for this reason, a proficient understanding of the local geology and moreover,

groundtruthing data, such as well logs, are key to determining appropriate interpretations of resistivity measurements.

Pereversoff et al. (2022) conducted a study that statistically summarized resistivities for several lithostratigraphic units observed in the same study area as this research. Salish Sediments were determined to have a median resistivity of 1730 Ωm, Capilano Sediments: 454 Ωm, Vashon Till: 96 Ωm, Quadra Sand: 951 Ωm, and shale of the Willow Point member of the Nanaimo Group: 28 Ωm. The ranges of resistivity resolved for each of these units are shown in Table 2.3.0.

Table 2.3.0. Typical resistivities of several regional lithostratigraphic units (modified from Pereversoff et al., 2022).

Lithostratigraphic Unit	Median resistivity value (Ωm)	Approximate range (Ωm)
Salish Sediments	1730	440-7730
Capilano Sediments	454	350-525
Vashon Drift	96	5-265
Quadra Sand	951	735-1250
Willow Point Member	28	18-85

3. Methods

3.1. Electrical Resistivity Surveying

Electrical resistivity surveying is a method that remotely senses the resistivity of materials below ground, allowing for the types of materials to be inferred. Geoelectrical methods, including electrical resistivity surveying, have dominantly been applied to hydrogeology research, as opposed to other geophysical techniques, due to their ability to address a wide range of problems, including delineating groundwater resources (e.g., Moncur, 1974; Lake, 1978), evaluating groundwater salinity (e.g., Asfahani, 2007; Moulds et al., 2023), and providing

valuable information that can be used to quantify hydraulic properties of aquifers (e.g., Kosinski & Kelly, 1981; Ikard et al., 2023).

In electrical resistivity surveys, four electrodes are inserted into the ground and are connected via cables to an instrument called a resistivity meter. This instrument transmits a low-frequency, alternating, electric current (I [amperes]) into the subsurface between two current electrodes designated A and B, and measures the difference in electric potential (ΔV [volts]) at the surface between two potential electrodes labelled M and N. The resistivity meter outputs the ratio of potential difference to injected current ($\Delta V / I$; resistance; Equation 3.1) as well as the calculated apparent resistivity (ρ_a [Ωm]). Apparent resistivity is a weighted average of the subsurface resistivities encountered by the transmitted current, and is calculated using Equation 3.1, where K, the geometric factor, is controlled by the relative positions of electrodes. These electrode configurations are referred to as electrode arrays, of which there are three common types used in electrical resistivity surveying.

Equation 3.1.

$$\rho_a = 2\pi \frac{\Delta V}{I} K$$

$$\rho_a = \text{apparent resistivity [}\Omega\text{m]}$$

$$2\pi = \text{constant}$$

$$\frac{\Delta V}{I} = \frac{\text{potential difference [V]}}{\text{current [A]}} = \text{resistance [}\Omega\text{]}$$

$$K = \text{geometric factor [m]}$$

3.1.1. Wenner Array

In the frequently used Wenner array, electrodes A, B, M, and N, are uniformly spaced around a central point, with the current electrodes on the outside, and the potential electrodes on the inside (Fig. 3.1.1). The equal spacing between each electrode is commonly denoted as ‘a’ and is incorporated into the geometric factor, K, from equation 3.1, making a new equation for apparent resistivity specific to Wenner arrays (Equation 3.1.1). The calculated apparent resistivity is associated with the materials directly beneath the centre point of the array. Wenner arrays have good vertical resolution and can be used to analyze the vertical and/or lateral variation in apparent resistivity of the subsurface. In the case of a vertical resistivity profile, all four electrodes are moved outwards, remaining centred about the same point, and maintaining the

equal spacing between adjacent electrodes. For lateral resistivity profiles, the spacing between electrodes stays constant, but the centre point moves laterally along the survey line requiring all four electrodes to be moved, while maintaining the spacing of 'a'. To obtain both lateral and vertical variation in apparent resistivity, producing a two-dimensional (2D) profile, a combination of the adjustments described above is employed. Conducting surveys with a Wenner array can be quite labour intensive since all four electrodes need to be shifted for each successive measurement.

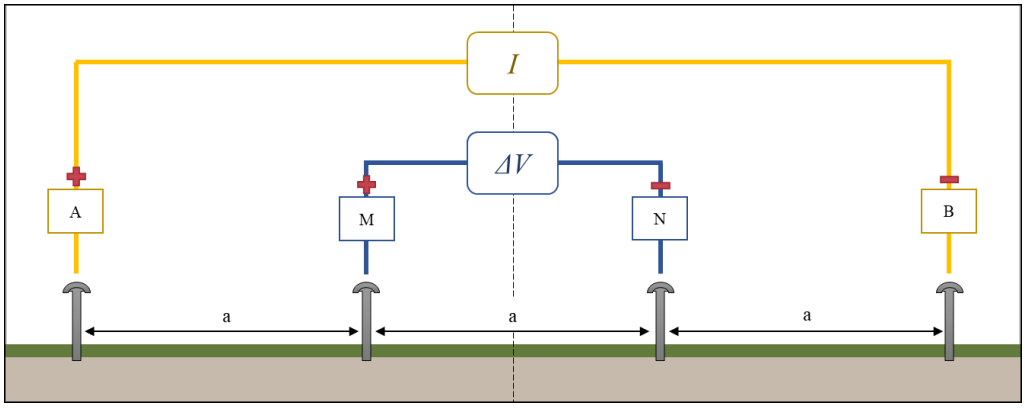

Figure 3.1.1. Schematic of a Wenner array. Current electrodes are labelled A and B and are connected by I, indicating the distance across which the injected current is passed. Potential electrodes are labelled M and N and are connected by ΔV, indicating the distance across which the potential difference is measured. The addition and subtraction symbols differentiate between the positive and negative terminals, respectively, in each electrode pair. Spacing 'a' is shown between adjacent electrodes.

Equation 3.1.1.

$$\rho_a = 2\pi \frac{\Delta V}{I} a$$

$$\rho_a = \text{apparent resistivity } [\Omega\text{m}]$$

$$2\pi = \text{constant}$$

$$\frac{\Delta V}{I} = \frac{\text{potential difference [V]}}{\text{current [A]}} = \text{resistance } [\Omega]$$

$$a = \text{electrode spacing [m]}$$

3.1.2. Schlumberger Array

The Schlumberger array has a similar arrangement of electrodes to the Wenner array in that the four electrodes are spaced about a centre point with the current electrodes, A and B, on the outside and the potential electrodes, M and N, on the inside. The difference between the Wenner and Schlumberger arrays are the spacings between electrodes. In the Schlumberger array, the

distance between each of the outer current electrodes (A and B) and the centre point is denoted as ‘ab’ and the distance between each of the potential electrodes (M and N) and the centre point is denoted as ‘mn’ (Fig. 3.1.2), producing an equation for apparent resistivity, specific to Schlumberger arrays, where the geometric factor, *K*, in Equation 3.1 is replaced by an expression relating to ‘ab’ and ‘mn’ (Equation 3.1.2). Like the Wenner array, the calculated apparent resistivity is representative of the material beneath the centre point. Schlumberger arrays are said to sense to slightly greater depths and have better resolution than Wenner arrays when comparing arrays with equivalent distances between current electrodes (e.g., Zohdy, Eaton & Mabey, 1974; Adeyemo, Ojo & Raheem, 2017). This may be attributed to the better distribution of relatively high currents beneath the Schlumberger array versus the Wenner array, where more area covered by higher currents results in better quality measurements (e.g., Reynolds, 2011). Analysis of lateral and/or vertical variation in resistivity of the subsurface can be achieved using this array. For lateral resistivity profiles, the spacing between electrodes stays constant where the spacing ‘ab’ is set to be much greater than the spacing of ‘mn’. The potential electrode pair can be moved independently to achieve a traverse, while leaving the outer electrodes in place. In the case of a vertical resistivity profile, current and potential electrodes are moved at separate times. To increase the depth of the sounding, current electrodes, A and B, are simultaneously moved outwards at equal distances from the centre, increasing the distance ‘ab’. This process is repeated until the spacing ‘ab’ exceeds five times the length of ‘mn’, at which time, to continue increasing the depth of the sounding, the potential electrodes are moved outwards from centre. Like electrodes A and B, electrodes M and N are moved outwards from centre at equal distances to maintain identical ‘mn’ spacing for each electrode. To obtain a 2D profile, a combination of the adjustments described above is employed. The Schlumberger array is less labour intensive than the Wenner array since there is less shifting of electrodes required to complete a survey.

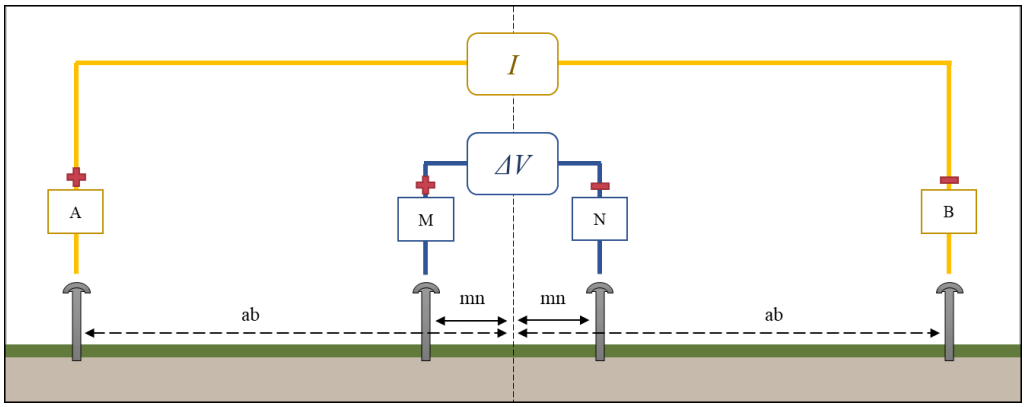

Figure 3.1.2. Schematic of a Schlumberger array. Current electrodes are labelled A and B and are connected by I, indicating the distance across which the injected current is passed. Potential electrodes are labelled M and N and are connected by ΔV, indicating the distance across which the potential difference is measured. The addition and subtraction symbols differentiate the positive and negative terminals, respectively, in each electrode pair. Spacings 'ab' and 'mn' are shown between electrodes and centre.

Equation 3.1.2.

$$\rho_a = \pi \frac{\Delta V}{I} \frac{(ab^2 - mn^2)}{2mn}$$

$$\rho_a = \text{apparent resistivity } [\Omega\text{m}]$$

$$\pi = \text{constant}$$

$$\frac{\Delta V}{I} = \frac{\text{potential difference [V]}}{\text{current [A]}} = \text{resistance } [\Omega]$$

$$ab = \text{distance between survey centre and current electrode [m]}$$

$$mn = \text{distance between survey centre and potential electrode [m]}$$

3.1.3. Dipole-Dipole Array

Unlike the previous two electrode arrays, the dipole-dipole array does not arrange the four electrodes over a centre point in the same way. In this array, the two current electrodes are placed adjacent to each other, spaced apart a distance equal to that between the two adjacent potential electrodes. The space between electrodes A and B, and M and N is denoted as 'a', while the distance between the two pairs of electrodes (AB and MN) is denoted as 'na', where 'n' is a multiplication factor of 'a' (Fig. 3.1.3). The general equation for apparent resistivity (Equation 3.1) can then be adjusted to represent the spacings 'a' and 'na', replacing the geometric factor, *K*, to produce Equation 3.1.3. The apparent resistivity calculation is representative of the material beneath the centre of the array. Vertical resolution of the dipole-

dipole array is relatively poor since the highest currents are focused at shallow depths beneath the two pairs of electrodes, and only a small fraction of the current reaches to greater depths (e.g., Reynolds, 2011). It does, however, have decent lateral resolution. For this reason, the dipole-dipole array is preferentially used to obtain lateral and 2D variation in apparent resistivity. Lateral apparent resistivity measurements are collected by shifting all four electrodes along the survey line simultaneously, keeping the spacings of 'a' and 'na' constant. To produce the 2D profile, essentially adding depth to the lateral measurements, shifting electrodes is done in a similar process however, the spacings 'a' and 'na' vary throughout the survey to probe different depths (Fig. 3.1.3.1).

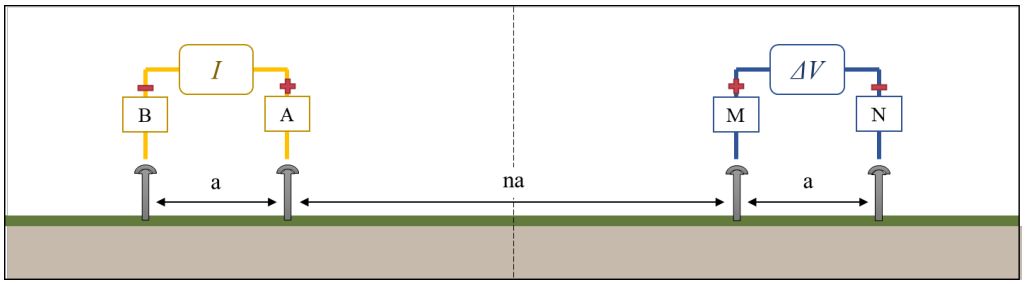

Figure 3.1.3. Schematic of a Dipole-Dipole array. Current electrodes are labelled A and B and are connected by *I*, indicating the distance across which the injected current is passed. Potential electrodes are labelled M and N and are connected by ΔV, indicating the distance across which the potential difference is measured. The addition and subtraction symbols differentiate the positive and negative terminals, respectively, in each electrode pair. Spacings 'a' and 'na' are shown between adjacent electrodes and electrode pairs.

Equation 3.1.3.

$$\rho_a = \pi \frac{\Delta V}{I} n(n+1)(n+2)a$$

$$\rho_a = \text{apparent resistivity } [\Omega\text{m}]$$

$$\pi = \text{constant}$$

$$\frac{\Delta V}{I} = \frac{\text{potential difference [V]}}{\text{current [A]}} = \text{resistance } [\Omega]$$

$$n = \text{multiplication factor}$$

$$a = \text{distance between adjacent electrodes [m]}$$

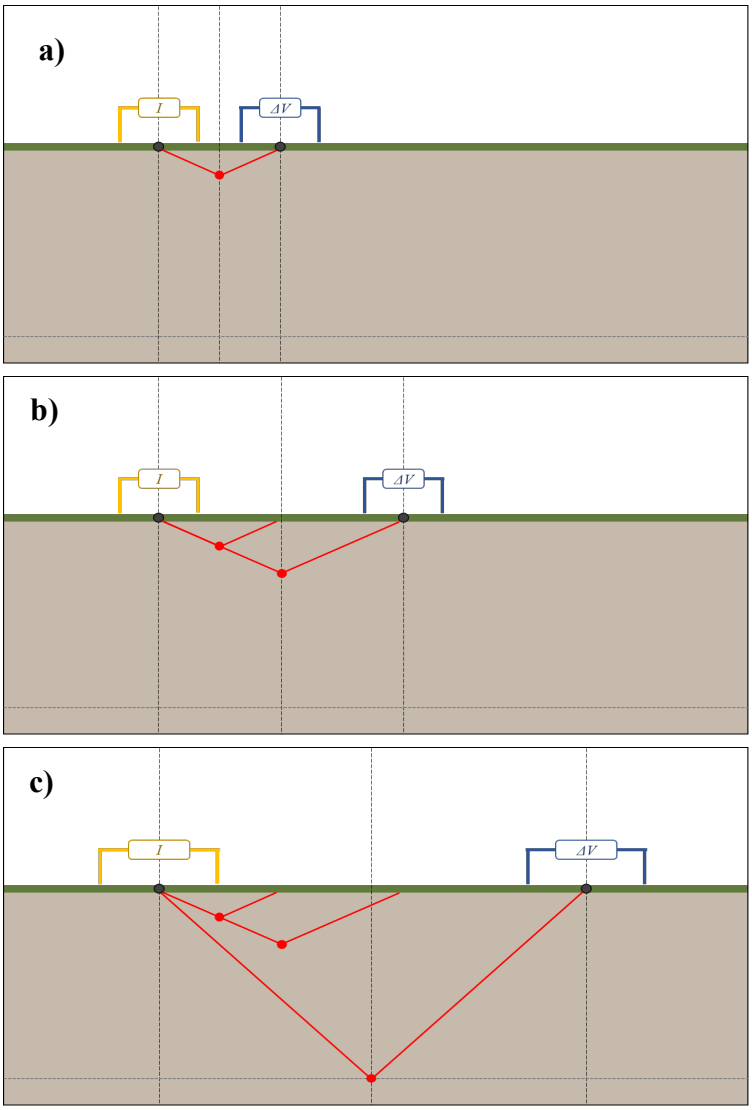

Figure 3.1.3.1. Series of schematics showing progressive measurements collected for a dipole-dipole array, 2D profile. a) Close spacing for 'a' and 'na'. b) Same spacing for 'a', increased 'na'. c) Increased spacings of both 'a' and 'na'. Red dots show points of data measurement. Note: the order of these panels is arbitrary.

3.2. Survey Dates and Locations

The design of the study was largely decided by the BWS, as they chose the locations where surveys were conducted, and organized the schedule of the data collection. The surveys in this study all took place during the week of July 11, 2023. Figures 3.2.0 and 3.2.1 show the locations of the surveys conducted in this study, while Table 3.2 summarizes the surveys by location/name, control well (well tag number(s); WTN), experiment type, and date completed.

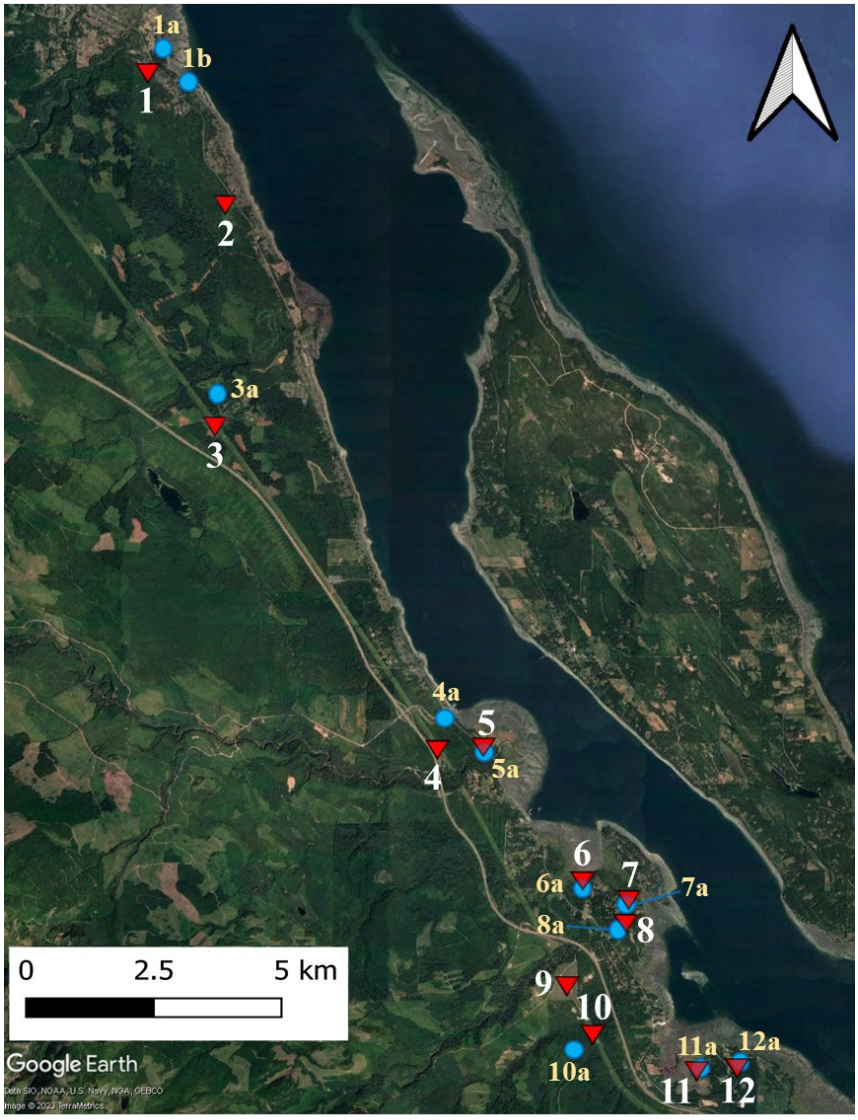

Figure 3.2.0. Locations of resistivity surveys (red triangles; white text) and control wells (blue circles; light yellow text). Sites are labelled 1-12, corresponding to the subsections in section 4.0, in which the results and interpretations of each site are described. The numbering system for both the surveys and controls wells are shown in Table 3.2. Control well locations from GWELLS (https://apps.nrs.gov.bc.ca/gwells/).

Figure 3.2.1. Locations of Fanny Bay and Ships Point ERT surveys (red line = Fanny Bay; yellow line = Ships Point) and control wells (blue dots). The numbers correspond to the locations of the same surveys in Figure 3.2.0. White numbers correlate to the subsections in section 4.0 for each site, where the results and interpretations are described. Control wells corresponding to each site are labelled in light yellow. The numbering system for both the surveys and controls wells are shown in Table 3.2. Control well locations from GWELLS (https://apps.nrs.gov.bc.ca/gwells/).

3.3. Vertical Electrical Sounding (VES)

3.3.1. Theory of VES

A vertical electrical sounding (VES) is a type of electrical resistivity survey designed to evaluate the variations of resistivity with depth, in one dimension (1D). In this study, each of the VES surveys were conducted with a straight-line, Schlumberger array, providing higher resolution data in a less labour-intensive electrode array than Wenner (e.g., Adeyemo, Ojo & Raheem, 2017; Haq et al., 2022), the other common array type for VES surveys. To achieve a profile of apparent resistivity over increasingly greater depths, the spacings between electrodes were successively increased about a fixed centre point with each measurement following the technique explained in section 3.1.2 for a vertical resistivity profile. Since the apparent resistivity is a weighted average of the various resistivities encountered by the propagating current, greater averaging occurs in the VES surveys. This is accounted for later when the data are modelled.

3.3.2. VES Equipment and Survey Setup

The VES surveys were completed using an AGI MiniSting Earth Resistivity and IP Meter with a 12V battery, electrode cables, cable connectors, and 48 stainless steel electrodes (Fig. 3.3.2a). Using 48 electrodes contributes to the efficiency of the survey since only cables had to be moved between measurements, not electrodes. Electrode positions were decided based on the desired resolution of vertical resistivity variation (Table 3.3.2.). The setup of each survey began by choosing a centre point that would represent the location of the VES sounding. Here, a wooden stake was driven into the ground, anchoring two tape measures at their 0-metre mark that were then laid out 150 metres in both directions (multiple tape measures of smaller lengths were used in this study). At the various predetermined positions, electrodes were inserted into the ground until approximately 12 centimetres were left exposed. At most survey locations, up to a half-litre of saltwater (seawater) was poured at the base of every electrode to improve the transmission of current from the electrode to the ground. With the MiniSting Resistivity Meter placed at the centre of the survey spread, cables were connected to the instrument and laid out to be attached to the four electrodes (Fig. 3.3.2b) at lengths that matched each Schlumberger configuration, beginning with spacing #1 (Table 3.3.2.). Cables were disconnected from two of the electrodes after each measurement to unspool further and be connected to the next set of electrodes further from the centre point for successively deeper measurements. For each change of ‘mn’ spacing, the last ‘ab’ spacing used was repeated with the new, greater ‘mn’ spacing as seen in Table 3.3.2. The electrode spacings used in a measurement were input as a parameter in the resistivity meter prior to each measurement. Every survey collected data with the following preset parameters: maximum current of 200 milliamperes (mA), maximum of 2 measurement cycles, 7.2 seconds per measurement, and 2% accuracy. Before dismantling the equipment setup, parameters and measurements recorded on the resistivity meter were downloaded to a laptop and saved for future data processing.

Table 3.2. Summary of surveys by name/location, control wells, survey type, and survey date. Site #s and Control Well #s correlate to those in Figures 3.2.0 and 3.2.1. * Label is not a Well Tag Number (WTN), rather a monitoring well on the Rosewall Hatchery property (DFO, unpublished data). ** Date of a failed ERT survey at Fanny Bay that was later completed on the second date provided (Control Well data from GWELLS, https://apps.nrs.gov.bc.ca/gwells/).

Site #	Site Name/Location	Control Well #	Control Well (WTN)	Survey Type	Survey Date
1	Royston	1a & 1b	81849 & 103795	VES	07/13/22
2	Argyle	-	-	VES	07/13/22
3	Macleod	3a	123217	VES	07/13/22
4	Buckley	4a	26165	VES	07/14/22
5	Tsable	5a	83159	VES	07/14/22
6	Fanny Bay	6a	121630	VES & ERT	07/11/22** & 07/15/22
7	Ships Point	7a	95528	ERT	04/14/22
8	Stelling	8a	77157	VES	07/11/22
9	Wilfred	-	-	VES	07/12/22
10	Qualicum	10a	12733	VES	07/15/22
11	Rosewall	11a	MW21-5*	VES	07/12/22
12	Berray	12a	81873	VES	07/12/22

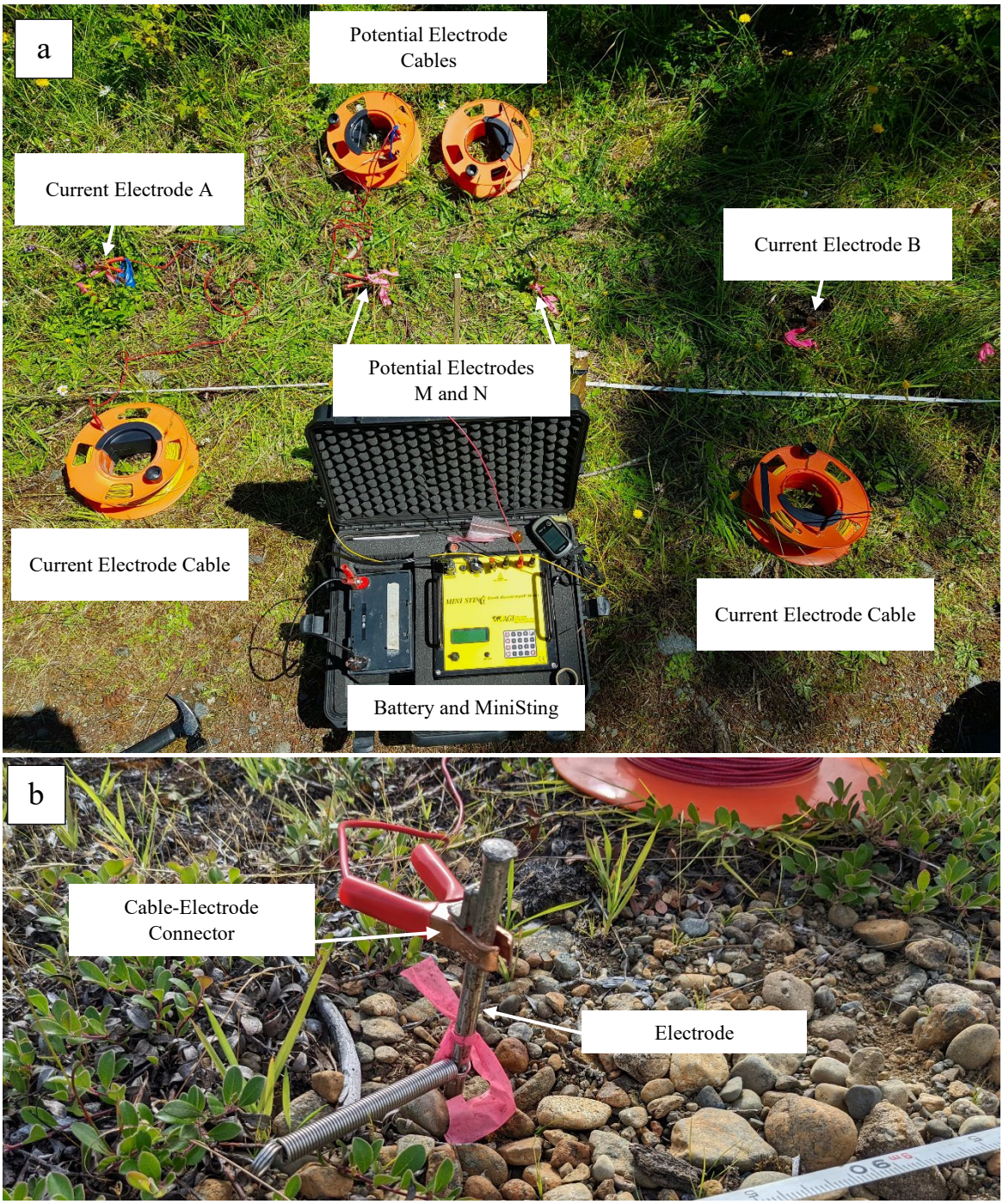

Figure 3.3.2. a) VES instrument setup showing all four electrodes, electrode cables, and the AGI MiniSting Resistivity Meter. b) Connection between electrode cable and potential electrode.

Table 3.3.2. Schlumberger array electrode spacings for VES surveys. Spacings 'ab' and 'mn' are positions relative to the fixed centre point (Fig. 3.2.1). Spacing #16 was not included in surveys until after the first two days of data collection (not included in VES surveys at Fanny Bay, Stelling, Rosewall, and Berray).

Spacing #	ab (m)	mn (m)
1	1	0.25
2	1.5	0.25
3	2	0.25
4	2.5	0.25
5, 6	3	0.25, 1
7	5	1
8	7	1
9, 10	10	1, 2.5
11	12	2.5
12	15	2.5
13	18	2.5
14, 15	25	2.5, 5
16	30	5
17	36	5
18, 19	50	5, 10
20	70	10
21	80	10
22, 23	100	10, 15
24	110	15
25	120	15
26	130	15
27	140	15
28, 29	150	15, 30

3.3.3. Cleaning VES Data

Cleaning the data was the first step of data processing, during which erroneous measurements were removed from the datasets. Erroneous measurements included those that were negative, since negative resistivities do not exist. Negative measurements in VES surveys were only recorded at one site where electrical interference led to this issue (section 4.8); much of this dataset was discarded. Other faulty measurements included ones that were collected when the spacings input into the resistivity meter did not match the cable-electrode setup. This occurred simply due to human error, where, although the spacings were predetermined, they were either incorrectly entered into the resistivity meter or cables were connected to incorrect electrodes. The last type of measurement that was removed from datasets were data points that had relatively high standard deviation (>25%). Some measurements had standard deviations as high as 90% which led to their removal from the datasets.

3.3.4. Modelling VES Data

The cleaned data were then imported into AGI EarthImager 1D software where apparent resistivity measurements were subject to partial differential calculations (Advanced Geosciences Inc., 2012) to produce subsurface models. Using inverse modelling techniques and the damped least squares inversion method, VES data were modelled over eight iterations with a depth factor of 1.1 to achieve a maximum model depth of 82.5 metres. The depth factor is a parameter that allows for the adjustment of the survey's penetration depth, where the penetration depth is defined by the product of the depth factor and the median depth of the survey as suggested by Edwards (1977) (Advanced Geosciences Inc., 2012). Other settings, such as the number of layers and damping factor were varied until the models produced were geologically reasonable, maintained critical details, and minimized root mean square error (RMSE).

The criteria mentioned above are explained thoroughly here. Geological reasonability is the concept of producing a subsurface model that is not overly detailed in stratigraphic structure. For instance, over the 82.5 metre penetration depth, with the knowledge of the regional geology, it would be unreasonable for a model to exceed 15 layers, which provides leeway for material variation within the lithostratigraphic units of the region, even if all were to occur in one profile. A geologically reasonable model is the result of not over-interpreting the data and keeping it simple. Critical details refer to high contrasts in the resistivities of the models. If the value of resistivity increases or decreases drastically across the interface between two layers, it was

important to maintain that high contrasting interface. While the number of layers were adjusted to find suitable models, I made sure to preserve these critical details. Lastly, RMSE is an evaluation of the goodness of fit between measured data points and synthetic (calculated) data points predicted from forward simulation of the inverse model. The RMSE values were represented as a percentage of the averaged misfit across a dataset, calculated with Equation 3.3.4 below (Advanced Geosciences Inc., 2012). The ideal RMSE for a model falls into the range of 1-5% (Advanced Geosciences Inc., 2012); however, RMSE values were simply minimized as the modelling process required a balance of the three criteria described.

Equation 3.3.4. Calculating RMSE where d^{Pred} is the predicted data, d^{Meas} is the measured data, and N is the total number of measurements (Advanced Geosciences Inc., 2012).

$$RSME = \sqrt{\frac{\sum_{i=1}^{N}\left(\frac{d_i^{Pred} - d_i^{Meas}}{d_i^{Meas}}\right)^2}{N}} \times 100\%$$

3.4. Electrical Resistivity Tomography (ERT)

3.4.1. Theory of ERT

When the variation of resistivity is desired in more than one vertical dimension, electrical resistivity tomography (ERT) is implemented to assess the lateral and vertical change in material resistivity, producing a 2D profile. In this study, ERT was used in two, nearby locations, that both occurred proximal to shorelines (Fig. 3.2.1), where there were concerns around potential saltwater intrusion. Implementing ERT surveys to analyze this issue is preferred over VES surveys since the data is continuous in two dimensions, and is therefore more informative and certain than vertical point data (VES). The ERT surveys were done to provide information on the lateral heterogeneity of the subsurface, including that of both geological materials and porewater salinity. To conduct each of the ERT surveys, a dipole-dipole array was used in an approximate straight line. Arranging electrodes in a dipole-dipole array is commonly done when a greater significance is placed on the lateral resolution of measurements as opposed to the vertical (e.g., Metwaly et al., 2010).

3.4.2. ERT Equipment and Survey Setup

The ERT surveys were completed using an AGI MiniSting Earth Resistivity and IP Meter, Swift Automatic Multi Electrode System, and Switch Box, along with a 12V battery, electrode cables, and 28 stainless steel electrodes (Fig. 3.4.2.0). The setup of these surveys began by choosing an end point where the equipment would be placed, and a tape measure would be anchored to extend 81 metres. Beginning at the 0-metre mark (at one end), electrodes were placed 3 metres apart and were also inserted into the ground until approximately 12 centimetres were left exposed. Electrode cables were laid out from the instruments to the last electrode 81 metres away, before being attached by steel springs to the electrodes and connected to the AGI equipment (Fig. 3.4.2.1). Prior to running the surveys, tests of contact resistance were completed to identify any problem electrodes, or cable connection issues. Advanced Geosciences Inc. (2009) defines 5000 ohms as a maximum value for acceptable contact resistance, but an ideal value as less than 2000 ohms. Approximately half a litre of saltwater (seawater) was initially poured at the base of each electrode to improve current transmission and reduce contact resistance. The ERT survey at Fanny Bay had a successful contact resistance test with all values less than 2200 ohms. The survey was able to proceed without further adjustments. In contrast, the test conducted at Ships Point determined much higher values of contact resistance, ranging between 1600 and 9100 ohms. Before measurements were collected, additional saltwater was poured on the ground at the base of most of the electrodes in order to further reduce contact resistance. The parameters set for both surveys included the electrode spacing of 3 metres, as well as a maximum current of 50 mA, maximum of 2 measurement cycles, 7.2 seconds per measurement and an accuracy of 2%. Like the VES surveys, experiment data were downloaded to a laptop and saved before the ERT equipment setup was taken apart.

3.4.3. Modelling ERT Data

The data file was imported into AGI EarthImager 2D software without any pre-analysis data cleaning since measurements were collected automatically by the instruments and therefore were less prone to human error. In this software, apparent resistivity data went through complex computations to produce subsurface models in a process similar to the modelling of the VES data, as described in section 3.3.4. A smooth model inversion method was chosen for both ERT surveys as it proved to produce outputs with the least amount of error (RMSE), also calculated using Equation 3.3.4. Like the modelling in section 3.3.4, ERT models went through eight

iterations for each trial. After running an initial model, data misfit was viewed in a histogram to identify and remove poorly fitted data and improve the models. This was done minimally as to not over-correct the data. Models that were geologically realistic, according to criteria similar to those outlined in section 3.2.4, and had appropriate RMSE values were chosen as final subsurface resistivity models. More specifically, the criteria followed in modelling the ERT data included the concept of keeping the model simple, not over-interpreting the data, as well as maintaining features in the contoured, modelled data where resistivities changed drastically over a short distance (tight contours). Balancing these criteria with minimizing the RMSE, following the same guidelines as for VES data, allowed for construction of an acceptable subsurface model.

Figure 3.4.2.0. Equipment used in the ERT surveys. The foreground shows the battery connected to the AGI MiniSting Resistivity Meter, which is connected by cables to the Swift Automatic Multi Electrode System, and Switch Box in the middle ground. In the background, electrode cables are laid out and connected to the 28 electrodes along the left side of the dirt path.

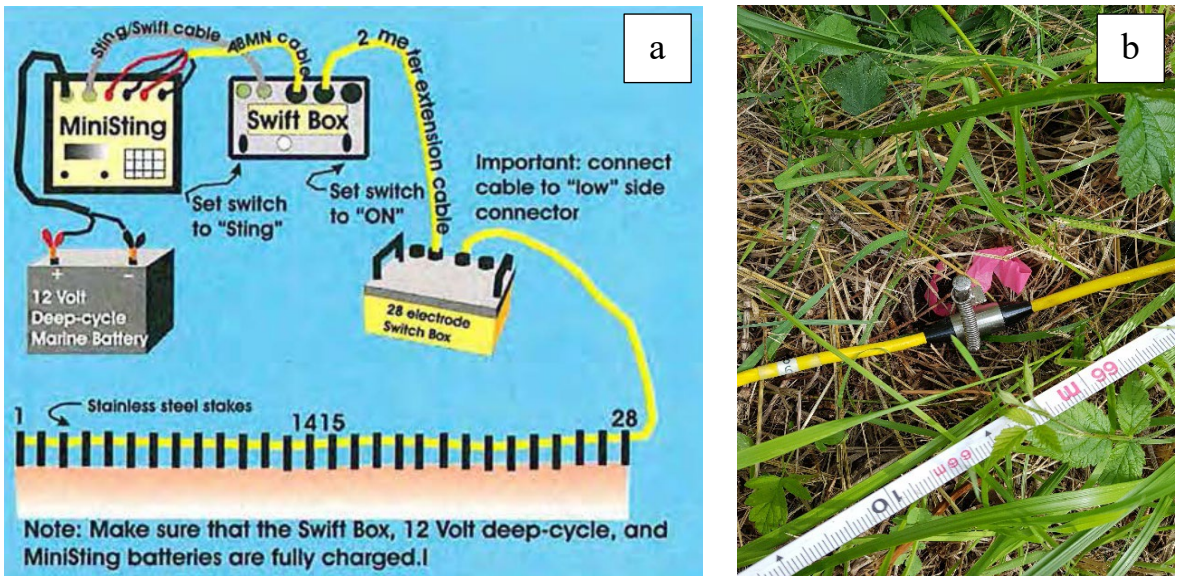

Figure 3.4.2.1. a) Diagram of cable connections to AGI instrumentation (Advanced Geosciences Inc., 2009) and b) photo of cable connection to an individual electrode.

4. Results and Interpretations

This section covers results and interpretations on a site-by-site basis. The modelling results for each survey are summarized in Table 4.0. Each survey site is introduced with the well tag number(s) for the corresponding control wells, followed by a brief description of the survey location, control well location(s), if applicable, and mapped geology. Resistivity data for the site are then presented and described along with the final resistivity model, followed by interpretation. Interpretations for each site cover the lithologies encountered and the hydrogeological potential of the interpreted lithologies, including the predicted aquifer yields which are based on lithologies in Table 6 of Berardinucci and Ronneseth (2002). In most cases, where adjacent lithologies have overlapping ranges of characteristic lithologies, interfaces of the layers are subject to uncertainty, shown by black dashed lines in the figures illustrating interpretations. For this reason, thicknesses of the interpreted layers could vary by several metres. All interpretations were determined through a combination of analyzing the modelled resistivities, control well records, and mapped geology (local stratigraphy). Throughout the results, survey sites are organised from north to south for simplicity.

Table 4.0. Summary of modelling results for all surveys including number of layers and RMSE. ERT surveys did not output a specific number of layers, so this value is left blank.

Survey Name	Number of Layers	RMSE (%)
Royston	7	5.25
Argyle	8	19.93
Macleod	7	7.85
Buckley	10	11.81
Tsable	8	6.00
Fanny Bay (VES; ERT)	9; -	2.20; 2.12
Ships Point	-	4.05
Stelling	5	35.63
Wilfred	8	5.16
Qualicum	10	5.27
Rosewall	8	11.94
Berray	7	5.29

4.1. Royston (WTN 81849 and WTN 103795)

4.1.1. Site Location and Mapped Geology

The VES survey completed in Royston was set up alongside a portion of the Esquimalt & Nanaimo (E&N) railway, on the south side of Trent River. The E&N railway was built upon a ridge of aggregate that has since become richer in organics at the surface due to the decay of surrounding vegetation in the forest. The survey was completed at an elevation of 28 metres above sea level (masl) with a vertical offset of 25 and 22 metres relative to the lower-elevation control wells, WTN 81849 and WTN 103795, respectively (GWELLS, https://apps.nrs.gov.bc.ca/gwells/well/81849; https://apps.nrs.gov.bc.ca/gwells/well/103795). Control well WTN 81849 was located roughly 810 metres southeast of the survey centre and WTN 1013795 was located approximately 575 metres to the northeast of the survey centre. Capilano marine sediments are mapped in this area overlying Vashon Till, where the surficial geology is described as “varied stony, gravelly, and sandy marine-veneer deposits” over “ground moraine deposits” (Fyles, 1960). Beneath the area’s unconsolidated sediments, bedrock is mapped as

Willow Point Member mudstone, siltstone, and minor conglomerate of the Nanaimo Group (Cathyl-Bickford and Hoffman, 1998).

4.1.2. VES Resistivity Data and Model

In the Royston survey, apparent resistivity measurements ranged between 27 and 2274 Ωm; resistivities for the layered subsurface model ranged between 27 and 2947 Ωm (Fig. 4.1.2). In this survey location, resistivity constantly decreased with depth, plummeting nearly 2900 Ωm in the top 0.5-1.1 metres of the profile. Below this depth, the resistivities of layers decreased more gradually, dropping roughly 10 Ωm between each of the three layers (Fig. 4.1.2). The final VES subsurface model for Royston had an RMSE of 5.25% and was a 7-layer model.

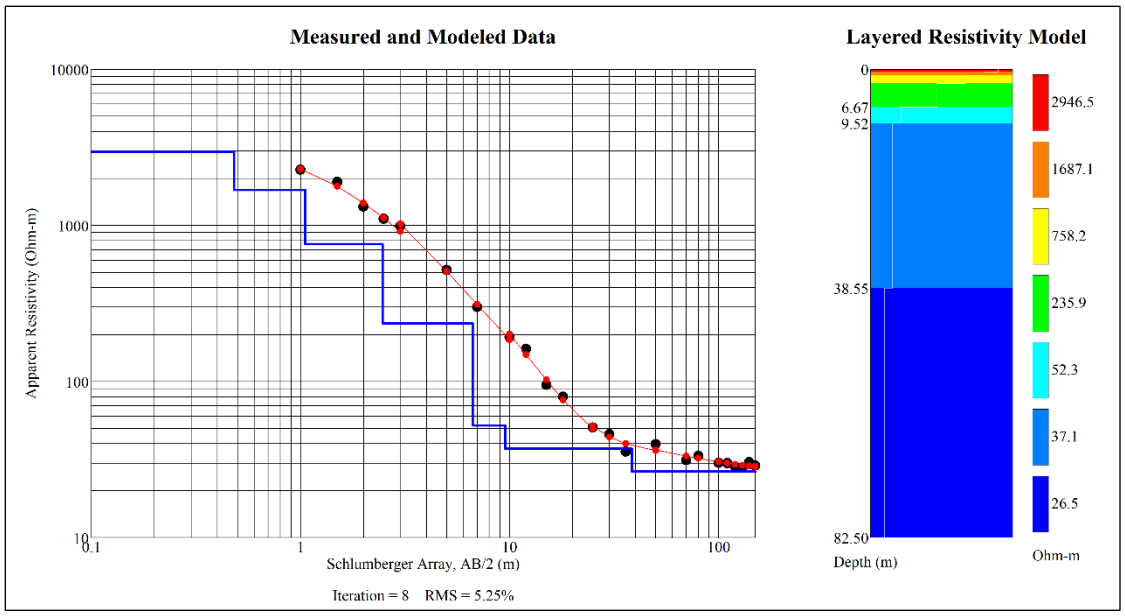

Figure 4.1.2. 7-Layer resistivity model and curve for the Schlumberger array, VES survey at Royston. Apparent resistivity measurements are plotted on the log-log graph as black circles, the model-predicted values are graphed in red, and the blue line plotted on the graph breaks down the model, showing layer thicknesses (interface depths in m on the x-axis) and resistivities (y-axis). The variance between the black circles and the red circles is measured in the RMSE value below the graph. The block diagram on the right is the layered subsurface resistivity model.

4.1.3. VES Interpretations

The subsurface at Royston was interpreted to have just three lithologically distinct layers (Fig. 4.1.3). Resistivities in the model were consistent with the ranges of values characteristic of lithologies such as sand and gravel, till, clay, shale, siltstone, and sandstone. Clay, siltstone, and sandstone were excluded from my interpretation due to their lack of suitability in the expected local stratigraphic sequence (predicted from control well lithologies and mapped geologies). The

top three layers of the model were interpreted to be moderately sorted (silty) sand and gravel, ~2.5 metres thick, and inferred to correspond to Capilano Sediments. Due to its presence at the surface, this unit may be considered a thin, unconfined, moderate-yielding aquifer if sufficiently thick and saturated. This was followed by another three modelled layers over the next ~36 metres, that I interpreted together to be till of the Vashon Drift, acting as an aquitard. The final layer of the model, starting at ~38.5 metres depth, was interpreted to be shale, corresponding to the Willow Point Member bedrock, and inferred to behave as a relatively confined, low-yielding aquifer. For this interpretation, mapped geology and modelled resistivities were the main data sources I used to guide my interpretation.

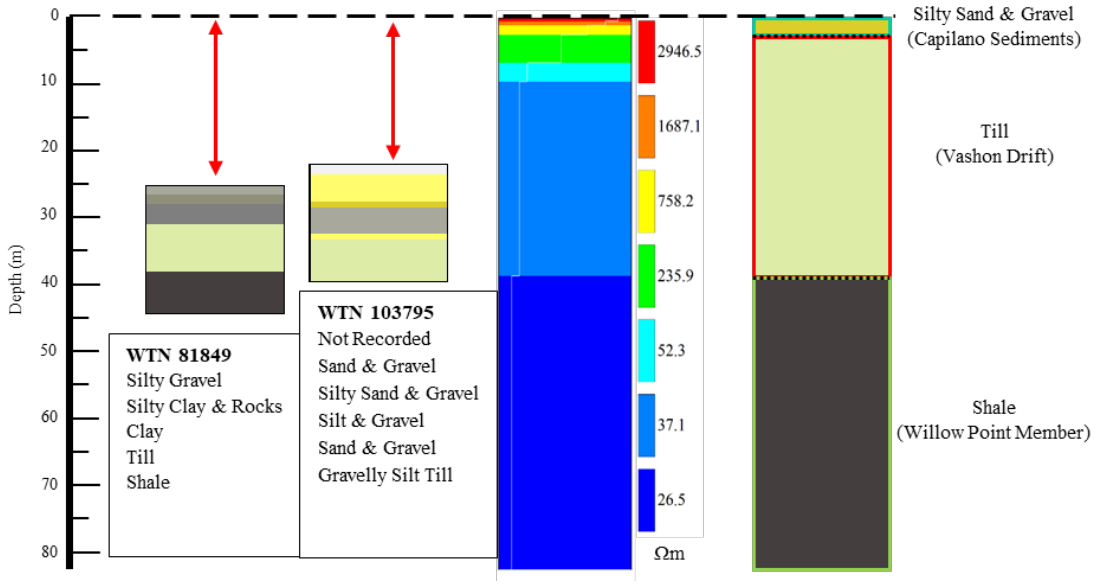

Figure 4.1.3. Royston's components of interpretation. Columns from left to right represent control well lithologies (listed beneath WTNs; GWELLS, https://apps.nrs.gov.bc.ca/gwells/well/81849; https://apps.nrs.gov.bc.ca/gwells/well/103795), resistivity model, interpretation of lithologies, stratigraphy, and hydrogeological potential (teal outline = moderate-yielding aquifer, red outline = aquitard, green outline = low-yielding aquifer). The dashed black line indicates ground surface, and red arrows show vertical offset. The dotted black line in the interpretation column indicates that the exact location of the boundary is uncertain and may be slightly shallower or deeper.

4.2. Argyle

4.2.1. Site Location and Mapped Geology

Like the Royston survey, Argyle's VES Schlumberger array was conducted on the edge of the E&N railway. Inland of Argyle Road in southern Royston, BC, an accessible part of the railway was chosen as the survey site, where the centre of the VES had an elevation of 32 masl.

There were no control wells used for this site, as the nearest wells with lithological data were greater than 2 kilometres away. However, mapped surficial and bedrock geology were used in combination with the resistivity data. These were identical to geology mapped at the Royston site, with Capilano Sediments (stony, gravelly, sandy marine-veneer) overlying Vashon Till (Fyles, 1960), and Willow Point Member bedrock underlying the unconsolidated sediments (Cathyl-Bickford and Hoffman, 1998).

4.2.2. VES Resistivity Data and Model

Apparent resistivity measurements at Argyle ranged between 21 and 1100 Ωm; resistivities for the layered subsurface model ranged between 25.4 and 2176.3 Ωm (Fig. 4.2.2). Below 0.8 metres depth, resistivities remained below 66 Ωm, with interfaces generally alternating between positive and negative resistivity contrasts, indicating the lack of a consistent trend of resistivity with depth. The lowest resistivity encountered occurred between 0.8 and 2 metres depth, indicating a relatively conductive material. The greatest contrasts in resistivity occurred in the top metre of the model, where resistivity decreased from 2176 to 565 Ωm, and then from 565.2 to 25.4 Ωm (Fig. 4.2.2). An 8-layer model was selected as the final subsurface model with an RMSE of 18.79%. The relatively high RMSE can be attributed to the three largest spacings, seen on the furthest right of the graphed data, where the signal-to-noise ratio is likely low.

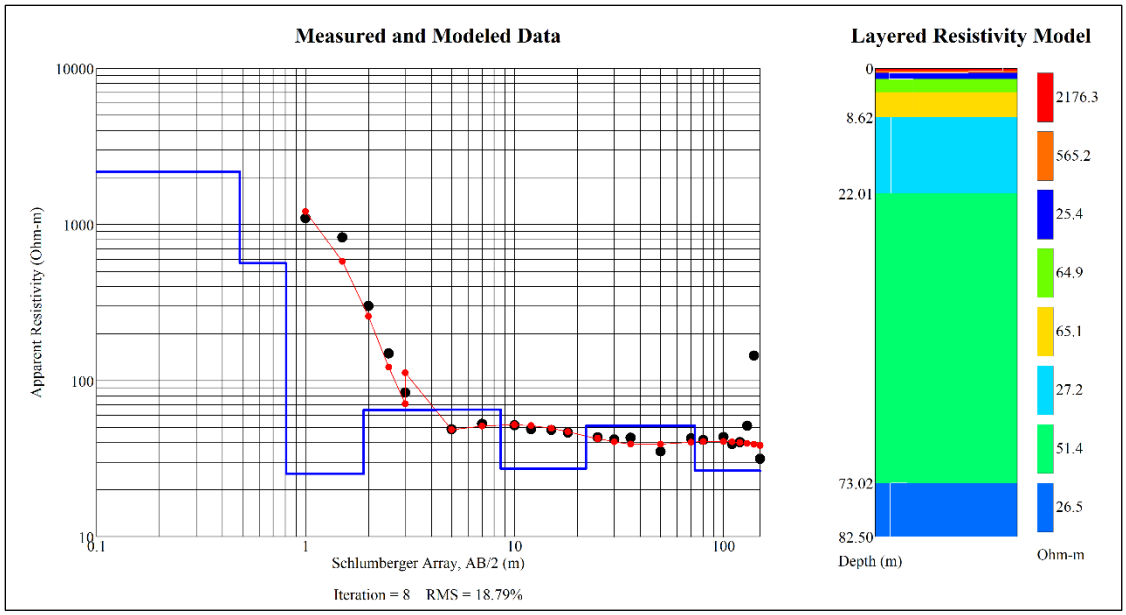

Figure 4.2.2. 8-Layer resistivity model and curve for the Schlumberger array, VES survey at Argyle. Apparent resistivity measurements are plotted on the log-log graph as black circles, the model-predicted values are graphed in red, and the blue line plotted on the graph breaks down the model, showing layer thicknesses (interface depths in m on the x-axis) and resistivities (y-axis). The variance between the black circles and the red circles is measured in the RMSE value below the graph. The block diagram on the right is the layered subsurface resistivity model.

4.2.3. VES Interpretations

At Argyle, I interpreted the subsurface to consist of six different layers of four lithologically distinct units (Fig. 4.2.3). Modelled resistivities were in the ranges of values characteristic of lithologies such as sand and gravel, till, clay, shale, siltstone, and sandstone. Sandstone was excluded from my interpretation due to its lack of fit in the expected local geology (predicted from control well lithologies and mapped geologies). The first two modelled layers were interpreted to comprise one unit of moderately sorted (silty) sand and gravel, which was comparable to the top layer at Royston, except here it was less than 1 metre thick. This silty sand and gravel unit was inferred to correspond to Capilano Sediments, but is unlikely to behave as an aquifer due to being at the surface and too thin for saturation to be probable year round. Between ~1 and 22 metres depth, I interpreted alternating layers of clay and till, where the third modelled layer with a resistivity of 25.4 Ωm was inferred to be clay, followed by ~6.5 metres of till, and then another ~13.5 metres of clay. The top clay layer is interpreted to correlate with Capilano Sediments, while the till and lower clay layer are interpreted to correlate with Vashon Drift. Together, these layers form an aquitard ~21 metres thick. The fifth interpreted layer comes from

the modelled layer with a resistivity of 51.4 Ωm, extending between ~22 and 73 metres depth, and was determined to represent siltstone of the Willow Point Member bedrock. This, combined with the final unit, interpreted to be shale of the Willow Point Member bedrock, are considered a relatively confined, low-yielding aquifer, at least 60 metres in thickness.

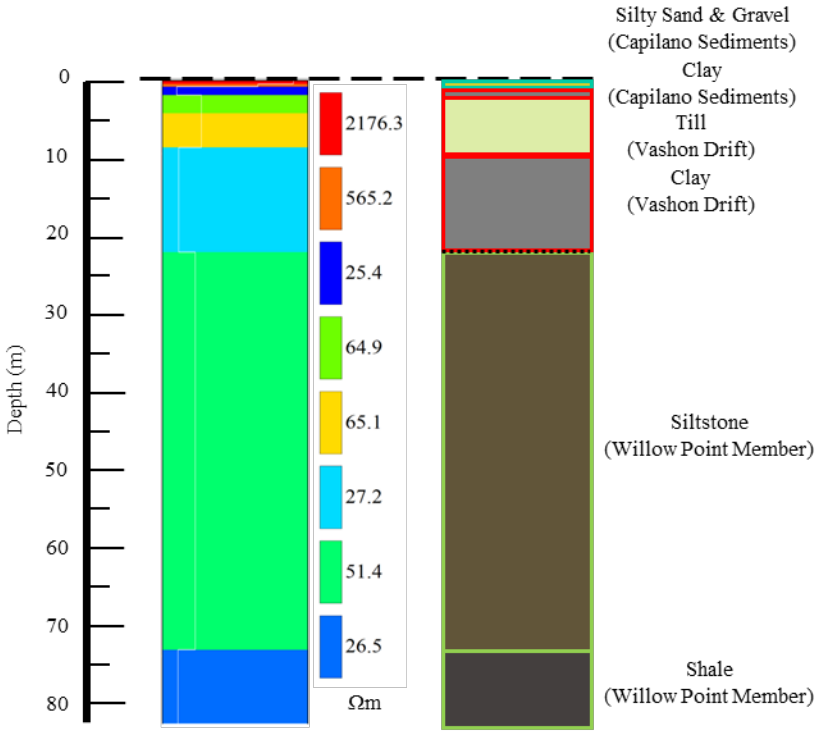

Figure 4.2.3. Argyle's components of interpretation. The left column represents the resistivity model, and the right column represents my interpretation of lithologies, stratigraphy, and hydrogeological potential (teal outline = moderate-yielding aquifer, red outline= aquitard, green = low-yielding aquifer). The dashed black line indicates ground surface and the dotted black line in the interpretation column indicates that the exact location of the boundary is uncertain and may be slightly shallower or deeper.

4.3. Macleod (WTN 123217)

4.3.1. Site Location and Mapped Geology

At the Macleod site, resistivity data were collected along the side of a BC Hydro Right of Way (R/W) in thick grass beside a dirt roadway. This survey site was at 104 masl and had a control well (WTN 123217; GWELLS, https://apps.nrs.gov.bc.ca/gwells/well/123217) located about 620 metres to the northeast at an elevation of 90 masl, resulting in a vertical offset of 14 metres between the survey centre and the lower-elevation control well. Surficial geology at Macleod is mapped as Capilano Sediments, specifically marine deposits consisting of clay, silt, sand, pebbly sand, and sandy gravel, commonly underlain by clay (Fyles, 1960). Macleod's

location is nearby a mapped boundary of bedrock lithologies between the Browns Member (sandstone; minor siltstone) and Puntledge Member (siltstone; minor sandstone) of the Nanaimo Group (Cathyl-Bickford & Hoffman, 1998), so some proportion of both siltstone and sandstone may be expected beneath the survey site.

4.3.2. VES Resistivity Data and Model

Raw apparent resistivity data from Macleod ranged between 50 and 282 Ωm; resistivities of the layered subsurface model ranged between 35 and 422 Ωm (Fig. 4.3.2). Four layers were modelled in the top ~5.4 metres with the majority of that thickness having resistivity values in the hundreds and the remaining material having a resistivity of ~46 Ωm. In the model, the lowest resistivity value of 35.2 Ωm occurs in the fifth layer, extending to ~13 metres depth. Below this, resistivities increase but remain less than 69.5 ohm-metres (Fig. 4.3.2). The chosen 7-layer subsurface model had an RMSE of 7.85%.

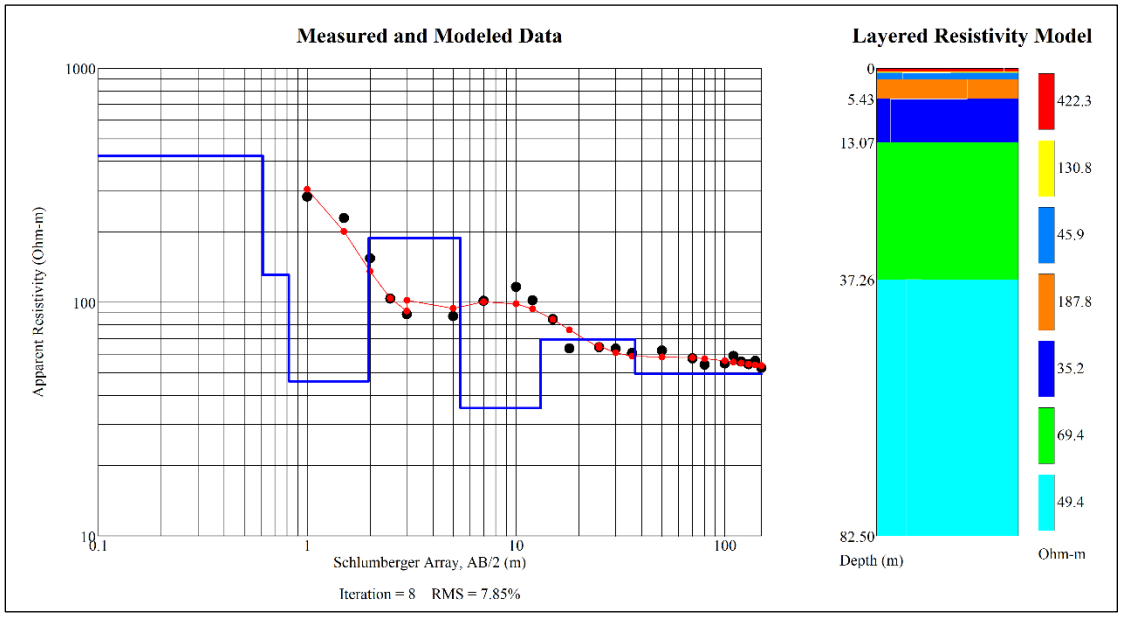

Figure 4.3.2. 7-Layer resistivity model and curve for the Schlumberger array, VES survey at Macleod. Apparent resistivity measurements are plotted on the log-log graph as black circles, the model-predicted values are graphed in red, and the blue line plotted on the graph breaks down the model, showing layer thicknesses (interface depths in m on the x-axis) and resistivities (y-axis). The variance between the black circles and the red circles is measured in the RMSE value below the graph. The block diagram on the right is the layered subsurface resistivity model.

4.3.3. VES Interpretations

The subsurface at Macleod was interpreted to have four lithologically distinct layers (Fig. 4.3.3). Resistivities in the model were consistent with the ranges of values for lithologies such as

sand and gravel, till, clay, shale, siltstone, and sandstone. Shale was excluded from my interpretation due to its lack of suitability in the expected local stratigraphic sequence (predicted from control well lithologies (GWELLS, https://apps.nrs.gov.bc.ca/gwells/well/123217) and mapped geologies (Fyles, 1960; Cathyl-Bickford & Hoffman, 1998)). I interpreted the top four layers of the model, i.e., the top ~5.5 metres, to be composed of moderately sorted (silty) sand and gravel separated by a lens of clay between 0.8 and 2 metres depth, and underlain by ~7.5 metres of clay, all corresponding to Capilano Sediments. Due to its presence at the surface, the upper portion of the silty sand and gravel unit may be considered to behave as a thin, unconfined, moderate-yielding aquifer if sufficiently thick and saturated, while the lower portion may be considered as a partially confined, moderate-yielding aquifer beneath a clay lens aquitard, if sufficiently thick and saturated. The underlying ~7.5 metres of clay is also considered an aquitard. Next, I interpreted a layer of till ~24 metres thick, which I inferred to correlate to Vashon Drift, and like the clay, behave as an aquitard. Finally, I interpreted the bottom-most modelled layer, extending from ~37 metres depth downward, to be comprised of siltstone and/or sandstone. This bedrock unit was inferred to correspond to either the Puntledge or Brown Member of bedrock, and is considered to behave as a relatively confined, low-yielding aquifer at least 45 metres in thickness.

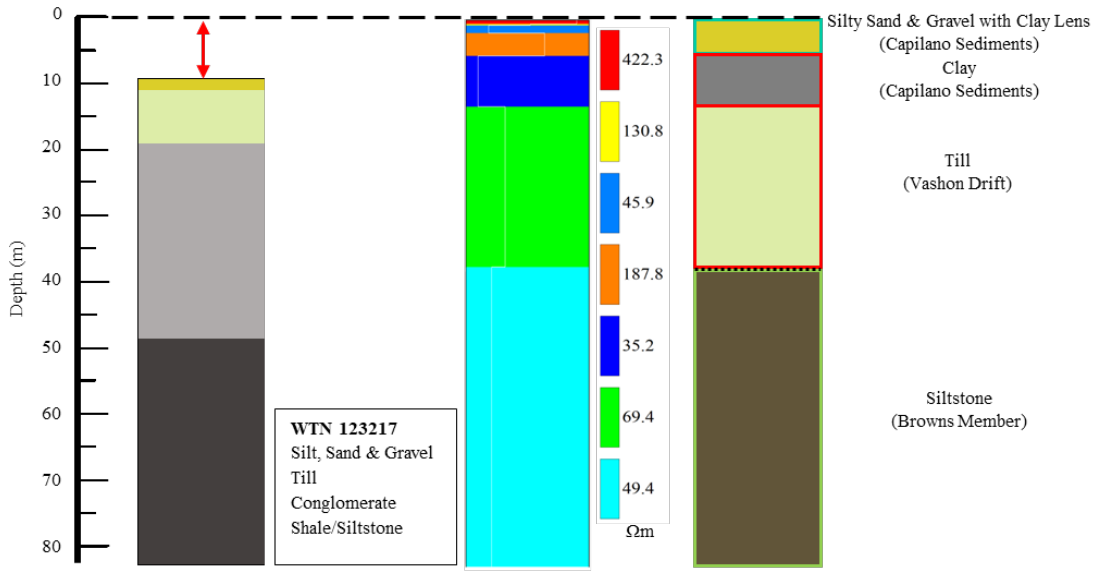

Figure 4.3.3. Macleod's components of interpretation. Columns from left to right represent control well lithologies (listed beneath WTN; GWELLS, https://apps.nrs.gov.bc.ca/gwells/well/123217), resistivity model, interpretation of lithologies, stratigraphy, and hydrogeological potential (teal outline = moderate-yielding aquifer, red outline = aquitard, green = low-yielding aquifer). The dashed black line indicates ground surface, and red arrows show vertical offset. The dotted black line in the interpretation column indicates that the exact location of the boundary is uncertain and may be slightly shallower or deeper.

4.4. Buckley (WTN 26165)

4.4.1. Site Location and Mapped Geology

South of the Macleod survey site, the Buckley VES survey was conducted on the same BC Hydro R/W, through long grass. At 57 masl, Buckley had a vertical offset of 41 metres above the lower-elevation control well, WTN 26165 (GWELLS, https://apps.nrs.gov.bc.ca/gwells/well/26165), that was approximately 650 metres to the northeast of the survey centre. Surficial and bedrock geology mapped at Buckley is identical to those mapped for Royston and Argyle: marine Capilano Sediments over Vashon Till (Fyles, 1960) and Willow Point Member bedrock (Cathyl-Bickford and Hoffman, 1998).

4.4.2. VES Resistivity Data and Model

Buckley survey measurements had a wide range of resistivities from 9 to 4554 Ωm; resistivities of the layered subsurface model had an even greater range of values from 3 to 12527 Ωm (Fig. 4.4.2). Despite the wide range, the spread of resistivity values was not evenly distributed; modelled resistivities were either less than 100 Ωm or greater than 2300 Ωm. The high-range resistivities greater than 2300 Ωm were modelled in the top 1.5 metres of the profile.

Below this, resistivities were more consistent. The bottom layer of the model was calculated to have a resistivity of 3.0 Ωm (Fig. 4.4.2), the lowest value modelled throughout the entire study. A 10-layer subsurface model was chosen as the final model for interpretation, with an RMSE of 11.81%.

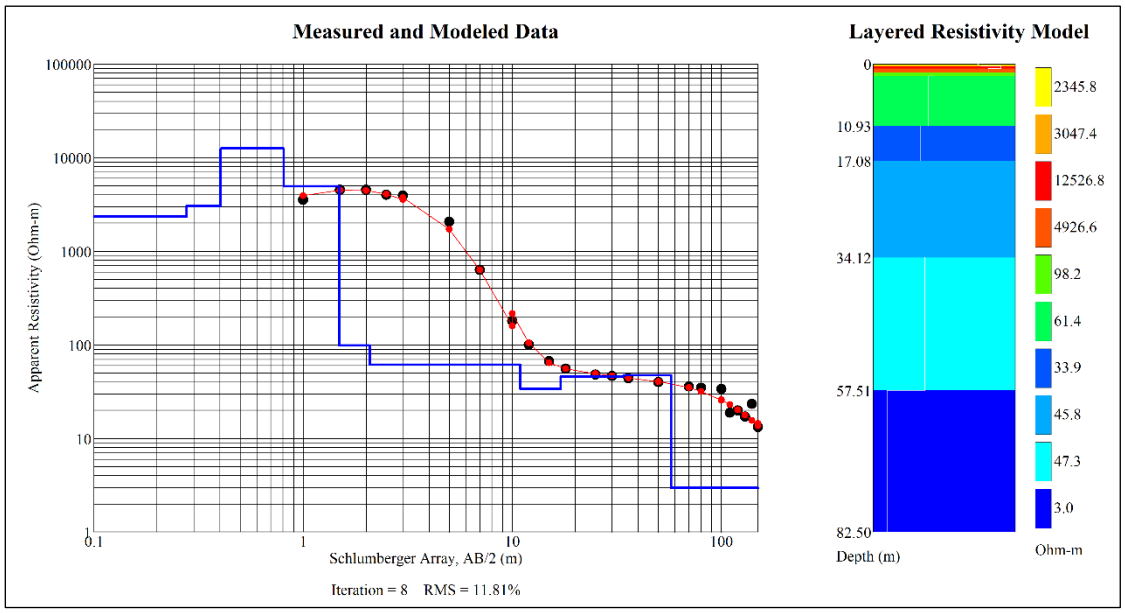

Figure 4.4.2. 10-Layer resistivity model and curve for the Schlumberger array, VES survey at Buckley. Apparent resistivity measurements are plotted on the log-log graph as black circles, the model-predicted values are graphed in red, and the blue line plotted on the graph breaks down the model, showing layer thicknesses (interface depths in m on the x-axis) and resistivities (y-axis). The variance between the black circles and the red circles is measured in the RMSE value below the graph. The block diagram on the right is the layered subsurface resistivity model.

4.4.3. VES Interpretations

Four lithologically distinct layers were interpreted in the subsurface at Buckley (Fig. 4.4.3). Resistivities in the model were consistent with the ranges of values characteristic of lithologies such as sand and gravel, till, clay, shale, siltstone, and sandstone as well as an anomalously high and low resistivity indicating drier sand and gravel and the presence of brackish or fresh water, respectively. Although WTN 26165 included clay in its lithological description (GWELLS, https://apps.nrs.gov.bc.ca/gwells/well/26165), it was listed in association with boulders and stones, which together, can also be described as till. For this reason, clay was excluded from my interpretation. Sandstone was also excluded due to its lack of suitability in the expected local stratigraphic sequence (predicted from control well lithologies (GWELLS, https://apps.nrs.gov.bc.ca/gwells/well/26165) and mapped geologies (Fyles, 1960; Cathyl-Bickford & Hoffman, 1998)). I interpreted a unit of sand and gravel, ~1.5 metres thick, at the top of the profile,

consisting of four modelled layers, and inferred to correspond to Capilano Sediments. This layer may be considered a thin, unconfined, high-yielding aquifer depending on its thickness and state of saturation, since it is present at the surface. The next ~9.5 metres were interpreted to be till of the Vashon Drift, comprising two of the modelled layers, and considered to act as an aquitard. Following the till, the next three modelled layers were interpreted to be siltstone of the Willow Point Member, extending to ~57.5 metres depth. This unit is considered a relatively confined, low-yielding aquifer. Lastly, from ~57.5 metres downwards, a layer with an anomalously low resistivity of 3.0 Ωm was interpreted to be heavily fractured, and therefore permeable, shale of the Willow Point Member. Considered to behave as a relatively confined, low to moderate-yielding aquifer, the shale unit's resistivity indicates the possible presence of brackish water, as with freshwater I would expect a slightly greater resistivity. While saltwater contamination of this aquifer cannot currently be concluded with certainty, further investigation of the water quality at this site should be considered to confirm the presence of brackish water.

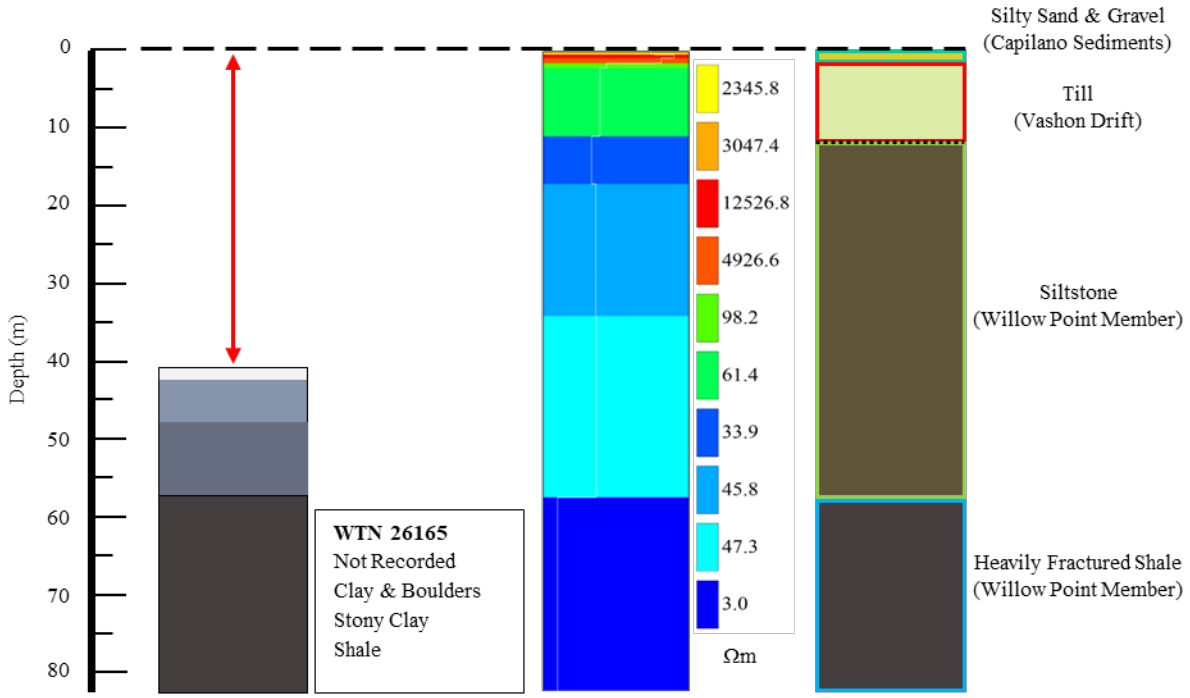

Figure 4.4.3. Buckley's components of interpretation. Columns from left to right represent control well lithologies (listed beneath WTN; GWELLS, https://apps.nrs.gov.bc.ca/gwells/well/26165), resistivity model, interpretation of lithologies, stratigraphy, and hydrogeological potential (teal outline = moderate-yielding aquifer, red outline = aquitard, green outline = low-yielding aquifer, blue = high-yielding aquifer). The dashed black line indicates ground surface, and red arrows show vertical offset. The dotted black line in the interpretation column indicates that the exact location of the boundary is uncertain and may be slightly shallower or deeper.

4.5. Tsable (WTN 83159/OBS Well 371)

4.5.1. Site Location and Mapped Geology

Set up parallel to Highway 19A or Island Highway S, the Tsable VES survey was conducted on a slope adjacent to the highway and was centred beside provincial observation well 371 (WTN 83159; GWELLS, https://apps.nrs.gov.bc.ca/gwells/well/83159). There was no vertical offset between the survey and control well as both were at an elevation of 6 masl. The lateral offset between the two was roughly 2 metres. Being less than 150 metres from Tsable River and just slightly further from its mouth, it is reasonable that Salish and Capilano Sediments are mapped at the surface in the vicinity of the survey centre (Fyles, 1960). These consist of shore, deltaic, and fluvial deposits of gravel, sand, silt, and clay (Fyles, 1960). Like many of the other sites, the bedrock below the sediments is mapped as the Willow Point Member (Cathyl-Bickford & Hoffman, 1998).

4.5.2. VES Resistivity Data and Model

Apparent resistivity measurements from the Tsable VES ranged between 28 and 3562 Ωm with considerable error on several measurements; modelled resistivities ranged between 25 and 8990 Ωm (Fig. 4.5.2). The overall trend in modelled resistivities is a near continuous decrease with depth. Like other subsurface models in this study, the highest resistivities occur in the top few layers (usually the top few metres). In this case, layers with resistivities greater than 1000 Ωm were all less than 3 metres below the surface (Fig. 4.5.2). Beyond 3 metres depth, layer resistivities decreased by an order of magnitude every couple of layers. Tsable was modelled with 8 layers, achieving a RMSE of 6.00% (Fig. 4.5.2).

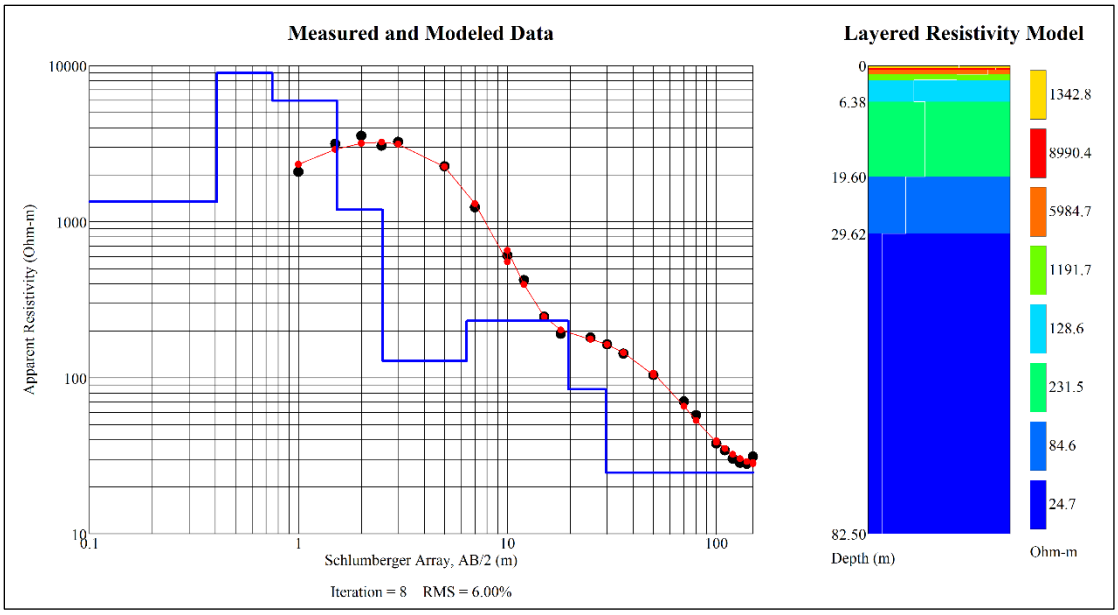

Figure 4.5.2. 8-Layer resistivity model and curve for the Schlumberger array, VES survey at Tsable. Apparent resistivity measurements are plotted on the log-log graph as black circles, the model-predicted values are graphed in red, and the blue line plotted on the graph breaks down the model, showing layer thicknesses (interface depths in m on the x-axis) and resistivities (y-axis). The variance between the black circles and the red circles is measured in the RMSE value below the graph. The block diagram on the right is the layered subsurface resistivity model.

4.5.3. VES Interpretations

The subsurface at Tsable was interpreted to have three distinct lithological layers (Fig. 4.5.3). Resistivities in the model were consistent with the ranges of values characteristic of lithologies such as sand and gravel, till, clay, shale, and sandstone. Clay and sandstone were both excluded due to their lack of suitability in the expected local stratigraphic sequence (predicted from control well lithologies (GWELLS, https://apps.nrs.gov.bc.ca/gwells/well/83159) and mapped geologies (Fyles, 1960; Cathyl-Bickford & Hoffman, 1998)). The top ~20 metres of the model, containing six modelled layers, was interpreted to be representative of sand and gravel, and inferred to correlate to Salish and Capilano Sediments. This sand and gravel unit is considered to behave as an unconfined, high-yielding aquifer. It was followed by a layer ~10 metres thick that I interpreted to be a till aquitard of the Vashon Drift. The bottom layer of the model, at least 53 metres in thickness, was inferred to be shale bedrock of the Willow Point Member and is considered to act as a relatively confined, low-yielding aquifer.

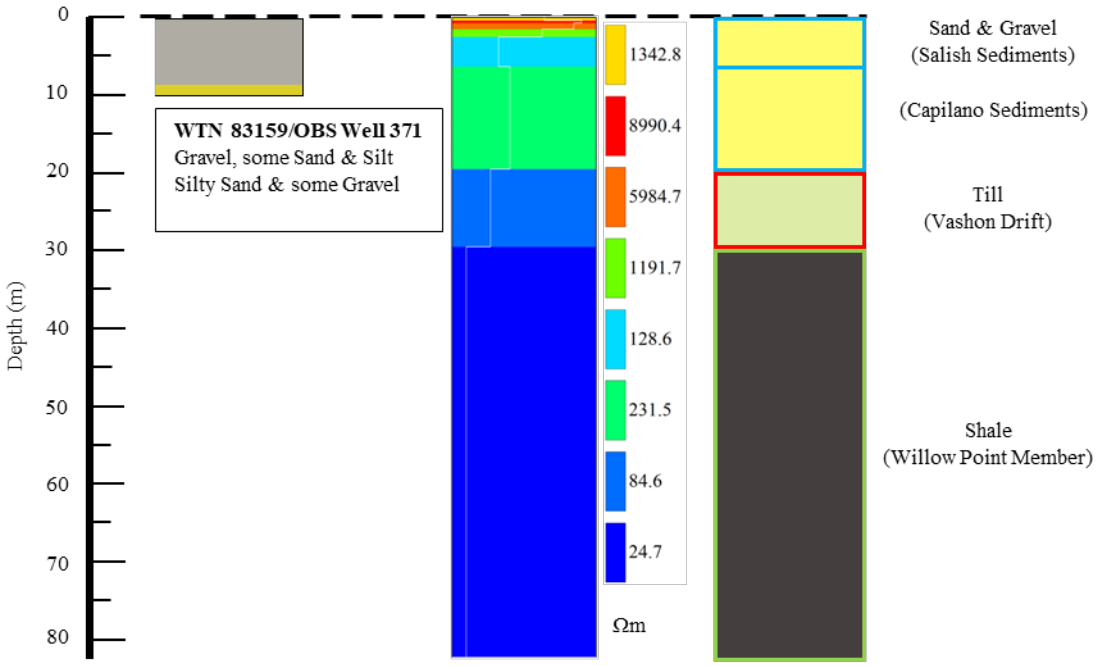

Figure 4.5.3. Tsable's components of interpretation. Columns from left to right represent control well lithologies (listed beneath WTN; GWELLS, https://apps.nrs.gov.bc.ca/gwells/well/83159), resistivity model, interpretation of lithologies, stratigraphy, and hydrogeological potential (blue outline = high-yielding aquifer, red outline = aquitard, green outline = low-yielding aquifer). The dashed black line indicates ground surface.

4.6. Fanny Bay (WTN 121630)

4.6.1. Site Location and Mapped Geology

The Fanny Bay surveys were conducted along a relatively flat hiking trail in a wooded area on the northwest edge of Ships Point Peninsula in Fanny Bay (Fig. 3.4.0 and 3.4.1). For the VES survey, the shoreline was approximately 50 metres northwest of the centre. For the ERT survey, the shoreline was nearest at the northeast end of the profile, coming within 20 metres of the ERT profile. The control well (WTN 121630; GWELLS, https://apps.nrs.gov.bc.ca/gwells/well/121630) near this location was roughly 120 metres to the south-southeast of the VES survey centre and the southwest end of the ERT profile. Vertical offset between the control well, VES centre, and western half of the ERT survey was negligible, while the eastern half of the ERT survey was 1 metre lower in elevation than the control well. Surficial geology at this location is mapped as Salish Sediments, consisting of shore, deltaic, and fluvial deposits including gravel, sand, silt, and clay (Fyles, 1963a; Fyles, 1963b). Bedrock for this area is mapped as the Willow Point Member of the Nanaimo Group (Cathyl-Bickford and Hoffman, 1998).

4.6.2. VES Resistivity Data and Model

Measurements of apparent resistivity ranged between 32 and 265 Ωm while modelled layer resistivities ranged between 28 and 369 Ωm (Fig. 4.6.2). Overall, the resistivities encountered beneath the Fanny Bay VES were relatively unvarying with the top 7 layers producing resistivities in the hundreds. Despite this, nearly 75% of the model was made up of 2 layers at the bottom of the profile, each with resistivities below 100 Ωm (Fig. 4.6.2). A 9-layer subsurface model with an RMSE of 1.83% was selected for interpretation. The high quality of the data may be attributed to the low contact resistance of the surficial sediments, averaging around 1300 Ωm, allowing higher current to pass through the electrodes.

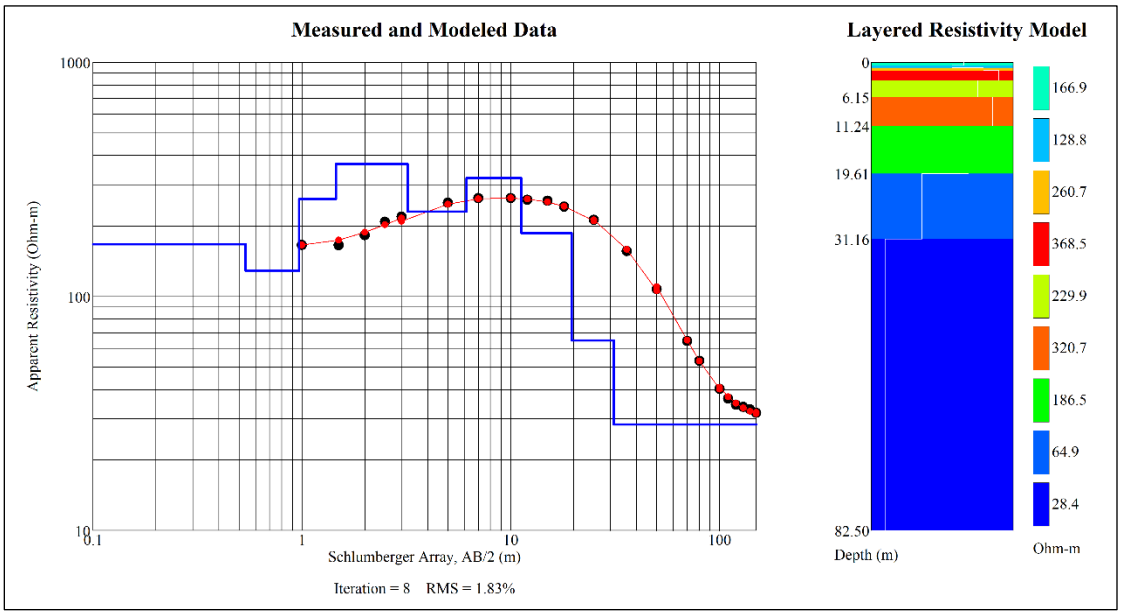

Figure 4.6.2. 9-Layer resistivity model and curve for the Schlumberger array, VES survey at Fanny Bay. Apparent resistivity measurements are plotted on the log-log graph as black circles, the model-predicted values are graphed in red, and the blue line plotted on the graph breaks down the model, showing layer thicknesses (interface depths in m on the x-axis) and resistivities (y-axis). The variance between the black circles and the red circles is measured in the RMSE value below the graph. The block diagram on the right is the layered subsurface resistivity model.

4.6.3. VES Interpretations

Four lithologically distinct layers were interpreted from the modelled nine layers of the Fanny Bay subsurface (Figure 4.6.3). Resistivities in the model were consistent with the ranges of values for sand and gravel, till, clay, shale, siltstone, and sandstone. Clay, siltstone, and sandstone were all excluded from my interpretations due to their lack of suitability in the expected local stratigraphic sequence (predicted from control well lithologies (GWELLS,

https://apps.nrs.gov.bc.ca/gwells/well/121630) and mapped geologies (Fyles, 1963b; Cathyl-Bickford & Hoffman, 1998)). The upper five layers in the model, or the top ~6 metres, were interpreted to represent moderately sorted (silty) sand and gravel correlating to Salish, and possibly Capilano, Sediments. Relatively low resistivities in this unit can be explained by the presence of silt when compared to the high resistivities of clean sand and gravel. The silty sand and gravel unit is considered to behave as an unconfined, moderate-yielding aquifer. Extending ~13.5 metres below the silty sand and gravel, the next two modelled layers were inferred to be better sorted sand and gravel, where the similar, low resistivities are explained by porewater content rather than silt. This sand and gravel unit was inferred to correspond to Capilano Sediments and to be hydraulically connected to the unit above, as an unconfined, high-yielding aquifer, corresponding to mapped aquifer number 419. If considered together, the top ~19.5 metres at Fanny Bay may be an unconfined, moderate to high-yielding aquifer. Till was the third lithological layer interpreted, spanning between ~19.5 and 31 metres depth as an aquitard. This unit was composed of just one modelled layer, and was inferred to correlate with Vashon Drift. Partially confined by the overlying till, the final modelled layer was interpreted to be a low-yielding aquifer, at least 51 metres thick, comprising shale corresponding to the Willow Point Member bedrock.

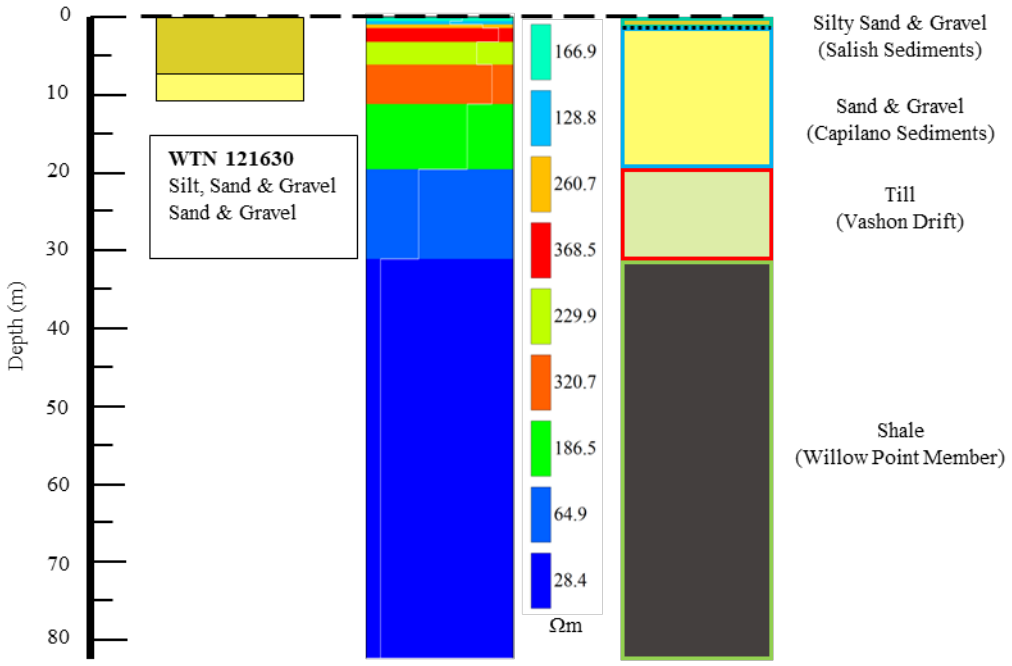

Figure 4.6.3. Fanny Bay's components of interpretation. Columns from left to right represent control well lithologies (listed beneath WTN; GWELLS, https://apps.nrs.gov.bc.ca/gwells/well/121630), resistivity model, interpretation of lithologies, stratigraphy, and hydrogeological potential (teal outline = moderate-yielding aquifer, blue outline = high-yielding aquifer, red outline = aquitard, green outline = low-yielding aquifer). The dashed black line indicates ground surface and the dotted black line in the interpretation column indicates that the exact location of the boundary is uncertain and may be slightly shallower or deeper.

4.6.4. ERT Resistivity Data and Model

The measurements of apparent resistivity collected in the dipole-dipole array remained on the order of 100 Ωm across the entire ERT profile, approximately ranging between 105 and 330 Ωm (Fig. 4.6.4). Modelled resistivities varied between 92 and 725 Ωm, replacing the apparent resistivities of the pseudosection in Figure 4.6.4a with true resistivities in this panel. The inverted resistivity section (Figure 4.6.4b) displayed a significant amount of conductive material on the left (in the northeast) of the profile, between the surface and ~4 metres depth and also between ~9 metres depth and the bottom of the profile. Between these bands of conductive material in the northeast, two regions of relatively high resistivity materials sit at a depth of ~5 metres. In the southwest (right of the profile), features in the subsurface were less pronounced than those in the northeast. While slightly more conductive materials appear along the surface on the right of the profile, the unit of conductive material is thinner than on the left. Although more subtle than on the left, resistive features on the right occupy a greater portion of the profile. A certain likeness

exists between the resistive features across the profile, with most occurring within the depths of ~4 to 5 metres. Similar to the 1D, VES model for Fanny Bay, the 2D subsurface model had a low RMSE of just 2.12%, again implying high data quality. These data are the result of a repeated ERT survey conducted on the last day of field work, as the first attempt on day one ended abruptly due to equipment failure.

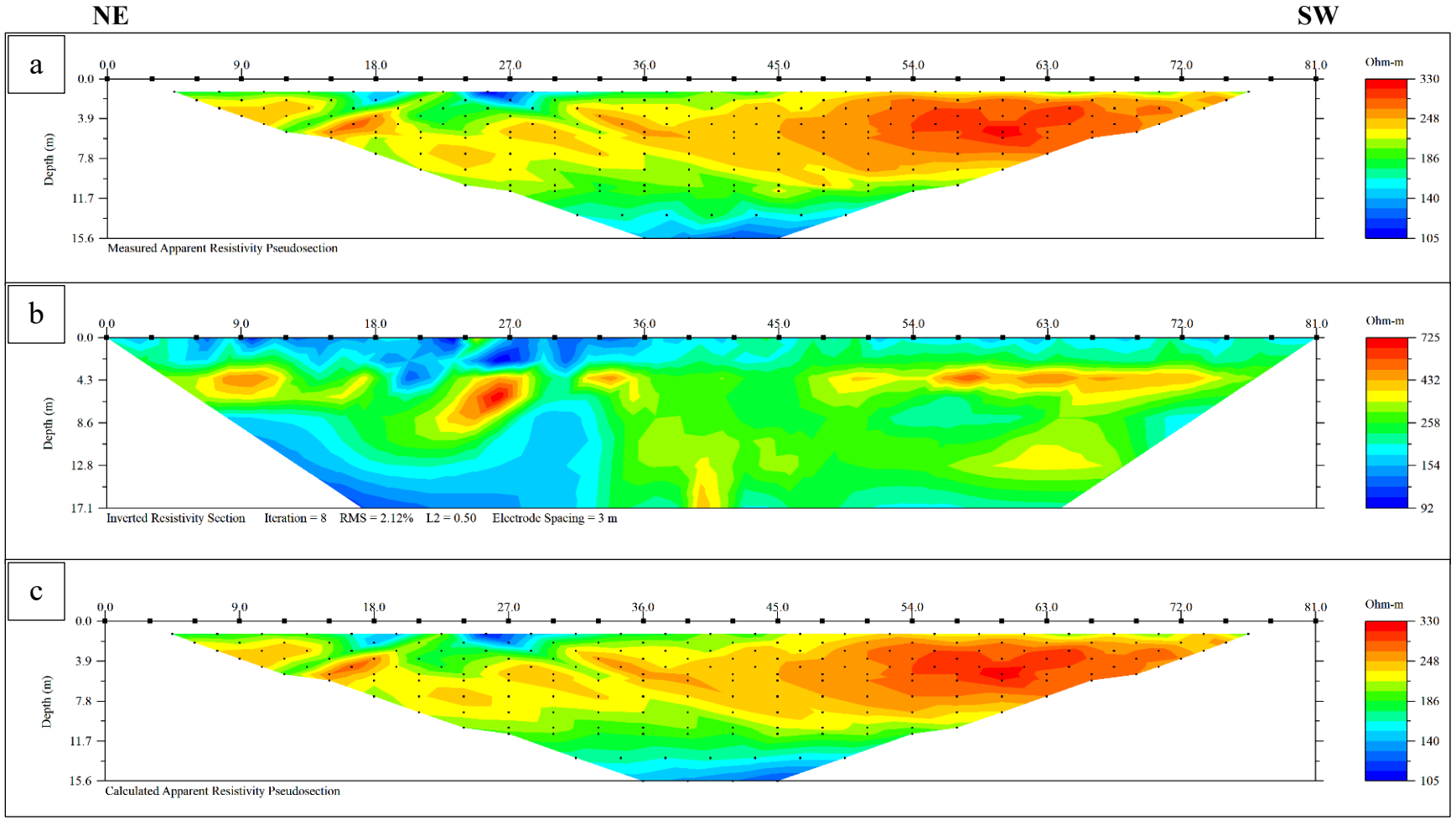

Figure 4.6.4. Fanny Bay: a) Dipole-dipole measured apparent resistivity pseudosection of field measurements. Black dots in the pseudosection show the average location of data collection points that produced the 2D model in b). b) Inverse resistivity model produced from smooth inverse modelling of data in panel a. The calculated RMSE compares panel a) to panel c). c) Calculated apparent resistivity pseudosection, produced by forward modelling results in panel b.

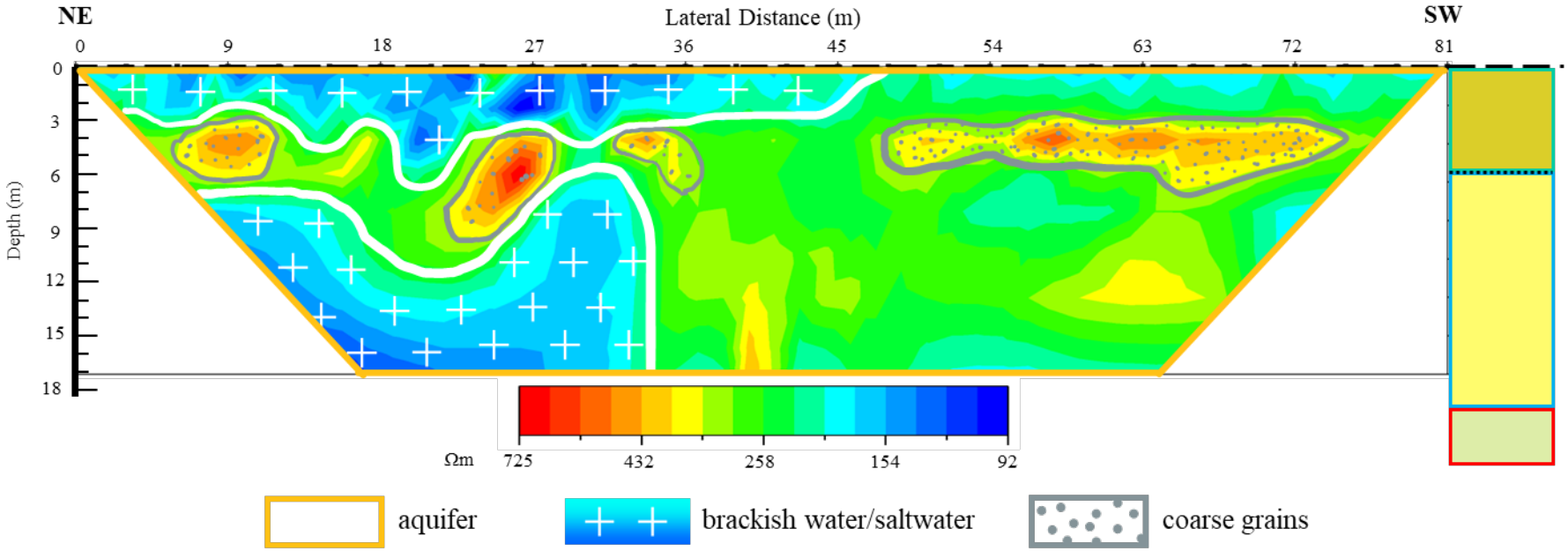

Figure 4.6.5. Interpretation of ERT model at Fanny Bay. The column on the right shows my interpretations from the adjacent VES survey to the approximate depth of the 2D profile. Areas in the profile that lack a pattern are interpreted simply as the aquifer. The entirety of the 2D profile is thought to represent the aquifer with minor heterogeneities in lithology (coarse grains), and variation in groundwater chemistry.

4.6.5. ERT Interpretations

The interpretations for the ERT model at Fanny Bay (Fig. 4.6.5) were made with consideration of the VES model and interpretations (Fig. 4.6.2 and 4.6.3). The centre of the VES survey was approximately located at the furthest southwest end of the survey, or roughly 81.0 metres on the 2D profile (Fig. 4.6.5). As a result of the VES penetrating ~83 metres depth, the ~17 metres depth covered by the ERT profile are theoretically contained within the upper quarter of the VES model. Resistivities in the southwest of the ERT are roughly consistent with the upper 20 metres of the 1D VES profile, and are therefore interpreted to represent the same lithologies – silty sand and gravel to sand and gravel. I infer that the higher resistivity materials approximately 4 to 8 metres deep contain greater proportions of coarse-grained sediments than the surrounding materials with lower resistivities. Although the northeastern part of the profile exhibits conductive material, I attribute this to fluid chemistry rather than variable lithologies such as the presence of till or bedrock, due to the unusual shape of the lower conductive material and the knowledge of the surficial geology for the upper conductive material. While the entire profile is near the shoreline, the closest approach occurred in the northeast, leading me to interpret the conductive material as the presence of brackish water or saltwater. The surficial conductive material is potentially the result of seepage of saltwater through the sediments as a result of high tides, whereas the deeper conductive material I infer to be saturated by saltwater as a result of seawater moving in from the sediments beneath the shoreline. The strength of the conductive regions may indicate pockets of greater permeability, and therefore slight variations in the sand and gravel lithology.

4.7. Ships Point (WTN 95528)

4.7.1. Site Location and Mapped Geology

The dipole-dipole ERT survey conducted at the Ships Point location was done along the south side of Ships Point Road on Ships Point Peninsula. The survey centre had an elevation of 1 masl and was located approximately 35 metres northeast of the control well (WTN 95528; GWELLS, https://apps.nrs.gov.bc.ca/gwells/well/95528), with no vertical offset. The survey line ran parallel to the road and came within 150 metres of the shoreline at the northeast end; however, more proximal to the survey line was a marsh area that likely contains brackish water closer to the survey site during high tides. Being on the opposite side of the Ships Point

Peninsula from the Fanny Bay site, a distance of roughly one kilometre, the mapped geology is identical (Fyles, 1963a; Fyles, 19643b; Cathyl-Bickford and Hoffman, 1998).

4.7.2. ERT Resistivity Data and Model

The measurements of apparent resistivity collected in the dipole-dipole array ranged between approximately 162 and 2527 Ωm (Fig. 4.7.2). The values in the inverted resistivity section varied between 14 and 5402 Ωm. In the modelled inverted resistivity section (Fig. 4.7.2b), the most significant conductive material exists in the bottom ~5 metres of the profile, specifically towards the southwest. A near-continuous band of resistive material spans the profile around 7 to 10 metres depth. Roughly two-thirds the length of the profile also displayed resistive material at the surface extending from the southwest and pinching out towards the northeast. This resistive material appears to be ~2 to 3 metres thick, before pinching out. Between the conductive and resistive materials, resistivity values ranged between ~171 and 755 Ωm.

4.7.3. ERT Interpretations

Considering the ERT profile at Ships Point was conducted across the peninsula from the ERT at Fanny Bay, and the two locations have similar expected stratigraphic sequences, interpretations for the Ships Point ERT (Fig. 4.7.3) are comparable to those for Fanny Bay. The majority of the 2D profile at Ships Point was interpreted to be comprised of sand and gravel, extending to ~12 metres depth. This sand and gravel unit was inferred to correlate with Salish and Capilano Sediments, and is considered an unconfined, high-yielding aquifer. Unlike the 2D profile for Fanny Bay, however, the sand and gravel unit was interpreted to be underlain by ~5 metres of till of the Vashon Drift, considered to behave as an aquitard. Although the resistivities at this depth may also be inferred to be bedrock, in particular shale or siltstone, this interpretation is less likely considering the stratigraphic sequence interpreted at Fanny Bay where a unit of till separates the sand and gravel from the bedrock. Supporting my interpretation, Pereversoff et al. (2022) conducted a VES survey nearby my Ships Point ERT location, from which they concluded a layer of till around 20 metres depth. The interface between the sand and gravel unit and the till in my ERT profile is slightly more shallow, but is within a reasonable range of the depth inferred by Pereversoff et al. (2022). In my profile, I interpret the “blue” area below ~12 m to be till, with all material above this inferred to be sand and gravel (Fig. 4.7.3) The interface between these lithologies appears to be irregular as it is not horizontal across the entire profile.

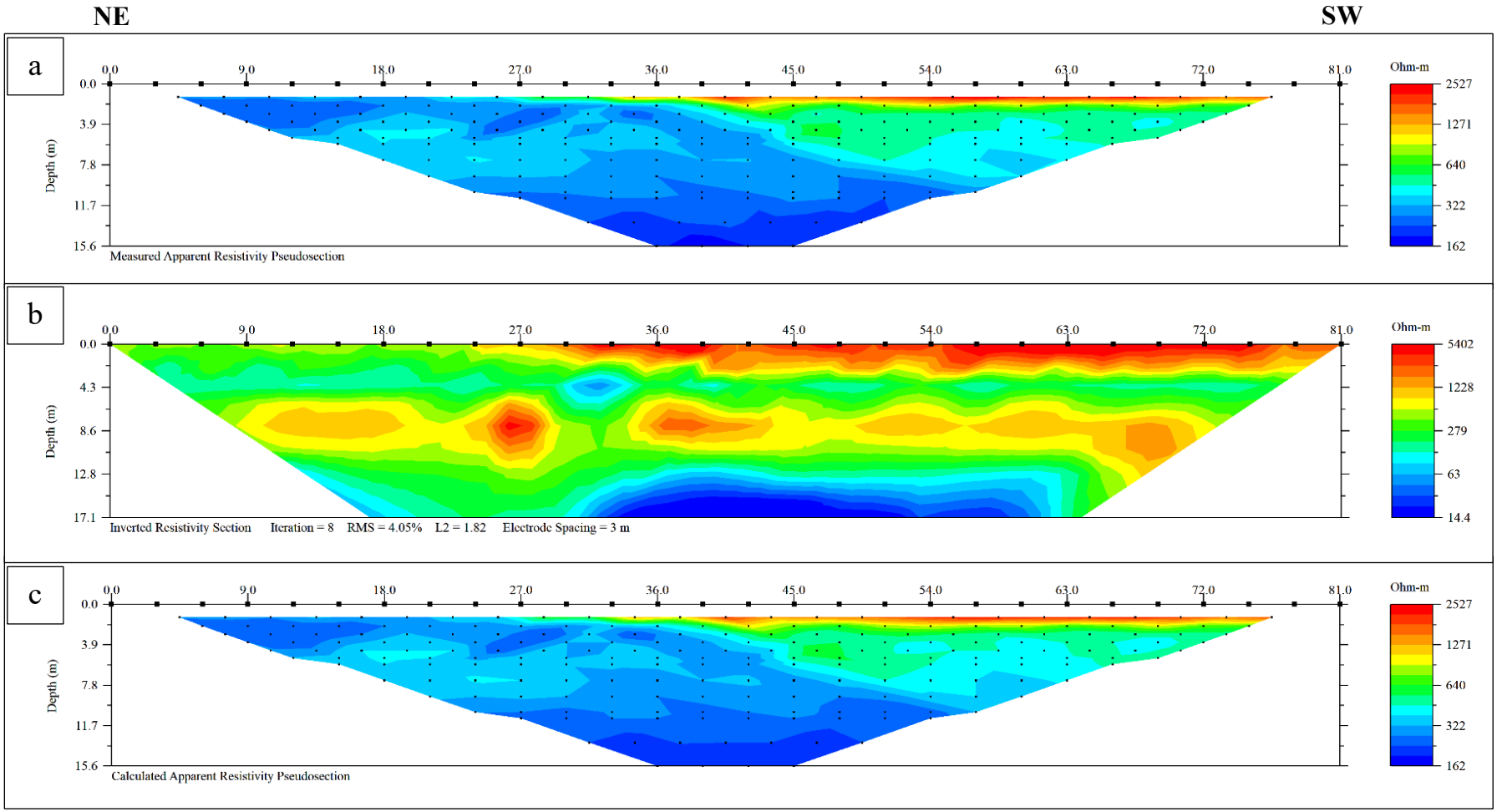

Figure 4.7.2. Ships Point: a) Dipole-dipole measured apparent resistivity pseudosection of field measurements. Black dots in the pseudosection show average location of data collection points that have been interpolated to produce the 2D model in b). b) Inverse resistivity model produced from smooth inverse modelling of data in panel a. The calculated RMS compares panel a) to panel c). c) Calculated apparent resistivity pseudosection, produced by forward modelling results in panel b.

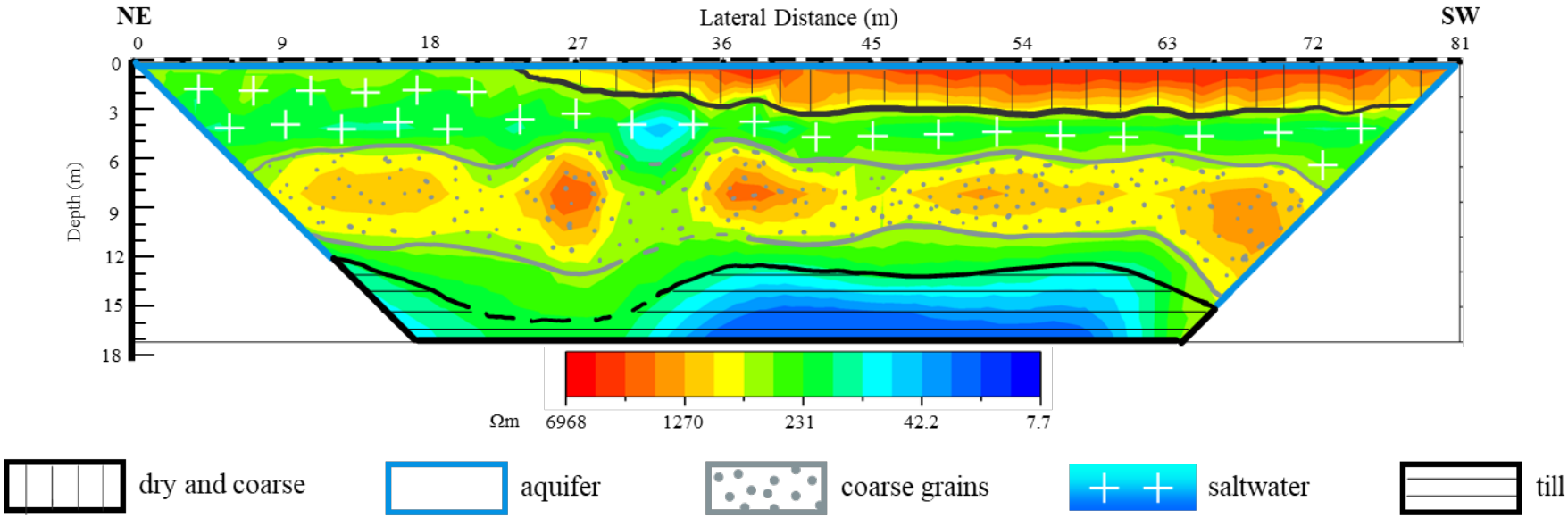

Figure 4.7.3. Interpretation of ERT model at Ships Point. Above the material interpreted as till, the blue outline indicates the aquifer. Within the aquifer, two-thirds of the surface are drier and more coarse, while the rest of the surface is inferred to be affected by the presence of saltwater. The saltwater presence continues across the profile beneath the drier more coarse material. Below this, minor heterogeneities exist in the lithology of the aquifer (coarse grains). Areas of the profile without a pattern simply indicate the aquifer. Dashed lines represent areas in the profile where the interface is uncertain.

Further distinguishing the materials in the profile, the sand and gravel aquifer in the upper 12 metres of the profile was interpreted to be influenced by the presence of saltwater. Due to the proximity of the ERT to the shoreline, particularly the northeast end of the profile, the explanation of saltwater causing the conductive readings is well grounded. The relatively high resistivity material along the surface for two-thirds of the profile was inferred to be drier than the material represented by "green" resistivities in the inverted resistivity section. These green-hue resistivities between ~170 and 750 Ωm were interpreted to represent sand and gravel infiltrated by saltwater. A band of material with relatively high resistivities that spans the width of the profile at ~7-10 m depth, and is sandwiched between two bands of inferred saltwater-saturated sediment, was interpreted to comprise a greater proportion of coarse grains like gravel, and possibly contain large cobble or boulder size rocks which appear as the concentric contours in orange to red hues. This band of coarse grained material is also thought to be infiltrated by saltwater.

4.7.4. Comparison with 2021 Profile

In summer 2021, an ERT survey was conducted at the Ships Point location (Pereversoff et al., 2022), slightly further south than the ERT survey completed in this study. The two profiles have an approximate spatial overlap of 40 metres but are almost exactly 12 months apart. This temporal variation is acceptable for comparison, since hydrologically, seasons are critical to groundwater conditions, and both surveys occurred at the same stage of summer. These temporal and spatial variations allowed for comparisons of the two ERT profiles at Ships Point. ERT data from 2021, collected by Pereversoff et al. (2022), were modelled to roughly match the published results. This modelling process was nearly identical to that of the ERT profiles discussed in previous sections. I then remodeled the 2022 data in the exact way I modelled 2021 data (Fig. 4.7.4), including constraining the scale of resistivity to match the 2021 scale. The identical modelling process allowed for fair comparison of the two temporally different ERT profiles, making similarities and differences more easily recognized and interpreted (Fig. 4.7.4).

Approximately 40 metres of each profile can be compared to the other to examine the temporal variation at the Ships Point location. Between July 2021 and July 2022, no drastic event occurred to alter the lithology, so variations in resistivities for common areas in the profiles are mostly attributed to changes in the pore fluids. For this comparison, lithological and

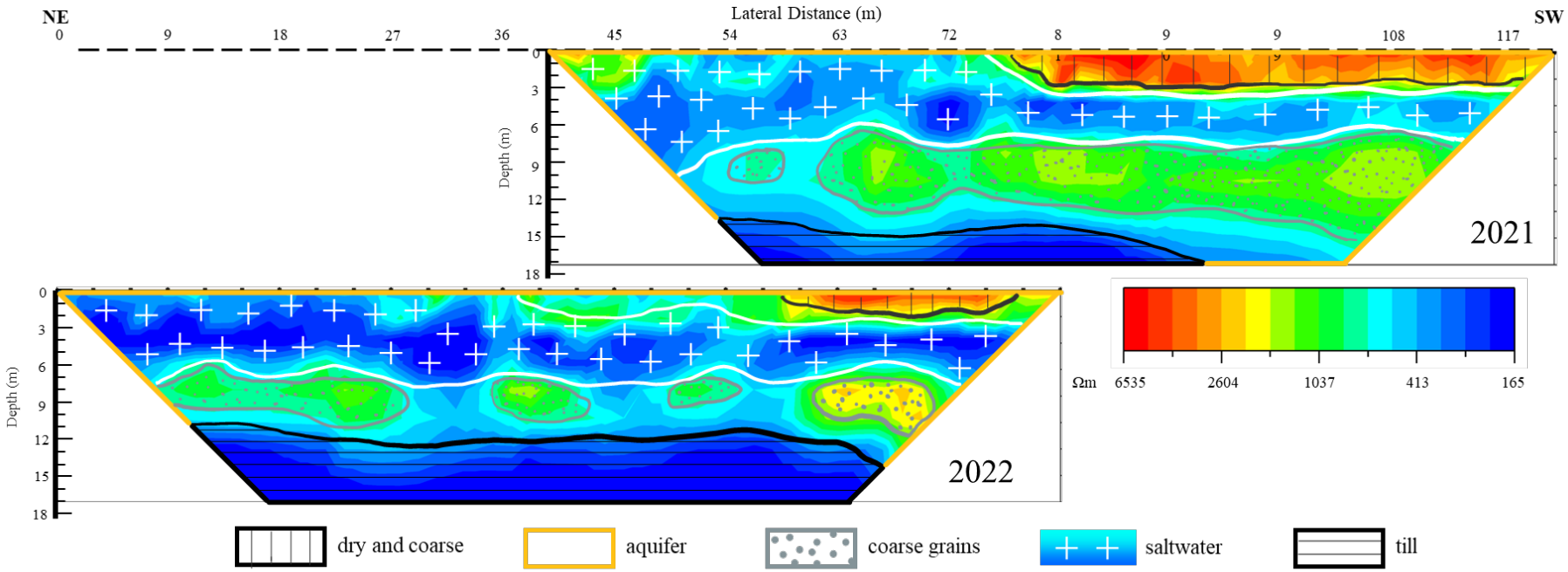

Figure 4.7.4. Comparison of Ships Point ERT profiles between 2021 and 2022. Both profiles share the same scale of resistivity and cover the same depth range. Models are stacked to show the part of the profiles that overlap; the ground level of each profile is identical. Above the material interpreted as till, the yellow outline indicates the aquifer. Within the aquifer, two-thirds of the surface are drier and more coarse, while the rest of the surface is inferred to be affected by the presence of saltwater. The saltwater presence continues across the profile beneath the drier more coarse material. Below this, minor heterogeneities exist in the lithology of the aquifer (coarse grains). Areas of the profile without a pattern simply indicate the aquifer. The darkening of "blue" resistivities in the upper conductive material of the 2022 profile is indicative of an increase in the presence of saltwater (2021 data from Pereversoff et al., 2022).

hydrogeological structure generally follows those of the model in Figure 4.7.3. One of the main changes from 2021 to 2022 was the increase in resistivity at the surface between 60 and 78 metres along the profile (as measured on the 2022 profile). This indicates a decrease in pore fluids, and therefore, drier surficial material. The other significant difference between the two profiles is the increase in conductivity in the upper band of conductive material. I speculate that the increase in conductivity is indicative of an increase in the salinity of the pore fluids present but cannot be certain without temporal analyses of water chemistry from a nearby control well. Lastly, a noticeable increase in resistivity occurred around 9 metres depth at the southwest end of the 2022 profile. This is one variation I attribute to slight lithological differences between the two profiles – perfect lateral alignment of the 2021 and 2022 ERT surveys is unlikely, so minor variations may exist as a result. The higher resistivities in the 2022 profile at this depth may be attributed to a lens of slightly coarser sediments, increasing the resistivity measurements compared to the 2021 profile which likely sensed more fine grains at that depth.

4.8. Stelling (WTN 77157)

4.8.1. Site Location and Mapped Geology

Conducted along the south shoulder of Stelling Road, the VES survey was set up in short, dense grass at an elevation of ~5 masl. A nearby control well (WTN 77157; GWELLS, https://apps.nrs.gov.bc.ca/gwells/well/77157) at 4 masl was located ~130 m southwest of the survey centre. Surficial and bedrock geology mapped at this location match the previous two study sites, Fanny Bay and Ships Point, having Salish Sediments at the surface and Willow Point Member bedrock at depth (Fyles, 1963b; Cathyl-Bickford & Hoffman, 1998).

4.8.2. VES Resistivity Data and Model

The Stelling VES collected just 19 data points, of which 15 had negative values of apparent resistivity. When electrode spacings surpassed a current electrode half-length of 50 metres and a potential electrode half-length of 10 metres, each measurement resulted in an error code "HVOVL" (high voltage overload), which often results from a disconnection or poor connection in the current transmission setup (electrodes A and B and associated cables). After confirming this was not the issue, it was determined that the overhead powerlines that ran parallel to the survey line, less than 10 metres to the south, were causing electrical interference (section 4.8.4). When several measurements came back with this error code, the survey was ended short, with the last measurement occurring at the spacing of 10 metres for the half-length between potential

electrodes and 50 metres for the half-length between current electrodes. Of the 19 data points that were collected, only four had positive apparent resistivities; the negative values were also attributed to the electrical interference caused by the powerlines. Including the negative measurements, apparent resistivities ranged between -17309 and 551 Ωm. Once negative points were removed, the four remaining data points ranged between 123 and 551 Ωm. Modelling the Stelling data resulted in a large RMSE of 35.63% due to the lack of useable data and the poor resolution caused by the spread of the useable data points (Fig. 4.8.2). Although set to 8 iterations, this model stopped at 6, indicating this was the best model AGI EarthImager 1D could produce. Set to just 5 layers reaching only 6.6 metres depth, modelled layer resistivities ranged from 21.9 to 1918.7 Ωm. The middle three layers had higher resistivities compared to the top and bottom layer; however, considering the problems encountered with this survey, I find these results unreliable (Fig. 4.8.2).

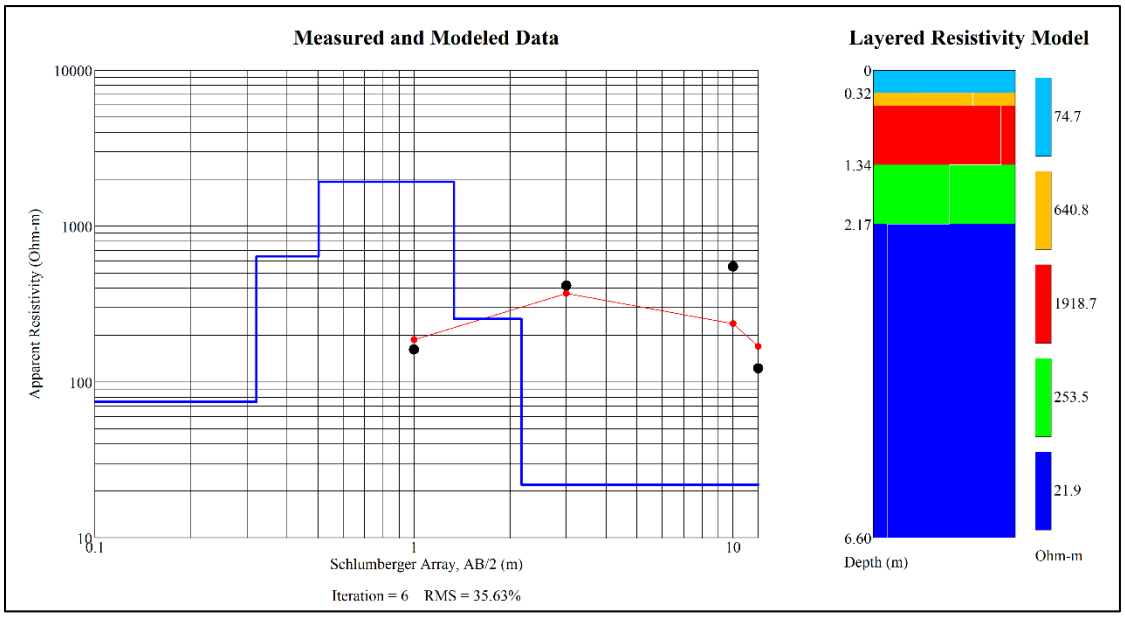

Figure 4.8.2. 5-Layer resistivity model and curve for the Schlumberger array, VES survey at Stelling. Apparent resistivity measurements are plotted on the log-log graph as black circles, the model-predicted values are graphed in red, and the blue line plotted on the graph breaks down the model, showing layer thicknesses (interface depths in m on the x-axis) and resistivities (y-axis). The variance between the black circles and the red circles is measured in the RMSE value below the graph. The block diagram on the right is the layered subsurface resistivity model.

4.8.3. VES Interpretations

The high level of uncertainty in the Stelling model led to greater uncertainty in my interpretations compared to at other sites (Fig. 4.8.3). The inferences I made from the resistivity model relied heavily on WTN 77157 that was located ~130 metres away (GWELLS,

https://apps.nrs.gov.bc.ca/gwells/well/77157). The overall depth of the model reached less than 7 metres, and since surficial geology was mapped as Salish Sediments, the stratigraphic sequence I interpreted consisted mainly of this unit and potentially some Capilano Sediments. Lithologically, the entire 6.6 metres of the model, including all five layers, was interpreted as sand and gravel, despite the low modelled resistivities at the top and bottom. I attribute these values to the poor resolution of the survey and the subsequent model error. The sand and gravel unit was considered to behave as an unconfined, high-yielding aquifer, at least 6.6 metres in thickness.

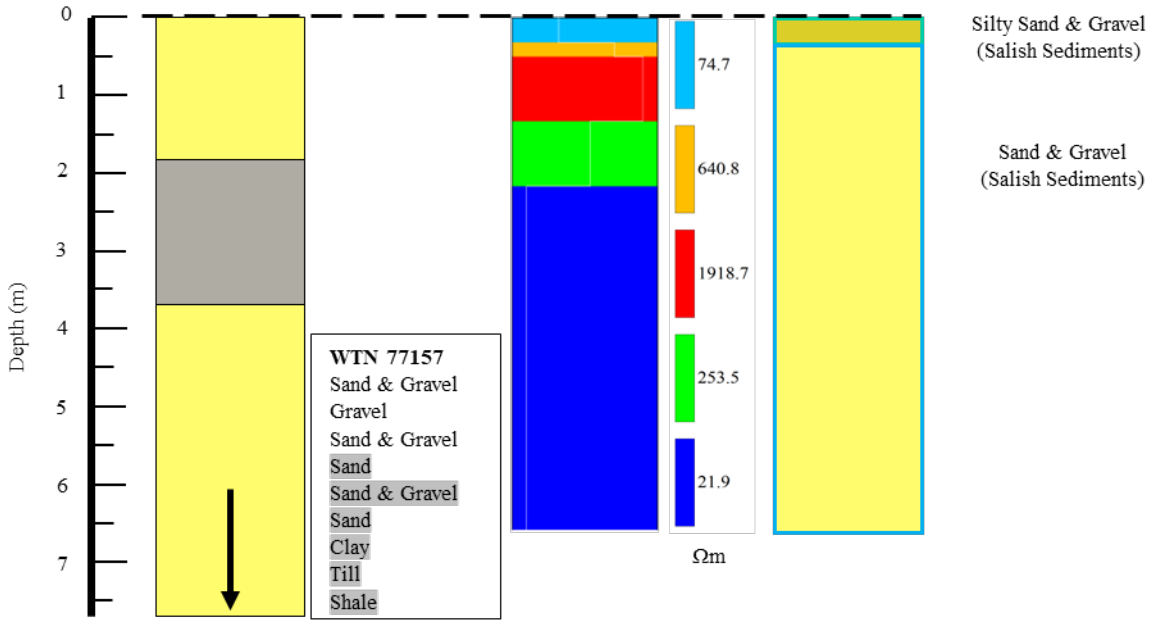

Figure 4.8.3. Stelling's components of interpretation. Columns from left to right represent control well lithologies (listed beneath WTN; GWELLS, https://apps.nrs.gov.bc.ca/gwells/well/77157), resistivity model, interpretation of lithologies, stratigraphy, and hydrogeological potential (teal outline = moderate-yielding aquifer, blue outline = high-yielding aquifer). The dashed black line indicates ground surface and the black arrow in the control well column indicates that the lithologies of the well extend past the bottom of the VES survey; these deeper well lithologies are highlighted grey in the lithology legend under the well tag number.

4.8.4. Electrical Interference

At this location, overhead power lines ran parallel to the VES survey, less than 10 metres south and ~20 metres above the ground (Fig. 4.8.4). Without having a solution during the data collection, the survey was discontinued in the interest of time, and surveys were completed at other sites. It was later determined that the error code appearing on the AGI MiniSting Resistivity Meter was likely a result of interference from the power lines with respect to the

chosen VES arrangement. Grounding between the power line towers is strongest directly beneath the overhead cables, and diminishes to either side (e.g., Greenwood, 2020). Being that the survey line was so close to the power lines, the grounding likely caused significant interference, leading to the "HVOVL" error and the negative apparent resistivity measurements. In hindsight, the issue may have been overcome if the survey was conducted further away from the power lines. If possible, a VES should be conducted perpendicular to power lines; if parallel, a VES profile should be at least 15% of the profile length away from power lines, or 45 m away for a 300-m profile (Greenwood, 2020). In this case, the VES profile was limited to the roadside, but could have been set up on the opposite side of the road ~15 metres from the power lines.

4.9. Wilfred

4.9.1. Site Location and Mapped Geology

The VES survey was conducted along a dirt roadway in a BCHROW southwest of Fanny Bay, BC. Artificial surficial material was quite obvious at this site due to a lack of vegetation and the dry conditions. The elevation at the Wilfred survey centre was 51 masl. The mapped surficial geology at this location is described as terraced fluvial delta deposits (Capilano Sediments) containing gravel and sand, commonly underlain by silt and clay (Fyles, 1963a; Fyles, 1963b). The Wilfred study site occurs near a boundary between the two members, so the exact mapped bedrock is uncertain, however I estimate the location of the survey to correspond with the location of the Puntledge Member (Cathyl-Bickford and Hoffman, 1998).

4.9.2. VES Resistivity Data and Model

The measured apparent resistivities at the Wilfred site spanned four orders of magnitude, ranging from 59 to 41541 Ωm. Modelled resistivity data had a minimum of 54 Ωm and a maximum of 88694 Ωm (Fig. 4.9.2). The Wilfred location encountered the highest resistivities as well as the greatest thickness of high-resistivity layers in the entire study. This also means that some of the largest resistivity contrasts were surveyed. In the top 17 metres of the model, layers exceeded resistivities of 8900 Ωm, but directly below this, the next layer had a resistivity of ~890 Ωm and was followed by a layer with a resistivity of 54 Ωm (Fig. 4.9.2). The boundaries between the bottom three layers were subject to a 10-fold decrease with depth between each subsequent layer. The selected 8-layer subsurface model not only produced a more clear stratigraphic sequence, but also the lowest RMSE (5.16%) of all the attempted models.

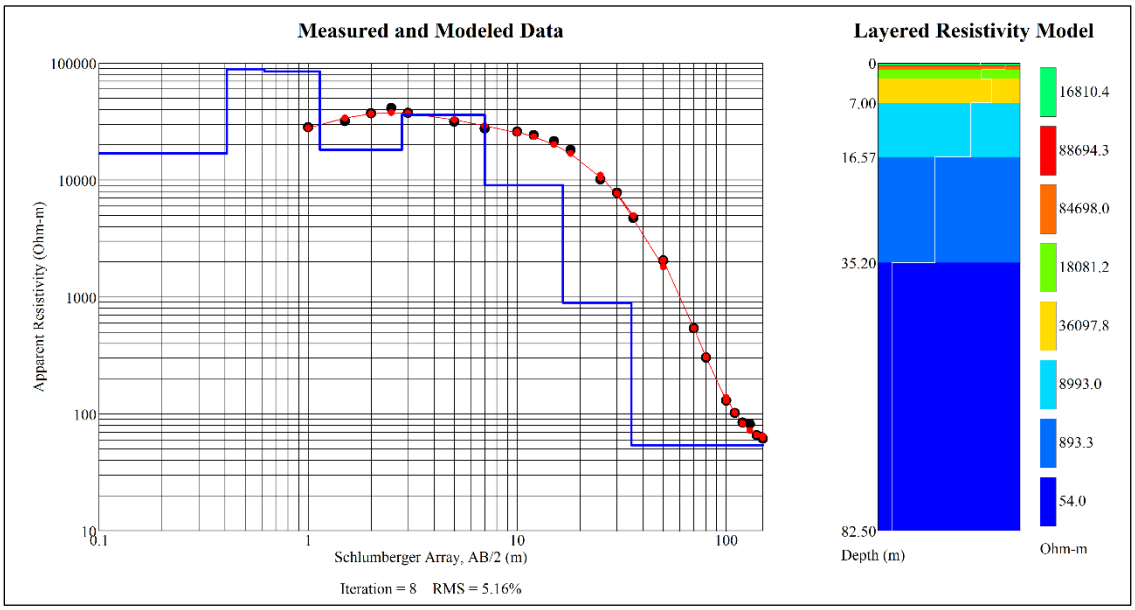

Figure 4.9.2. 8-Layer resistivity model and curve for the Schlumberger array, VES survey at Wilfred. Apparent resistivity measurements are plotted on the log-log graph as black circles, the model-predicted values are graphed in red, and the blue line plotted on the graph breaks down the model, showing layer thicknesses (interface depths in m on the x-axis) and resistivities (y-axis). The variance between the black circles and the red circles is measured in the RMSE value below the graph. The block diagram on the right is the layered subsurface resistivity model.

4.9.3. VES Interpretations

At Wilfred, the subsurface was determined to comprise three, natural, lithologically distinct layers (Fig. 4.9.3). Resistivities in the model were consistent with the ranges of values for sand and gravel, till, clay, siltstone, and sandstone. Clay and sandstone were excluded from my interpretation due to their lack of fit in the expected stratigraphic sequence from the regional surficial and bedrock geology. At the surface, ~1 metre of artificial gravel was interpreted, labelled as fill in Figure 4.9.3. A unit of sand and gravel ~15.5 metres thick was the upper-most, natural layer in my interpretation, inferred to correlate to Capilano Sediments, and considered to behave as an unconfined, high-yielding aquifer. Although the top seven layers in the model, extending to ~35 metres depth, had resistivities characteristic of sand and gravel, the bottom layer of that group, between ~16.5 and 35 metres depth, was interpreted to be till, as the resistivity was also characteristic of this lithology, and the trend of stratigraphic sequences observed in the surrounding areas had till underlying sand and gravel. This till was determined to correspond to Vashon Drift and is considered an aquitard. While this layer may also be representative of water-bearing sand and gravel, I was less certain of this interpretation due to a

lack of control wells available to estimate the approximate location of the water table at this site. Below the unit of till, extending from ~35 metres downward, I interpreted siltstone bedrock, which is considered to act as a relatively confined, low-yielding aquifer. The siltstone was inferred to correlate to Willow Point Member bedrock.

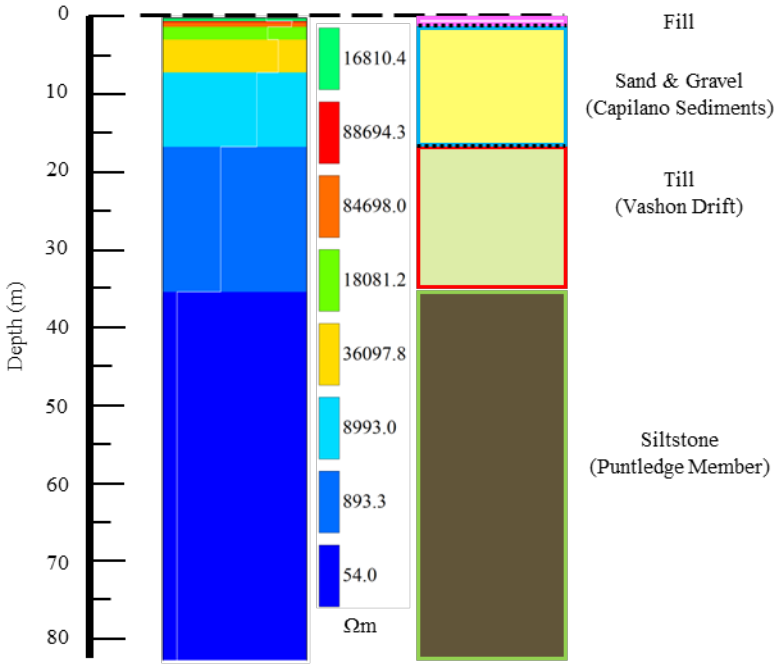

Figure 4.9.3. Wilfred's components of interpretation. The left column represents the resistivity model, and the right column represents my interpretation of lithologies, stratigraphy, and hydrogeological potential (pink outline = artificial material, blue outline = high-yielding aquifer, red outline = aquitard, green = low-yielding aquifer). The dashed black line indicates ground surface and the dotted black line in the interpretation column indicates that the exact location of the boundary is uncertain and may be slightly shallower or deeper.

4.10. Qualicum (WTN 12733)

4.10.1. Site Location and Mapped Geology

Roughly one kilometre south of the Wilfred VES, on the same portion of BCHROW, the Qualicum survey was conducted. At 38 masl, the centre of the Qualicum survey had a 46-metre vertical offset from the higher-elevation control well (WTN 12733; GWELLS, https://apps.nrs.gov.bc.ca/gwells/well/12733) located approximately 400 metres west. Like the Wilfred location, mapped surficial geology is described as terraced fluvial delta deposits (Capilano Sediments) containing gravel and sand, commonly underlain by silt and clay (Fyles, 1963a; Fyles, 1963b). The bedrock in the area may be the Willow Point Member or the Puntledge

Member (Cathyl-Bickford and Hoffman, 1998); it is unclear since the bedrock geology map does not extend south of the Wilfred location, so lithological boundaries must be extrapolated.

4.10.2. VES Resistivity Data and Model

While nearly half of the apparent resistivity measurements were greater than 1000 Ωm, values ranged between 10 and 5881 Ωm. The modelled range of resistivities was larger, spanning from 81 to 11858 Ωm (Fig. 4.10.2). The general trend over the depth of the model was for the layer resistivities to decrease. This can be seen in the layered resistivity model, where colours gradually change from warm tones at the top to cool tones at the bottom (Fig. 4.10.2). The highest resistivity layers occur in the upper 2 metres of the model and are followed by roughly 10 metres of moderately high resistivity layers. Between about 12 metres depth and the bottom of the model, layer resistivities remain relatively low (80-130 ohm-m). The 10-layer subsurface model was selected for interpretation, with an RMSE of 5.27%.

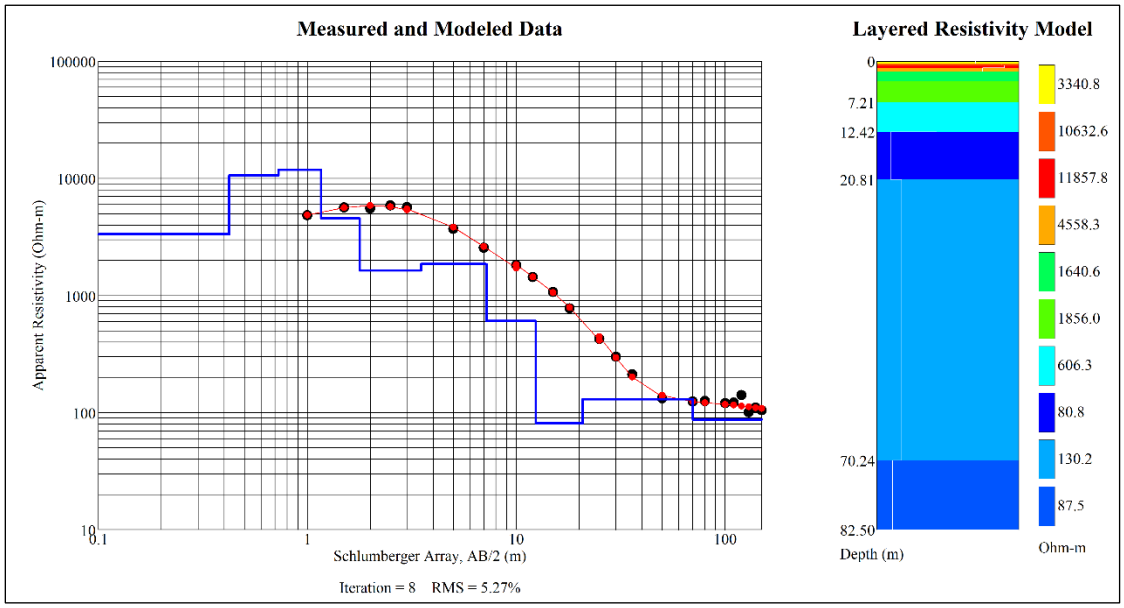

Figure 4.10.2. 10-Layer resistivity model and curve for the Schlumberger array, VES survey at Qualicum. Apparent resistivity measurements are plotted on the log-log graph as black circles, the model-predicted values are graphed in red, and the blue line plotted on the graph breaks down the model, showing layer thicknesses (interface depths in m on the x-axis) and resistivities (y-axis). The variance between the black circles and the red circles is measured in the RMSE value below the graph. The block diagram on the right is the layered subsurface resistivity model.

4.10.3. VES Interpretations

Three, natural, lithologically distinct units of material were interpreted in the subsurface at Qualicum, with interfaces at depths of ~12.5 and 21 metres depth (Fig. 4.10.3). Resistivities in

the model were consistent with the ranges of values for sand and gravel, till, clay, siltstone, and sandstone. Bedrock geology beneath this site is unmapped but was inferred to occur at much greater depths than sensed by the VES, based on bedrock elevations in nearby well logs. WTN 12733 placed bedrock at an elevation of roughly -62 masl, and when compared to the minimum elevation sensed by the VES survey of roughly -45 masl, it is possible that bedrock was simply out of reach of the survey. For this reason, siltstone and sandstone are excluded from my interpretation. At the surface of Qualicum, I interpreted fill composed of gravel just like at Wilfred, but here it was ~2 metres thick and included the first four modelled layers. The next three modelled layers were interpreted to comprise a unit of sand and gravel ~10.5 metres thick, inferred to correspond to Capilano Sediments. The sand and gravel unit is considered to behave as an unconfined, high-yielding aquifer. Initially, the bottom ~70 metres of the profile were interpreted as till from the Vashon Drift; however, the Vashon Drift has a maximum observed thickness of ~60 metres (e.g., Bednarski, 2015), which made this interpretation less reliable. Instead, immediately beneath the sand and gravel, I interpreted a unit of silty clay ~8 metres thick, represented by the model's resistivity minimum, 80.8 Ωm, and I inferred it to represent a lower unit of Capilano Sediments. This interpretation is more geologically reasonable since the mapped surficial geology, Capilano Sediments, is often associated with silt and clay underlying sand and gravel deposits. The silty clay interpretation also allowed for the rest of the profile to be interpreted as Vashon Drift till, as the lowest unit decreased from ~70 metres thick to ~62 metres, more consistent with the maximum observed thickness. Both the silty clay and till are considered a thick aquitard, confining whatever lithologies exist below.

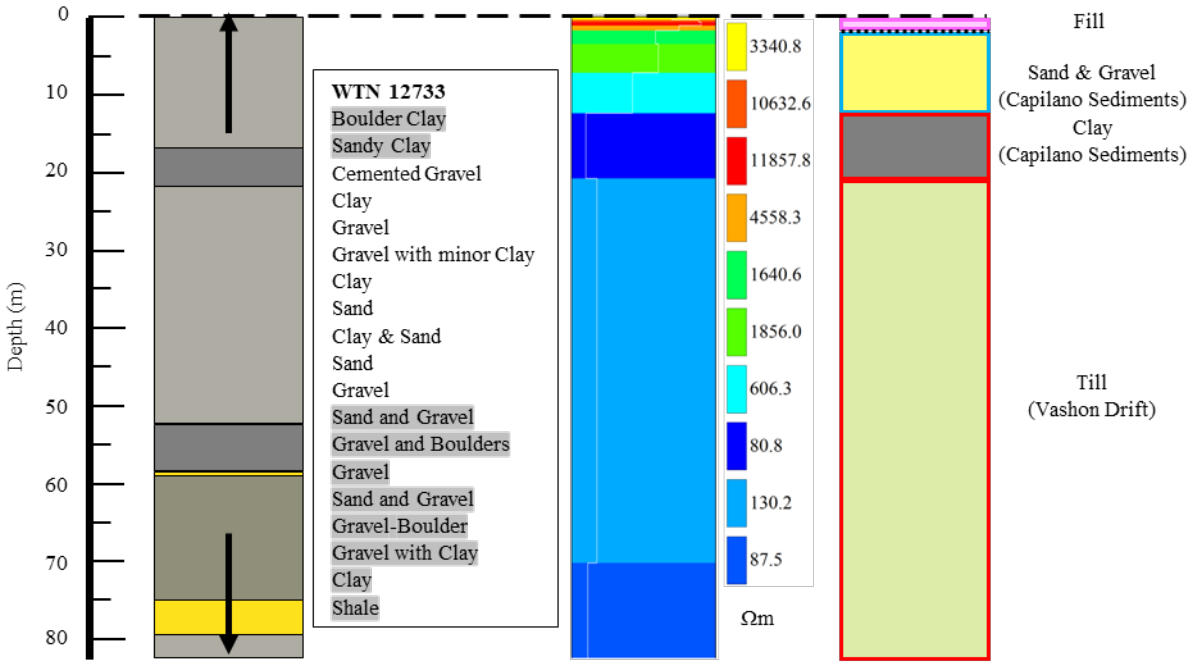

Figure 4.10.3. Qualicum's components of interpretation. Columns from left to right represent control well lithologies (listed beneath WTN; GWELLS, https://apps.nrs.gov.bc.ca/gwells/well/12733), resistivity model, interpretation of lithologies, stratigraphy, and hydrogeological potential (pink outline = artificial material, blue outline = high-yielding aquifer, red outline = aquitard, green = low-yielding aquifer). The dashed black line indicates ground surface and the dotted black line in the interpretation column indicates that the exact location of the boundary is uncertain and may be slightly shallower or deeper. The black arrows in the control well column indicate that the well contains lithological records that extend above and below the VES survey; these well lithologies are highlighted grey in the lithology legend under the well tag number.

4.11. Rosewall (MW21-5)

4.11.1. Site Location and Mapped Geology

On the Department of Fisheries and Oceans (DFO) property of the Fanny Bay Salmonoid Enhancement Society, the Rosewall VES survey was set up along the side of a dirt pathway, running subparallel to the shoreline, which was located roughly 40 metres from the survey centre. The survey centre, at an elevation of 4 masl, was located approximately 100 metres southwest of the slightly lower-elevation control well (MW21-5; DFO, unpublished data), with a vertical offset of roughly 0.6 metres. Salish Sediments composed of gravel, sand, silt, and clay in shore, deltaic, and fluvial deposits are mapped as the surficial geology (Fyles, 1963a; Fyles, 1963b). Specific bedrock geology of the area is unknown but is likely some member of the Nanaimo Group bedrock, most probably the Willow Point Member.

4.11.2. VES Resistivity Data and Model

Apparent resistivity measurements ranged from 27 to 14194 Ωm and the layered resistivity model ranged in value from 18 to 34917 Ωm (Fig. 4.11.2). The highest resistivities occurred in the top 1.5 metres of the profile and modelled resistivities successively dropped by an order of magnitude for each of the next three layers. Nearly 77 metres of the model (all material below ~6 m depth) are represented by layers with resistivities less than 100 Ωm. Similar to Qualicum, a general decrease in resistivity of the layered model can be seen in the colours of layers from top to bottom, changing from warm tones to cool tones, but with the most conductive layer occurring between ~20 and 51 m depth (Fig. 4.11.2). An 8-layer model with an RMSE of 11.94% was chosen for interpretation as a subsurface model.

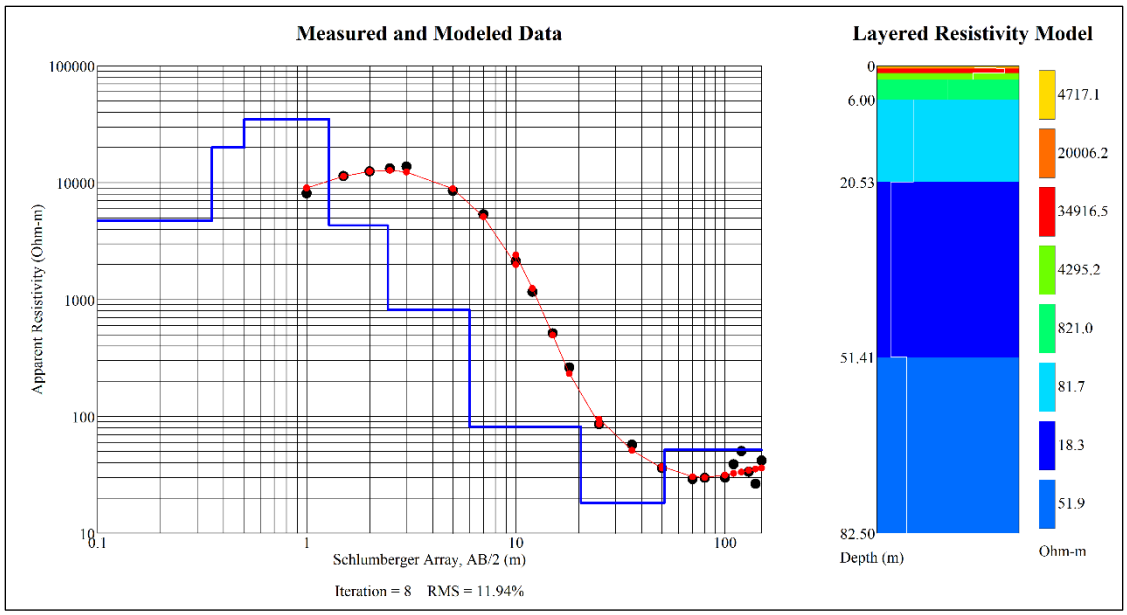

Figure 4.11.2. 8-Layer resistivity model and curve for the Schlumberger array, VES survey at Rosewall. Apparent resistivity measurements are plotted on the log-log graph as black circles, the model-predicted values are graphed in red, and the blue line plotted on the graph breaks down the model, showing layer thicknesses (interface depths in m on the x-axis) and resistivities (y-axis). The variance between the black circles and the red circles is measured in the RMSE value below the graph. The block diagram on the right is the layered subsurface resistivity model.

4.11.3. VES Interpretations

Four, natural, lithological units were interpreted from the Rosewall model of the subsurface (Fig. 4.11.3.0). The modelled resistivities were characteristic of sand and gravel, till, clay, shale, siltstone, and sandstone. The top three layers of the model were interpreted to represent artificial gravel or fill like the previous two survey sites, measuring ~1 metre thick. I interpreted a unit of

sand and gravel ~5 metres thick to follow the fill and inferred it to correlate with Salish, and possibly, Capilano Sediments. This unit is considered to behave as an unconfined, high-yielding aquifer. Below this, the next modelled layer was interpreted as ~14.5 metres of silty sand, also correlating with Salish and/or Capilano Sediments, but inferred to act as a moderate-yielding aquifer. The next modelled layer was interpreted as the third lithological unit in the sequence, inferred to be clay, either corresponding to the Capilano Sediments as marine clay or the Vashon Drift as glaciomarine clay. This unit is ~31 metres thick, extending from ~20.5 to 51.5 metres depth, and was inferred to behave as an aquitard. Till of the Vashon Drift was excluded from my interpretation due to its absence from nearby wells penetrating to depths within the range of 20 to 50 metres. The last unit I interpreted was siltstone, extending from ~51.5 metres depth downwards, and inferred to be a relatively confined, moderate-yielding aquifer, of the Willow Point Member bedrock. Interpretations for the Rosewall VES incorporated another type of data: mapped faults (Fig. 4.11.3.1; British Columbia Digital Geology, https://catalogue.data.gov.bc.ca/dataset/geology-faults). This information was used to help construct my interpreted lithostratigraphic sequence, given uncertainty in the depth of bedrock, as there is a lack of wells that penetrate bedrock in the area. The nearest constraint on bedrock depth is from a site ~1.6 km to the northwest of the Rosewall survey, where bedrock occurs at ~12 metres below ground level, at -9 masl (WTN 98193; GWELLS, https://apps.nrs.gov.bc.ca/gwells/well/98193) . The wells in the area closer to Rosewall, however, penetrated up to ~27 metres depth without encountering bedrock. To better understand whether bedrock was sensed in the VES survey, I consulted fault maps from the BC Geological Survey on iMaps BC (https://maps.gov.bc.ca/ess/hm/imap4m/) and identified a NE-trending fault located between the Rosewall survey and nearby wells and the well with bedrock at ~12 metres below ground level (Fig. 4.11.3.1). It is unclear what motion occurs on this fault, but in the case of it being a normal or extensional fault common in the area, downward movement on the SE side of the fault could explain the greater bedrock depth at Rosewall compared to at WTN 98193 on the NW side of the fault. This helped guide my interpretation of the bedrock depth, and led to my Rosewall interpretation including bedrock at a depth of at least 51.5 metres below the ground surface.

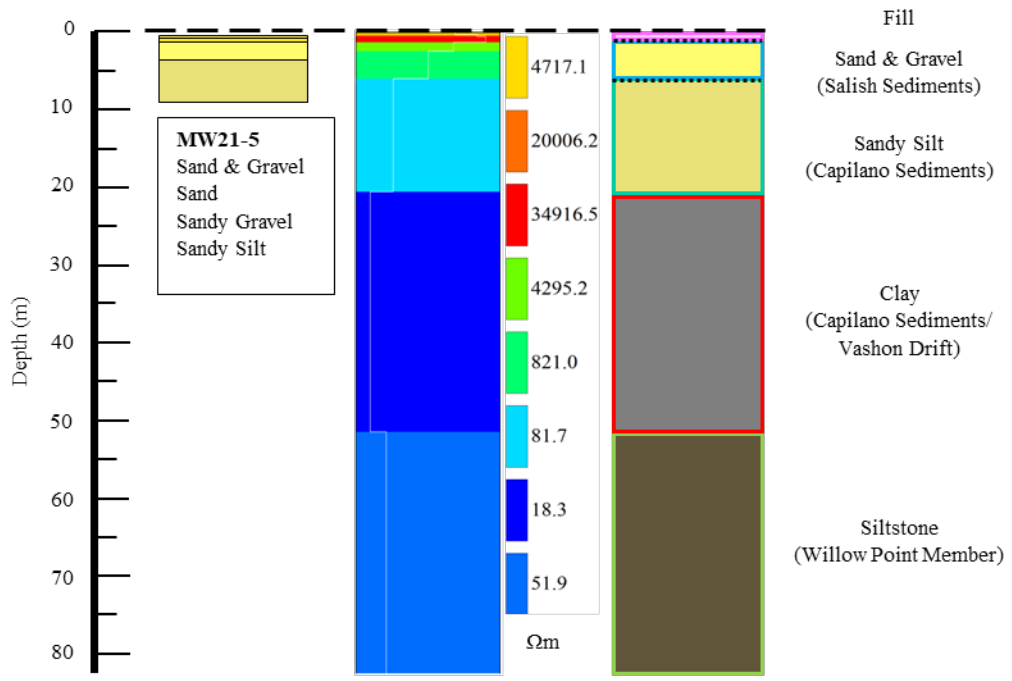

Figure 4.11.3.0. Rosewall's components of interpretation. Columns from left to right represent control well lithologies (listed beneath WTN; DFO, unpublished data), resistivity model, interpretation of lithologies, stratigraphy, and hydrogeological potential (pink outline = artificial material, blue outline = high-yielding aquifer, red outline = aquitard, green = low-yielding aquifer). The dashed black line indicates ground surface and the dotted black line in the interpretation column indicates that the exact location of the boundary is uncertain and may be slightly shallower or deeper.

Figure 4.11.3.1. Map of NE-trending fault (British Columbia Digital Geology, https://catalogue.data.gov.bc.ca/dataset/geology-faults) between Rosewall study site (red triangle) and WTN 98193 (blue circle; GWELLS, https://apps.nrs.gov.bc.ca/gwells/well/81873).

4.12. Berray (WTN 81873)

4.12.1. Site Location and Mapped Geology

Approximately 700 metres east of the Rosewall survey centre, the Berray VES was conducted along the shoulder of a road. Relative to the survey centre (13 masl), the control well, WTN 81873 (GWELLS, https://apps.nrs.gov.bc.ca/gwells/well/81873), was located 2 metres lower and roughly 100 metres northeast. Surficial geology at Berray matches that mapped at the Rosewall site (Fyles, 1963a; Fyles; 1963b), and similarly, the bedrock is assumed to broadly be of the Nanaimo Group since specific details of the bedrock are not mapped.

4.12.2. VES Resistivity Data and Model

Raw, apparent resistivity data ranged between 10 and 955 Ωm. In comparison, the modelled layer resistivities ranged from 83 to 2584 Ωm (Fig. 4.12.2). As seen in the plotted resistivities, the Berray model does not follow a simple trend, such as the gradual decreases seen in other models in this study; rather, resistivities first decrease with depth, followed by a sharp increase, and another steeper decrease (Fig. 4.12.2). A 7-layer model with an RMSE of 5.29% was selected for interpretation as the subsurface model.

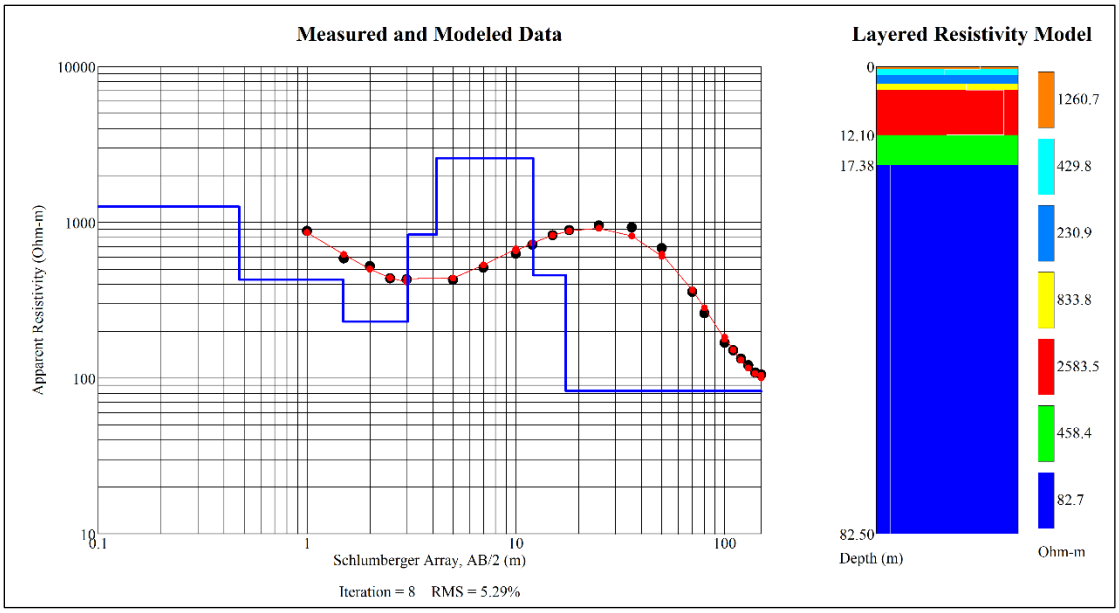

Figure 4.12.2. 7-Layer resistivity model and curve for the Schlumberger array, VES survey at Berray. Apparent resistivity measurements are plotted on the log-log graph as black circles, the model-predicted values are graphed in red, and the blue line plotted on the graph breaks down the model, showing layer thicknesses (interface depths in m on the x-axis) and resistivities (y-axis). The variance between the black circles and the red circles is measured in the RMSE value below the graph. The block diagram on the right is the layered subsurface resistivity model.

4.12.3. VES Interpretations

Only two lithological units were interpreted in the subsurface of Berray from the model, in which resistivities were characteristic of sand and gravel, till, clay, and sandstone (Fig. 4.12.3). Six of the seven modelled layers were less than ~17.4 metres deep, and were interpreted as sand and gravel of the Salish, and possibly Capilano, Sediments. This unit was inferred to behave as an unconfined, high-yielding aquifer. Below ~17.4 metres depth was a modelled layer exceeding ~65 metres in thickness. With a resistivity characteristic of clay, till, and sandstone, there were many factors to consider in the lithological interpretation. Since the Berray survey was conducted roughly 700 metres east of the Rosewall survey, wells in the surrounding area were common between the two sites. In those wells that penetrated up to ~27 metres depth, bedrock was not encountered, ruling sandstone out of my interpretation of the bottom layer. In the case of till, which stratigraphically would be Vashon Drift, Bednarski (2015) notes that the maximum observed thickness is 60 metres. While it is possible that this maximum is exceeded beneath the ground where we cannot observe it, this constraint on thickness led to uncertainty in identifying the bottom modelled layer, 65 metres or more in thickness, as till. Instead, the unit was

interpreted as a deposit of clay, not only as a result of the process of elimination, but also as it was the most geologically reasonable explanation. Although the thickness may seem unusual, the interpretation of a deposit of clay spanning both the time ranges of the Vashon Drift (marine clay) and Capilano Sediments (glaciomarine clay) is plausible. Alternatively, this unit may be a combination of clay and till that were so close in resistivity that the model grouped them as one layer, masking the presence of two lithologies. Without more information, this assumption has large uncertainty, and my interpretation remains a single unit of clay – an aquitard greater than 65 metres in thickness.

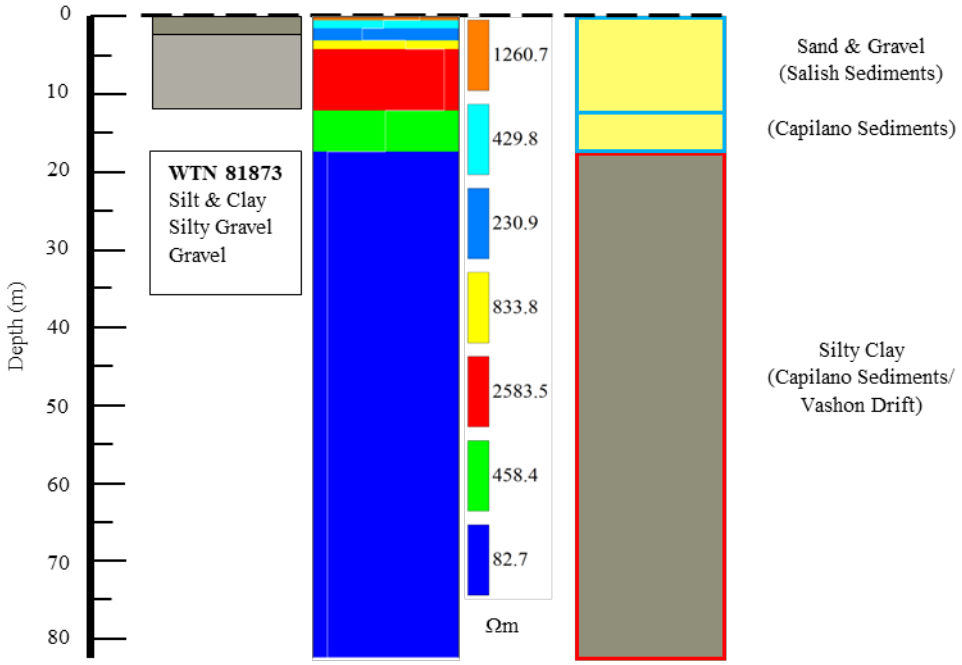

Figure 4.12.3. Berray's components of interpretation. Columns from left to right represent control well lithologies (listed beneath WTN; GWELLS, https://apps.nrs.gov.bc.ca/gwells/well/81873), resistivity model, interpretation of lithologies, stratigraphy, and hydrogeological potential (blue outline = high-yielding aquifer, red = aquitard). In this case, the bottom two layers were similar enough in lithology, I grouped them together. The dashed black line indicates ground surface.

5. Discussion

5.1. Regional Lithostratigraphy

Throughout the Beaufort Watershed region, three unconsolidated lithostratigraphic units were consistently inferred to correlate with subsurface materials. From youngest to oldest, these units were the Salish Sediments, Capilano Sediments, and the Vashon Drift. In terms of the lithostratigraphic units of bedrock, there was one member of the Nanaimo Group that was

dominantly interpreted; however, one or two other members were inferred to be present in the study area. In respective order, these were the Willow Point Member, the Puntledge Member and/or the Browns Member. In the following subsections, each of the lithostratigraphic units encountered in this study are summarized, with the exception of the interpretations made for Stelling due to the level of uncertainty and lack of information provided by the shallow VES. As a result, the interpretations are summarized with respect to the 11 other survey sites. Table 5.1 contains these summarized interpretations and Figure 5.1 illustrates the lithostratigraphic units correlating to lithologies in this study. In the final subsection (5.1.6.), I theorize why the other Quaternary lithostratigraphic units are absent from the 11 study sites.

Table 5.1. Summary of the locally correlated lithostratigraphic units.*Excluding Stelling due to its large error and uncertainty. **Values from ERT sites not used.

Lithostratigraphic Unit	Materials	Range of Thickness (m)	Average Resistivity (Ωm)	Number of Sites*, Number of Values**
Salish Sediments	Variations of Sand & Gravel	~1-12	2028	5, 15
Capilano Sediments	Variations of Sand & Gravel; Clays	~1-18.5; insufficient data[1]	3890; 48	11, 26; 5, 5
Vashon Drift	Till; Clay	~6.5-62+; insufficient data[1]	88; 42.7	9, 13[3]; 3, 3
Willow Point Member	Shale; Siltstone	-	~26.5; ~46	5, 4[3]; 3, 5
Puntledge Member	Siltstone	-	54.0[2]	1, 1
Browns Member	Siltstone	-	59.4[2]	1, 1

[1] Unknown interface depths.
[2] Not an average; only a single value was correlated to this unit.
[3] Anomalous values were omitted from calculation of average.

5.1.1. Salish Sediments

The lithology of materials inferred to correlate with Salish Sediments was always a variation of sand and gravel, whether it was silty or clean, and had a range in thickness between ~1 and 12 metres. The modelled resistivities associated with the lithologies corresponding to Salish Sediments ranged between 128.6 and 8990.4 Ωm, averaging around 2028 Ωm. These characteristics were summarized from models and interpretations at six of the 11 valid survey sites, all of which occurred in the southern part of the study area, south of, and including, the Tsable study site. At the six sites where Salish Sediments were hypothesized to occur (Tsable, Fanny Bay, Ships Point, Stelling, Rosewall, and Berray), survey centre elevations were less than 15 masl; in fact all but one of these sites were 6 metres or less above sea level. In contrast, the remaining six sites at which this lithostratigraphic unit was not inferred to be present had elevations greater than 28 masl at their survey centres. As the definition of Salish Sediments implies, the occurrence of the unit is strongly linked to elevation above present day base level (e.g., Bednarski, 2015), explaining the lack of Salish Sediments at half of the study sites where the typical elevation of the unit (~5 masl) is greatly exceeded.

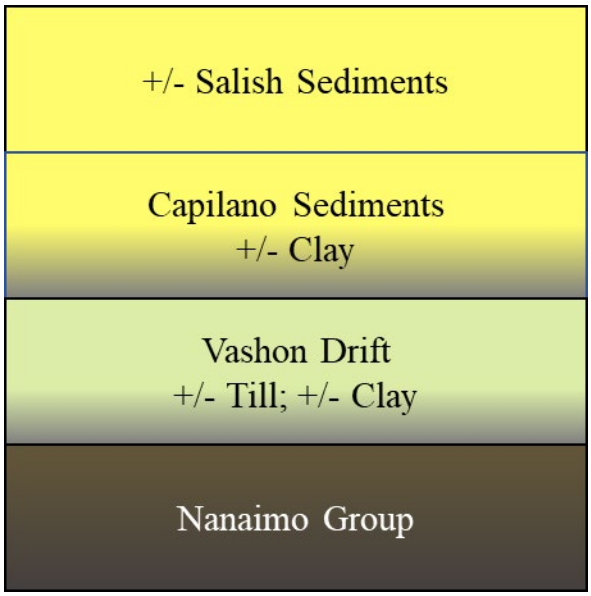

Figure 5.1. Generalized illustration of the inferred local lithostratigraphy. Thicknesses are not to scale due to the large ranges possible. Colours match the most common lithologies (yellow = variation of sand and gravel, grey = clay, light green = till, brown = siltstone, dark grey = shale), and the plus or minus (+/-) symbolize the variable presence/absence of the unit throughout the study area. Nanaimo Group may be any of the three members of bedrock inferred in this study, or possibly other members defined by Cathyl-Bickford (1992).

5.1.2. Capilano Sediments

Capilano Sediments, on the other hand, were inferred to correlate to material at all 11 of the study sites, corresponding to a more diverse range of lithologies due to the depositional nature of the lithostratigraphic unit. The prominent lithology associated with this interpretation was sand and gravel that varied from silty to clean. The range in thickness of the sand and gravel lithology in this unit was also more variable than the Salish Sediments, being as thin as 0.8 metres and as thick as 18.5 metres. The thinner units of Capilano sand and gravel occurred in the region of the study area north of Tsable, at four sites that were associated with an absence of Salish Sediments. Resistivity of the sand and gravel materials interpreted as Capilano Sediments ranged between 81.7 and 36097.8 Ωm, averaging around 3890 Ωm. The other lithology interpreted from the models and inferred to correlate with Capilano Sediments was clay (or silty clay), and was determined to be present at five of the 11 study sites. This part of the unit occurred in layers as thin as ~1 metre and potentially exceeded 65 metres in southern locations. The maximum thickness of Capilano clay is uncertain due to the interpretation of some of these clay units jointly correlating to both Capilano Sediments and Vashon Drift. For clays interpreted at sites near current day sea level, the likely depositional origin of the clays is glacio-marine, which could have been deposited across the time intervals associated with both the Vashon Drift and Capilano Sediments. In this case, the interface between the two lithostratigraphic units would be disguised by the continuous deposition of the same material, and the thickness of the lithostratigraphic unit would be unknown. A range and an average can be approximated for the resistivities of the Capilano clays, however, since the clays from either lithostratigraphic unit would be considered identical. The Capilano clays range between 18.3 and 82.7 Ωm, and average around 48 Ωm. To understand the distribution of the Capilano clays throughout the study area, more research would need to be conducted on the local sea level over the Quaternary period. I speculate that the sites at which the Capilano clays have been interpreted were in isostatically depressed coastal areas (e.g., Bednarski, 2015) where the ground was below local base level during this time interval.

5.1.3. Vashon Drift

The last unconsolidated lithostratigraphic unit inferred to correlate with materials throughout the study area was Vashon Drift, including till and glaciomarine clay. Vashon Drift till was interpreted at nine of the 11 survey sites (all but Rosewall and Berray), and ranged in resistivity

from 37.1 to 893.3 Ωm, but the maximum was an outlier as most corresponding resistivities were less than 100 Ωm. An average resistivity for the Vashon Drift till was calculated at around 88 Ωm, omitting the 893.3 Ωm outlier. The till was determined to have a range in thickness of ~6.5 to 61.7 metres, mostly agreeing with the maximum observed thickness of this lithostratigraphic unit of 60 metres (e.g., Bednarski, 2015). At three of the 11 study sites (Argyle, Rosewall, and Berray), I interpreted a unit of clay to potentially correlate with Vashon Drift. At Argyle, this unit was distinct from Capilano clay since it was overlain by Vashon till as opposed to the other two sites where Vashon clay was interpreted without the presence of Vashon till. For the same reason I could not provide a range in thickness for Capilano clay, the thickness range for Vashon clay is unknown. Resistivity of this unit, however, ranged between 18.3 and 82.7 Ωm and averaged around 42.7 Ωm. I attribute the absence of Vashon till at the two study sites to the relative local sea level during the Vashon Drift time interval; over this time, I hypothesize that the Rosewall and Berray study sites were below sea level, and therefore experienced marine deposition conditions rather than glacial moraine deposition conditions, leading to clay deposits instead of till. In comparison to the Argyle study site where both till and clay of the Vashon Drift were interpreted, I suggest that the area was below sea level for the first part of the time interval over which the Vashon Drift was deposited, allowing for clay to be overlain by till.

5.1.4. Willow Point Member

Willow Point Member bedrock was interpreted at seven of the study sites. The bedrock lithologies varied between shale and siltstone, and at some locations both were interpreted to be present. Thicknesses of these units were not summarized, since they often extend to depths beyond the scope of the surveys, but the resistivities were. This was possible since the dimensions of the bedrock unit were not necessary for measuring and summarizing the rock's physical property of resistivity. Shale, which was interpreted at just five of the 11 sites, had a small range in resistivities from 24.7 to 28.44 Ωm, excluding the anomalously low resistivity of 3.0 Ωm modelled at Buckley, interpreted as heavily fractured shale, saturated in water that was potentially brackish. While also omitting this outlier, the average resistivity for Willow Point shale was calculated to be ~26.5 Ωm. Siltstone of the Willow Point Member was interpreted at three study sites, ranging in resistivity between 33.9 and 51.9 Ωm, and averaging ~46 Ωm. Spatially, the interpretation of these two bedrock lithologies relied heavily on bedrock maps from Cathyl-Bickford and Hoffman (1998). With the complex tectonic history of Vancouver Island

and the age of the Nanaimo Group bedrock (>66.0 Ma), the presence and absence of the Willow Point Member bedrock in the study area can most simply be explained by the coupled factors of unconsolidated sediment thickness overlying the bedrock, and the absolute elevation of the bedrock linked to the dip of the Nanaimo Group.

5.1.5. Puntledge Member and Browns Member

Both the Puntledge and Browns Member lithostratigraphic units were interpreted at only one study site each. The Puntledge Member was correlated to siltstone interpreted at the Wilfred survey site in the south part of the study region, characterized by a resistivity of 54.0 Ωm. The Browns Member was also correlated to a siltstone unit, but instead, in the north part of the study region at the Macleod survey site. The Browns siltstone was characterized by a resistivity of 49.4 Ωm. Like the Willow Point Member, the thickness of each of these bedrock units were not summarized since it is unknown whether or not the lower extent exceeds the depth that the surveys probed. Also, similar to the Willow Point Member, the presence and absence of these bedrock members is attributed to the thickness of unconsolidated sediments and related bedrock elevation, controlled by the dipping nature of the Nanaimo Group.

5.1.6. Absence of Unconsolidated Lithostratigraphic Units

After analysis and interpretation of the resistivity surveys across the study area, it was determined that four of the regional lithostratigraphic units described in section 2.1.2 were not inferred to correlate to any material sensed beneath the survey sites. These units were all older than Vashon Drift, and included the Quadra Sand, Cowichan Head Formation, Dashwood Drift, and Mapleguard Sediments. South of the study area, Fyles (1963b) constructed a small schematic of an exposure consisting of all four of these units; however, this section was nearby an area of Quadra Sand mapped at the surface. Within the study area, between Fanny Bay and Royston, Fyles (1960; 1963b) did not identify any surficial deposits of Quadra Sand, but he did map a unit that is potentially equivalent in time to Quadra Sand. The absence of lithostratigraphic units older than Vashon Drift in my interpretations can be attributed to the erosional nature of the glaciers flowing over Vancouver Island, that deposited the till. At the survey sites in this study, erosion by glaciers is the most logical explanation as for why Quadra Sand and older units are absent. While the surveys in this study were relatively dispersed, providing a decent sampling of the entire study area, it cannot be certain that my interpretations of stratigraphic sequences hold true for the surrounding areas where surveys were not conducted. As a result, I cannot

confidently conclude that the four units absent from my interpretations are absent from the entire region.

5.2. Implications for the Beaufort Watershed and Summary of Hydrogeological Units

The hydrogeological implications of the lithostratigraphic units either present or absent in this study are discussed in the following subsections along with a summary of the aquifers and aquitards inferred from my lithological interpretations. The characteristics of the aquifers and aquitards are summarized in Table 5.2.

5.2.1. Sand and Gravel Aquifers

Sand and gravel units from the Salish and Capilano Sediments were inferred to behave as unified, partially confined, moderate to high-yielding aquifers, stretching up to 19.6 metres thick. At each site they were present together, the sand and gravel from the two lithostratigraphic units were considered as a single sand and gravel layer due to uncertainty in their interface as well as the likelihood of hydraulic connection. The relatively high resistivity readings of these sand and gravel units that resulted in high average resistivities (Table 5.1) may be attributed to the degree of dryness of the sediments, with a dominant portion of these sands and gravels being undersaturated.

In the northern part of the study area where the Buckley, Macleod, Argyle, and Royston survey sites were located, Salish sand and gravel was determined to be absent, but thin layers of Capilano sand and gravel was interpreted to be present. Despite this, the deposits of sand and gravel present are generally too thin (0.8 – 5.4 metres thick) for aquifer development to be reasonable in this area; this is supported by the lack of wells drawing water from sand and gravel between the Buckley and Royston sites (GWELLS, https://apps.nrs.gov.bc.ca/gwells/). Sand and gravel units at Tsable, and all other sites further south, were between ~10 and 20 metres thick (average of ~17.5 metres), providing sufficient material to develop an aquifer, as can be seen by the current number of wells drilled into this sand and gravel unit throughout the southern part of the study area (GWELLS, https://apps.nrs.gov.bc.ca/gwells/). At three of these sites, a gravel fill was interpreted as a thin layer at the surface, but due to the permeable nature of the artificial material, it can theoretically be included in the surficial sand and gravel aquifer. With the exception of the Wilfred study site, where extremely high resistivities indicated dry conditions within the aquifer, all southern locations included this sand and gravel aquifer at ground level.

Confinement of these aquifers was considered to be partial since the sand and gravel units at most sites were fully exposed to the surface, but a lens of clay interpreted within the sand and gravel at Macleod suggested the potential for partial confinement of the sand and gravel directly below it. Furthermore, it is not uncommon for lenses of various lithologies to form in the lithostratigraphic units, so it is reasonable to hypothesize that other parts of the sand and gravel aquifer throughout the study area may be partially confined by other clay lenses in the Capilano Sediments.

Yields of this aquifer were estimated to be moderate to high based on lithologies and Table 6 of Berardinucci and Ronneseth (2002). After evaluation of various yields from wells in the study area that drew water from surficial sand and gravel (WTN: 108240, 108269, 127037, 124028, 121630, 74999, 81873; GWELLS, https://apps.nrs.gov.bc.ca/gwells/), it was determined that the sand and gravel aquifers I interpreted (inferred to correlate with the aquifer in the analyzed wells), in fact yielded moderate to high quantities of groundwater (15-100 US gallons per minute [GPM]; Berardinucci & Ronneseth, 2002). Heterogeneity of the variably sorted sand and gravel in this aquifer likely explains the variation in yields throughout the aquifer.

A consequence of the aquifer being only partially confined and highly developed is the vulnerability to saltwater intrusion. Community members from Ships Point peninsula raised concern over this, inspiring the design of the study to include ERT surveys along either side of the peninsula. The resulting 2D profiles revealed what was interpreted to be the presence of saltwater/brackish water in the sand and gravel aquifer. Comparing the 2022 Ships Point ERT survey to the one conducted in 2021 displayed a potential increase in the presence of saltwater, possibly indicating an increase in the strength of saltwater intrusion. While sand and gravel interpreted in the VES surveys were not inferred to be affected by the presence of brackish water or saltwater, I cannot confidently conclude that the phenomenon is not occurring at any other site. Section 5.3 discusses future research that can be done to look at this issue in greater detail.

I propose that the boundaries of previously mapped sand and gravel aquifers in the southern part of the study area can be either extended to include all locations where I interpreted a sand and gravel aquifer, or for locations I made this interpretation outside the boundaries of previously mapped sand and gravel aquifers, a new aquifer can be delineated to contain these locations (Fig. 5.2).

5.2.2. Bedrock Aquifers

I classified most of the bedrock units interpreted in this study as a single, relatively confined, low-yielding aquifer. Each of the three members of the Nanaimo Group correlated to bedrock in this study had similar lithologies, all of which were fine-grained and believed to be fractured to varying degrees. The average depth to the bedrock aquifer throughout the study area is ~32 metres.

All bedrock aquifers I interpreted in the study area are considered to be relatively confined. The majority of bedrock is heavily confined beneath a thick layer of till and/or clay, but in areas where bedrock outcrops at the surface or surficial sediments are very thin and lack aquitard qualities, the bedrock aquifers are unconfined. These unconfined areas are much less common than the confined areas, so the aquifer is more confined than not. For this reason, the bedrock aquifer is less vulnerable to contamination than the sand and gravel aquifer in the study area.

Berardinucci and Ronneseth classify fractured bedrock as a low-yielding aquifer (2002), which is further supported by yields of ~1 GPM consistently reported for wells drilled into fractured bedrock in the study area (WTN: 127323, 127321, 107383; GWELLS, https://apps.nrs.gov.bc.ca/gwells/). Assuming the bedrock interpreted in the study area is consistent with the previously mapped bedrock for which these yields were reported, the bedrock aquifer I inferred is characterized as a low-yielding aquifer. This assumption excludes the heavily fractured shale bedrock beneath the Buckley site, where I suggest the aquifer to yield low to moderate quantities of groundwater.

Bedrock was interpreted at almost every one of the study sites in this survey. At the locations it was not interpreted, it can be inferred that the bedrock occurs at depths beyond what was sensed by the electrical resistivity surveys. A bedrock aquifer is therefore deemed to be present throughout the study area. I propose that the boundaries of the bedrock aquifer currently mapped in the north of the study area be extended at least to the southern extent of the study area (Fig. 5.2).

5.2.3. Aquitard

All clays and tills interpreted in this study were considered aquitard units. These lithologies were either Capilano Sediments, Vashon Drift, or some blend of both. At several survey sites, both lithologies were interpreted and occurred adjacent to one another allowing for the identification of a single aquitard, combining the extent of the two lithologies. In locations where

one or the other was present, the thickness was simply dictated by a single lithology. On average, the thickness of this aquitard was ~30.5 metres. This aquitard was interpreted at every site except Stelling (due to the limited depth sensed), indicating a regional instance of this aquitard. The depth to the aquitard varied between the north and south of the study area, where the average depth to the aquitard in the north, beyond Tsable, was ~2.5 metres, and from Tsable southwards, the average was ~18 metres depth.

Table 5.2. Summary of significant hydrogeological units inferred in the study area. * Based on definitions by Berardinucci and Ronneseth (2002), and using data from GWELLS (https://apps.nrs.gov.bc.ca/gwells/). Blank spaces indicate fields non-applicable to the hydrogeological unit.

Hydrogeological Unit	Sand & Gravel Aquifer	Bedrock Aquifer	Aquitard	
Study Area	Southern	Full	Northern	Southern
Average Depth (m)	Ground Level	32.0	2.48	17.68
Average Thickness (m)	~17.5	-	30.5	
Confinement	Partially Confined	Majorly Confined	-	-
Yield	Moderate-High*	Low*	-	-
Saltwater Presence	Yes	Maybe	-	-

5.2.4. Hydrogeological Implications of Inferred Lithostratigraphy

The Quadra Sand lithostratigraphic unit comprises the most exploited aquifer on the east coast of Vancouver Island (e.g., Benoit et al., 2015). This is significant for two reasons. First, as mentioned in section 2.1.4, the previously mapped, sand and gravel aquifer in Fanny Bay was identified as a Quadra Sand aquifer. In contrast, I interpreted the aquifer in the Fanny Bay area to correlate to the Capilano and Salish Sediments, as these units were more consistent with the various datasets I consulted, as well as the other sand and gravel aquifers mapped to either side, which are recognized as Salish Sediments. Unless the fault system at Fanny Bay is such that to either side of aquifer number 419, there are normal/extensional faults resulting in a vertical offset of the sediments at Fanny Bay, raising them relative to those on either side (Tsable River and

Rosewall Creek), it is unreasonable to have a Quadra Sand aquifer (aquifer number 419; GWELLS, https://apps.nrs.gov.bc.ca/gwells/aquifers/419) at roughly the same elevation as the much younger Salish Sediments aquifers (aquifer numbers 414 (GWELLS, https://apps.nrs.gov.bc.ca/gwells/aquifers/414) and 415 (GWELLS, https://apps.nrs.gov.bc.ca/gwells/aquifers/415)). Secondly, Quadra Sand was determined to be absent at every one of the sites in this study, implying a general scarcity of Quadra Sand in the study region between Royston and Fanny Bay. Therefore, Quadra Sand is not considered an aquifer in the context of this study area, and other lithostratigraphic units must be considered for access to groundwater. Although less prominent in hydrogeological use, the absence of the Cowichan Head Formation, Dashwood Drift, and Mapleguard Sediments also result in fewer sources of sand and gravel aquifers in the study area.

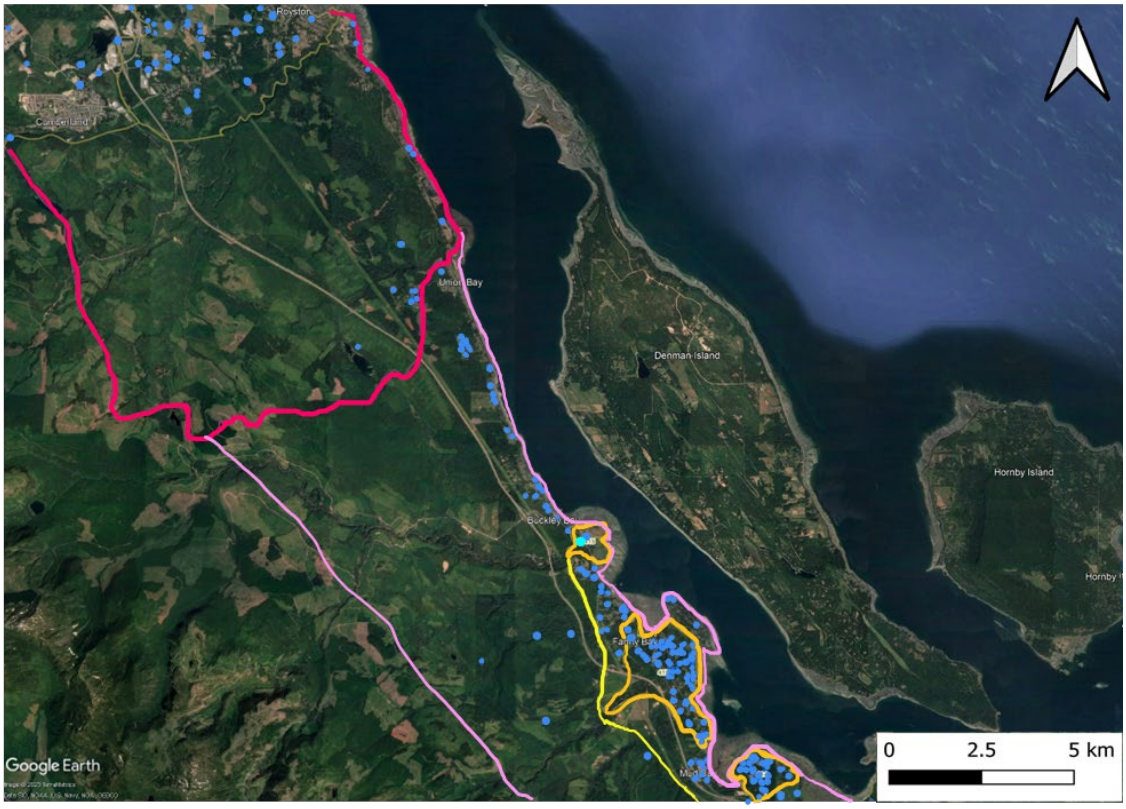

Figure 5.2. Map of proposed extension of aquifer boundaries. The dark pink outline is the previously mapped bedrock aquifer; the light pink outline is my proposed extension of the bedrock aquifer. The gold outlines are the previously mapped sand and gravel aquifers; the bright yellow outline is my proposed sand and gravel aquifer boundary. Groundwater wells are depicted as blue dots, with the cyan well signifying a provincial observation well. (data from GWELLS, https://apps.nrs.gov.bc.ca/gwells/).

The identification and characterization of the Salish and Capilano sand and gravel aquifer in the southern part of the study area revealed that the groundwater resource is slightly more pervasive than previously mapped to show. The average thickness of the aquifer will impact the

development of the resource as it is closely tied to the aquifer's hydraulic properties, while the knowledge gained on the depth and degree of confinement will have consequences for the protection and management of the groundwater in this aquifer. The inferred saltwater intrusion into this aquifer at Fanny Bay will also impact the strategies put into place for monitoring and mitigating the severity of the phenomenon. From the identification and characterization of the bedrock aquifer throughout the study area, average depths of the bedrock will contribute to the planning processes during development of the groundwater from this unit. The inferred regional presence of the bedrock aquifer also provides an alternative source of groundwater when a sand and gravel aquifer is not available.

6. Conclusion

In this study, I used the geophysical technique of electrical resistivity surveying to investigate the lithology and hydrogeology of the Beaufort Watershed study area. Numerous vertical electrical sounding surveys and two electrical resistivity tomography surveys were conducted throughout the region to locate and characterize aquifers and aquitards in this area of the Beaufort Watershed. The data from the vertical electrical soundings were modelled and interpreted allowing for the location and materials of aquitards and aquifers to be identified, and the thickness of each to be determined. With the interpretations of both aquitards and aquifers together, it was possible to resolve the relative degree of confinement of the aquifers in the study area. These interpretations revealed a surficial, partially confined sand and gravel aquifer in the southern part of the study area, determined to be a moderate to high-yielding aquifer, ranging between approximately 10 and 20 metres thick. An aquitard was inferred to cover the entire region, situated beneath the sand and gravel aquifer in the south, and within ~2.5 metres of the surface in the north. Averaging around 30.5 metres thick, this aquitard was determined to significantly confine the underlying bedrock aquifer that was also inferred to span the entire region. The bedrock aquifer had an average depth of 32 metres below the ground surface and was determined to be a low-yielding aquifer and heavily, although not completely, confined. For the population in the Beaufort Watershed, this provides useful information applicable to the protection and management of groundwater in the region.

6.1. Recommendations for Future Research

Although significant progress has been made to improve the understanding of aquifers and aquitards in the Beaufort Watershed study area, further research should be conducted to allow for the best possible groundwater management and protection. Characterization of the aquifers in this study was mostly qualitative so it would be useful for future studies to provide aquifer characteristics that are quantitative such as their hydraulic properties. These describe how the groundwater flows and behaves when the aquifer is actively pumped, and can be determined through analyses of pumping tests conducted at various locations throughout the aquifers. It would also be beneficial for more detailed groundtruthing work to be completed to confirm or support interpretations made in this study, such as finding bedrock outcrops throughout the study area and determining the degree to which it is fractured. Verification of the groundwater chemistry at Ships Point Peninsula would also improve the interpretations made in this study. Carrying out chemical analyses of groundwater from multiple wells around Ships Point Peninsula over a period of time, while observing the rate of groundwater withdrawal from the aquifer over the same time period, may clarify whether the sand and gravel aquifer in this location is experiencing worsening saltwater intrusion. Similarly, the groundwater chemistry at Buckley should be evaluated to determine if the deep, anomalously low resistivity was indicative of brackish water in the bedrock or if it was simply significant quantities of freshwater. The overall knowledge of the hydrogeology in the Beaufort Watershed region would also be advanced by conducting more studies like this one, in which more resistivity data are collected at different locations throughout the area.

F

7. References

Adeyemo, I. A., Ojo, B. T., & Raheem, W. O. (2017). Comparison of thickness and depth resolution power of Wenner and Schlumberger Arrays: A case study of temidire quarters, Akure, Nigeria. Journal of Geoscience and Environment Protection, 05(03), 233–239. https://doi.org/10.4236/gep.2017.53016

Advanced Geosciences Inc. (2009). Instruction Manual for EarthImager 2D. Austin, TX: Advanced Geosciences Inc.

Advanced Geosciences Inc. (2012). Instruction Manual for EarthImager 1D. Austin, TX: Advanced Geosciences Inc.

Armstrong, J.E., & Clague, J.J. (1977). Two major Wisconsin lithostratigraphic units in southwest British Columbia. Canadian Journal of Earth Sciences, 14(7), 1471 – 1480.

Asfahani, J. (2007). Electrical earth resistivity surveying for delineating the characteristics of ground water in a semi-arid region in the Khanasser Valley, Northern Syria. Hydrological Processes, 21(8), 1085–1097. https://doi.org/10.1002/hyp.6290

Barroso, S., Geo, P., Ormond, R., & Lapcevic, P. (2016). Groundwater Quality Survey of Aquifers in South Wellington, Cassidy and North Oyster, Vancouver Island. Water Science Series 2015-05.

Bednarski, J. M. (2015). Surficial geology and Pleistocene stratigraphy from Deep Bay to Nanoose Harbour, Vancouver Island, British Columbia. Geological Survey of Canada Open File 7681. doi:10.4095/295609

Benoit, N., Paradis, D., Bednarski, J. M., Hamblin, T., & Russell, H. A. J. (2015). Three dimensional hydrostratigraphic model of the Nanoose-Deep Bay area, Nanaimo Lowland, British Columbia. Geological Survey of Canada Open File 7796. doi:10.4095/296302

Berardinucci, L. & Ronneseth, M. (2002). Guide to using the BC aquifer classification maps for the protection and management of groundwater. Ministry of Water, Land and Air Protection, Environmental Protection Division, Victoria, BC, Canada.

Burger, H. R., Sheehan, A. F., & Jones, C. H. (2006). Introduction to applied geophysics: Exploring the shallow subsurface (Vol. 550). New York, NY: W.W. Norton.

Buzzanga, B. (2017). Precipitation and sea level rise impacts on groundwater levels in Virginia Beach, Virginia. Master's thesis, Old Dominion University, Norfolk, VA. doi: 10.25777 /qsft-gq17.

Cathyl-Bickford, C. G. (1992). Geology and energy resource potential of the Tsable River and Denman Island (92F/10, 11). British Columbia Geological Survey Geological Fieldwork 1991, Paper 1992-1, 419-426.

Cathyl-Bickford, C. G., & Hoffman, G. L. (1998). Geology of the Tsable River area, Comox Coalfield, British Columbia (Open File 1998-07, Sheets 6 and 7 of 8). British Columbia Ministry of Energy and Mines, Geological Survey Branch.

Clague, J. J. (1976). Quadra Sand and its relation to the late Wisconsin glaciation of southwest British Columbia. Canadian Journal of Earth Sciences, 13(6), 803–815. https://doi.org/10.1139/e76-083

Earle, S. (2019). Physical Geology – 2nd Edition. Victoria, B.C.: BCcampus. Retrieved from https://opentextbc.ca/physicalgeology2ed/

Edwards, L. S. (1977). A modified pseudosection for resistivity and induced polarization. Geophysics, 42, 1020-1036.

ENV, 2022a. Aquifer fact sheet: Aquifer 411. Accessed March 30, 2023. https://apps.nrs.gov.bc.ca/gwells/aquifers/411

ENV, 2022b. Aquifer fact sheet: Aquifer 415. Accessed March 30, 2023. https://apps.nrs.gov.bc.ca/gwells/aquifers/415

ENV, 2022c. Aquifer fact sheet: Aquifer 419. Accessed March 30, 2023. https://apps.nrs.gov.bc.ca/gwells/aquifers/419

ENV, 2022d. Aquifer fact sheet: Aquifer 414. Accessed March 30, 2023. https://apps.nrs.gov.bc.ca/gwells/aquifers/414

Freeze, R. A., & Cherry, J. A. (1979). Groundwater. Prentice-Hall, Inc.

Fyles, J.G. (1960). Surface Geology of Courtenay, Comox, Nelson, Nanaimo and Newcastle Districts, Vancouver Island, British Columbia, Ottawa: Geological Survey of Canada.

Fyles, J. G. (1963a). Surficial geology of the Horne Lake and Parksville map-areas, Vancouver Island, British Columbia (Memoir 318). Ottawa, ON: Geological Survey of Canada.

Fyles, J. G. (1963b). Surficial geology of Horne Lake Vancouver Island, British Columbia [Map]. Ottawa, ON: Geological Survey of Canada.

Greenwood, J. (2020, April 30). *Grounding and Corrosion Protection* [Webinar]. Advanced Geosciences Inc. https://www.agiusa.com/blog/agi-webinar-archive-april-2020

Hamblin, A. P. (2015). Detailed measured sections, bedrock aquifer/aquitard facies and potential bedrock aquifer systems of the Upper Cretaceous Nanaimo Group, Nanaimo Lowland, eastern Vancouver Island, British Columbia, Canada. Geological Survey of Canada Open File 7849. doi:10.4095/296979

Haq, F. U., Naeem, U.A., Ahmad, I., Waseem, M., & Iqbal, M. (2022). Electrical resistivity in the assessment of subsurface lithology and groundwater depth - a case study in Rawalpindi, Pakistan. Environmental Earth Sciences, 81(8), 1-15. https://doi.org/10.1007/s12517-022-10819-7

Ikard, S.J., Minsley, B.J., Rigby, J.R., Lane Jr., J.W., Knight, R.J., Llopis, J.L., & Bristow, C.S. (2023). A model of transmissivity and hydraulic conductivity from electrical resistivity distribution derived from airborne electromagnetic surveys of the Mississippi River Valley Alluvial Aquifer, Midwest USA. Hydrogeology Journal, 31(2), 313-334. https://doi.org/10.1007/s10040-022-02590-6

Lake, M. I. (1978). A report of a resistivity survey of the South Pilling area of North West Lancashire. Unpublished manuscript, University of Birmingham, Birmingham, UK.

Lapcevic, P., Kenny, S., & Wei, M. (2006). Long-term monitoring of groundwater conditions in fractured bedrock aquifers on Vancouver Island and the Gulf Islands, British Columbia. Sea to Sky Geotechnique, 1538 – 1545.

Metwaly, M. (2010). Integrated geoelectrical survey for groundwater and shallow subsurface evaluation: Case study at Siliyin spring, El-Fayoum, Egypt. International Journal of Earth Sciences, 99(4), 823-836. doi: 10.1007/s00531-009-0458-9.

Moore, R. B., Factors related to well yield in the fractured-bedrock aquifer of New Hampshire (2002). Reston, VA; U.S. Dept. of the Interior, U.S. Geological Survey.

Moncur, M. C. (1974). Groundwater investigations on Mayne Island: Report No. 3. Groundwater exploration on Mayne Island (Water Investigations Branch, B.C. Water Resources Service, File 0239013). British Columbia, Canada.

Moulds, M., Gould, I., Wright, I., Binley, A., Slater, L., & Rutter, H. (2023). Use of electrical resistivity tomography to reveal the shallow freshwater–saline interface in The Fens coastal groundwater, eastern England (UK). Hydrogeology Journal, 31(1), 335-349. https://doi.org/10.1007/s10040-022-02586-2

Mustard, P. S. (1994). The Upper Cretaceous Nanaimo Group, Georgia Basin. In J. W. H. Monger (Ed.), Geological and Geological Hazards of the Vancouver Region, Southwestern British Columbia (pp. 27-95). Geological Survey of Canada, Bulletin, 481.

Palacky, G. J. (1988). Resistivity characteristics of geologic targets. Electromagnetic methods in applied geophysics, 1, 53-129.

Pereversoff, V. G., Leonard, L. J., Lake, M. I., Wei, M., & Barroso, S. (2022). Evaluating the use of electrical resistivity sounding to characterize aquifers in the Beaufort Watershed, BC Water Science Series, WSS2022-08. Province of British Columbia, Victoria.

Church, M. & Ryder, J.M. (2010). Chapter 2: Hydrologic processes in forest ecosystems. In Compendium of forest hydrology and geomorphology in British Columbia (pp. 17-45).

Province of B.C. (2016). Water Sustainability Act: Overview and frequently asked questions. Retrieved from https://www2.gov.bc.ca/gov/content/environment/air-land-water/water/laws-rules/water-sustainability-act

Province of B.C. (2022). BC Data Catalogue Map Layers (Freshwater Atlas, Water Rights, Groundwater Wells, Aquifer Intrinsic Vulnerability, Aquifer Vulnerability to Saltwater Intrusion). Victoria, B.C.

Reynolds, J. M. (2011). An Introduction to Applied and Environmental Geophysics (2nd ed.). John Wiley & Sons.

Shiklomanov, I. A. (2000). Appraisal and assessment of world water resources. *Water International*, 25(1), 11–32.

Zohdy, A.A.R., Eaton, G.P., & Mabey, D.R. (1974). Chapter D1: Application of surface geophysics to ground-water investigations. Techniques of Water-Resources Investigations of the United States Geological Survey, p. 1-116.